Using Intrinsic Conducting Polymers (ICPs) in Electromagnetic Interference (EMI) Shielding for Wi-Fi and Mobile Phone Devices

By

Whamid AL-SHABIB

BSc (Elect Eng Hon) Iraq, MPhil (Mob Comms) Bradford UK,

MSc (Mob Comms) Lancaster UK, MSc (Comp.Sci) Huddersfield UK,

MSc (Manuf. Eng.) Bradford UK, MPhil (Physics) NUT UK

SCHOOL OF HEALTH, ENGINEERING AND SCIENCE

EDITH COWAN UNIVERSITY

2022

USE OF THESIS

Abstract

This research investigated whether there is potential to replace the materials now used in EMI shielding for mobile phones and Wi-Fi devices with Intrinsically Conducting Polymers (ICPs), which can be tuned to the frequency spectrum between 1 - 6 GHz. It also investigated other benefits that might result from use of ICPs in EMI shielding.

Using only simple experiments and simulation, this thesis demonstrated that ICPs tuneable to the frequency range between 1 - 6 GHz do have potential to replace the current EMI shielding for mobile phones and Wi-Fi devices. ICPs can perform EMI shielding at least as effectively as the forms of shielding currently in use. Comparison of the experimental modelling results showed the possibility of implementing the simulation model and applying it universally across all the shielding devices made from different IPC materials. Both liquid and felt forms of ICPs proved effective as EMR shielding. The highest level of transmission loss S_{21} occurred when ICP device material was made of woven fabric rather than a liquid PEDOT or PAni solution.

Narrowband experiments suggested the ICP transmission loss S_{21} could be improved by using a liquid rather than a woven PPy fabric, from solid to liquid and varying the frequency. The wideband experiments suggest liquid ICP shielding devices could be further improved by combining different doping chemicals with the PAni and the PEDOT, all experiments were protected by aluminium conducting tape to protect the shielding devices from edge diffraction on the corners of the shielding device under test.

Basic COMSOL Models fitted to the experimental data provide prediction rules for various ICP shielding devices in similar situations. More accurate measurements of material properties of the ICPs investigated requires further improvement of the modelling results.

At present, the ICP materials investigated are expensive, difficult to manufacture and require ingredients not readily obtainable. Use of those materials in EMI shielding devices would, however, provide impetus for further development of ICP materials and enhancement of their technological performance.

This research highlighted scope for the use of ICPs in a wider range of applications and suggested directions for further research including processes to speed up production of high-yield ICP materials with an accurate conductivity. Evidence that ICPs can enhance or replace the current shielding materials should promote the reduction or elimination of metals and carbon shielding materials in a new generation of mobile phones and Wi-Fi devices. This can offer benefits in terms of performance and reduction of health and environmental impacts.

Declaration

I certify that this thesis does not, to the best of my knowledge and belief:

i. incorporate without acknowledgment any material previously submitted for a degree or diploma in any institution of higher education;

ii. contain any material previously published or written by another person except where due reference is made in the text of this thesis; or

iii. contain any defamatory material.

[signature]

Signed *WhamidAlshabib* *Date* *18/12/2022*

ACKNOWLEDGMENTS

I would like to thank Prof Daryoush Habibi for accepting my original research proposal and allowing me to start my research journey. I would also like to thank the ECU vice-chancellor and Dr. Mehdi Khiadani for their support towards my thesis coach, Dr Marie-Louise McDermott. I would like to acknowledge and thank my supervisors, Dr Stefan W. Lachowicz and Dr Octavian Bas for supporting my research proposal. I would also like to thank, Dr Asfar Al-Shibib (microbiology) for the professional assistance of chapter 7 results. I would like 3A Kathy Communications Ltd., for publishing my thesis and supporting me.

I thank the research writer Dr Greg Maguire for his corrections to parts of this thesis and Professor William Stock, Associate Dean (Research) for checking the research summary. I thank my thesis coach, Dr Marie-Louise McDermott for her support.

I would like also to thank APA and ECU for providing me with funding for this project. I am also grateful to Ms Deb Duff with the Equity, Diversity and Disability Office for providing me with a one year license for COMSOL and HFSS simulations. I would like to thank Dr. Jamshid Avloni Managing Director of Enoyx (USA) for supplying me with ICP materials. I thank Dr Franz Schlagenhaufer from the International Centre for Radio Astronomy Research (ICRAR) for allowing me funding for my paper and access to their laboratory to verify the data from the OEMI experiments. I would like to express my profound gratitude and love to my wife Katherine Muller for her understanding and endless patience, when it was most needed during difficult times of this research. I give special thanks to my son, Adam Ahmed, and my daughters, Aishah and Aliah, who have always encouraged me to finish my research. I am also grateful to Emma Pettit for her interest, contact, encouragement and help during the period of my research.

I would like to thank my friends Dr. Waleed Al Sadi, Dr. Thair Mahmood, Dr. Maha Ahmed, Mr. Amro Qandour and Mr. Steven Silva for their continuous support of my research.

Table of contents

List of figures

List of tables

List of symbols, abbreviations and acronyms

λ	Wavelength
ρ	Charge Density (C/m***3***)
tanθ	Loss tangent
μ	magnetic permeability
A	Absorption loss
AFM	Atomic Force Microscopy
B	Magnetic flux density (Wb/m***2***)
E	Electric field (V/m)
σ	Electrical conductivity
∂	Skin depth
D	Electric Flux Density (C/m***2***)
ECU	Edith Cowan University
EME	Electromagnetic Energy
EMF	Electromotive Force
EMI	Electromagnetic Interference
EMR	Electromagnetic Radiation
EMP	Electromagnetic Pulse
f	Frequency
FDTD	Finite-Difference Time-Domain
FEM	Finite Element Method
FIT	Finite Integration Technique
FSS	Frequency Selective Surface
GSM	Global System for Mobile Communication
H	Magnetic Field (A/m)
ICP	Intrinsic Conducting Polymer
ICNIRP	International Commission for Non-Ionisation Radiation Protection
IEEE	Institute of Electrical and Electronics Engineering
INIRC	International Non-Ionising Radiation Committee
IR	Infrared
IRPA	International Radiation Protection Association

J	Electric current Density (A/m$^{2)}$
m	Magnetic permeability
MAN	Metropolitan area network
MoM	Method of Moment
MWCNTs	Multiwalled Carbon Nanotube
OEMI	Open Electromagnetic Interference
PAni	Polyaniline
PPy	Polypyrrole
μ	Permeability
ε	Permittivity
PEDOT	Poly(3-4-ethylenedioxythiophene)
R	Reflection loss
RF	Radio Frequency
S	Scattering Parameters
SE	Shielding Effectiveness
TM	Transverse Magnetic
UMTS	Universal Mobile Telecommunication System
U-NII	Unlicensed National Information Infrastructure
W	Width
WHO	World Health Organisation
WiMAX	Worldwide Interoperability for Microwave Access
Wi-Fi	Wireless Fidelity

Chapter 1 INTRODUCTION

Background

Electromagnetic Interference (EMI) emissions are increasing worldwide due to the growing use of smart phones, second and third generation mobile phones, iPods, TVs, computers, tablets, GPS systems, e-readers, video game consoles and other electronic-based products and the increasing levels of electronic circuitry found in cars, planes, home appliances and machine tools.[1] The increasingly complex designs of Wi-Fi devices coupled with the rising speed of the digital communications circuits such as clocks, control buses, and power supplies has increased demand for faster reliable data transfer.

Users of smart phones now expect to connect to the Internet wirelessly from any remote access point. They also expect their smart phones and other Wi-Fi devices to be accurate, reliable and safe and to operate without unwanted interference from other electronic devices. This has greatly stimulated interest in the provision of cost-effective ways to shield mobile and Wi-Fi devices, laptops, PCs and other devices from Electromagnetic Interference (EMI) produced by electromagnetic radiation emitting devices.

The scope for interference is now huge and growing, since all digital circuits can act as EM radiators and conductors can act like concealed antennas [2], [3], and [4] that can degrade the performance of other wireless devices. Signals emitted by Wi-Fi devices stretch over many kilometres, if their standard non-directional antennae are changed to directional antennae.

Over the last 30 years, regulators in the USA, European Union (EU), Australia and New Zealand have developed and published regulations and standards to protect electronic devices [5][6]. Those regulations have influenced communication device designs, and stimulated and encouraged use of shielding devices to maintain the EM transmission performance of mobile phones and other wireless devices. The need

to shield mobile phones and Wi-Fi devices from unwanted communication signals always need to be balanced against the need to preserve the amount of electromagnetic interference radiated and/or absorbed from the device/system. This balance, called Electromagnetic Compatibility (EMC) is the subject of directives (such as European Directive 89/336/EEC. Within Australia, EMC is stringently regulated and suppliers, manufacturers, importers and of all communication equipment are all required to comply with the Australian Communications and Media Authority (ACMA) regulations on EMC.

Essentially, EMI shielding allows transmission of desired frequencies, while absorbing or reflecting EMI energy that would otherwise cause interference. EMI shielding can be divided into four types depending on the frequency range and whether it is operating continuously or pulse. Electromagnetic Pulse (EMP) is a broadband frequency range, with high intensity short duration bursts of electromagnetic energy [d1988emp] akin to nuclear explosion and electric discharge. Within the EMI power spectrum, there are three key segments, namely:

- the range 1 - 100 KHz [8],
- the radio frequency range 100 KHz to 1GHz [3],
- Microwave and beyond frequency band now used in wireless LAN protocols (such as Bluetooth and the IEEE 802.11 specifications, that use microwaves in the 2.4 GHz band) [4][5]

The recent need for higher bandwidth in wireless communications has seen its frequency region shift from the radio wave region into the microwave region [2], namely the 5 GHz frequency using IEEE 802.11a standards [6] Unlicensed National Information Infrastructure (U-NII) use frequencies in the 5 GHz range, while Metropolitan area network (MAN) protocols, such as WiMAX (Worldwide Interoperability for Microwave Access) are based on standards such as IEEE 802.16 designed to operate between 2 to 11 GHz. Shielding devices currently used in mobile phones achieve attenuation levels around 40dB to 60dB according to commercial shielding companies.

With the standards for the next generation of mobile phones likely to move to even higher GHz frequencies [154], there is growing demand for cost-effective EMI shielding to help maintain mobile phone performance [9][143] in GHz microwave frequencies. Unfortunately, the materials currently used in EMI shielding will not be able to provide effective shielding for these future frequency increases as these materials tend to produce more losses as the frequency increases [11]. Providing more cost-effective ways of providing the required level of shielding performance is therefore likely to require investigation of a wider range of materials than those currently used in EMI shielding of mobile devices.

Current metal-based forms of EMI Shielding

Since around 2001, the mobile phone shielding has typically used a metal-based conductive coating patterned over a plastic material as shown in Figure 1A

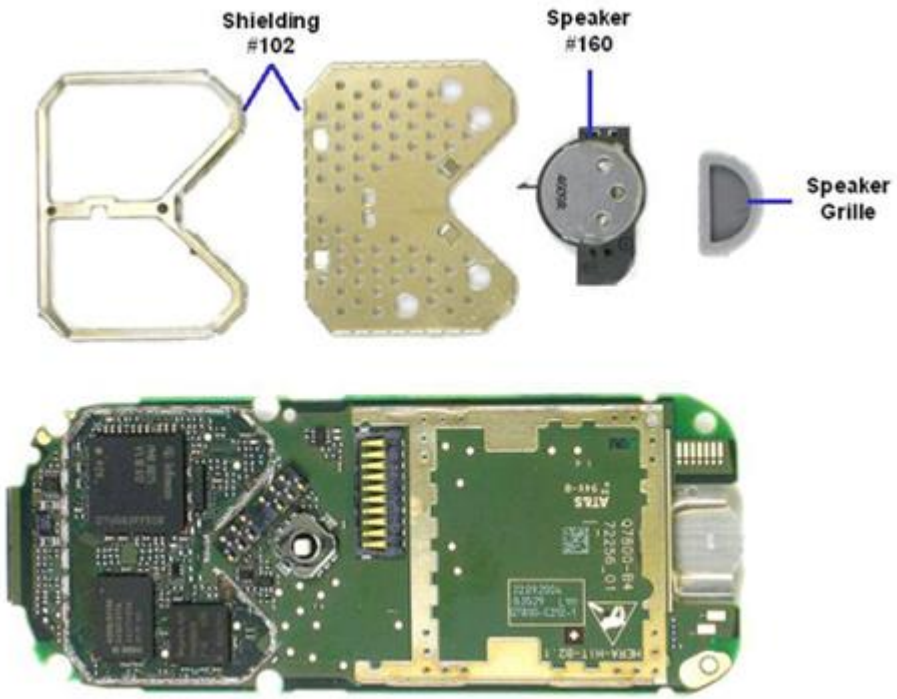

Figure 1-1 Shielding materials in a mobile phone (Curtsey IHS)

Figure 1-1 shows the ability of shielding materials in mobile phones to provide the required EMI shielding by reflecting the unwanted radiation within the frequency spectrum of 30-10 000 MHz [11]. The attenuation is spread over more than 10 GHz without concentrating on shielding a specific frequency band within that range.

The current EMI shielding technology uses metal shielding devices, which achieves an excellent shielding performance in terms of transmission loss, but adds to the cost and weight of mobile phones and as well as introducing problems of corrosion [8]. Manufacturers currently using metal composite polymers are seeking to deliver satisfactory phone performance whilst minimising both the use of costly metals and the weight of the phone.

Alternative EMI shielding materials

In addition to metal fibres, metal powders, aluminium structures, coatings, nickel and copper metalized fabrics, the required EMI shielding can also be achieved by using carbon to absorb unwanted radiation. Carbon fibre composites have already found widespread acceptance in the automotive and aerospace industries because compared to steel and other structural materials, these composites are strong, lightweight and less susceptible to corrosion. With carbon black now 20 times cheaper than nanocarbon and 7 times cheaper than carbon fibres, interest in the use of carbon is growing despite carbon shielding devices having problems relating to cost, sloughing, health and long-term environmental issues. [12] The paper's findings of the case studies concludes that the use of nanotubes can exist not only in the production stages, but also in the usage and disposal stages of nanotube applications. The chances and the shape of release is governed by the way CNT are used into the shielding material.

Other current choices for the shielding device material include polyacrylonitrile (PAN) nickel-coated reinforced polymers, and, more recently, nano-reinforced polymer composites (NRPCs). Polymeric materials are appealing, because they can

be manufactured to have structures that respond to the EM radiation in ways that depend on the chemical structure used, and the EM frequency applied. [13][14][15].

One class of polymer that is already being used in electronic materials and circuits and having some obvious potential for use in EMI shielding are the Intrinsic Conducting Polymers (ICPs), organic polymers that conduct electricity. Although these ICPs are sometimes called synthetic metals, [140] they weigh less than metals and do not corrode like metals. As they are manufactured rather than mined, production costs for ICPs can be expected to decrease over time.

While both the materials and the investigative methods adopted need to be affordable and cost-effective, it is important to be confident of the EMI data measured at a wide frequency range. There are many methods and standards that are currently used in testing shielding devices. The test depends on the type of shielding device, the material and their applications. Several existing standards such as ASTM D4935-99, ASTM ES7-83, MIL-STD-188-125A, IEEE-STD-299-1991, MIL-STD-461C, and MIL-STD-462 are available to characterise a specific scattering parameter S_{21} of shielding devices.

Scope for solutions based on new conductive materials

The increasing demand for cost-effective, environmentally-friendly and health-promoting EMI-shielding devices to protect the environment and workplace, strengthen the need for new conductors that are lightweight, chemically stable and more easily adapted to a wider range of environments. Irfan Ullah (2012)[16] investigated the use of Energy Saving Glass (ESG), in conjunction with Frequency Selective Surface (FSS) metal materials, in measuring and filtering microwave radiations. He recommended that an Electromagnetic Wave Interceptor (EWI), which is a special type of EMR attenuating polymer painted on the receiving side of the handset, that should also be installed in mobile phones.

One current trend is the use of conductive paint as a shielding device method because the spray can be easily applied, re-moulded and are cost effective. Water paints are increasingly used in building paints to decrease the amount of volatile organic compounds.

While common metal powders (silver, nickel) are among the most common conductive substances, dispersed metal particles get rusty in water-based paint. Non-metallic conductive fabrics, which do not corrode, have the potential for use in bedding, drapes, clothing, hats, windows, curtains, screen and tents to shield the user/wearer/environment from EM radiation. Polymer matrices incorporate the metal/carbon fibres and colour substances can produce a shielding device with good material properties.

Newer materials might also help to minimise some of the health and environmental concerns relating to the materials currently used to provide EMI shielding.

Aims and research questions

The overarching question this research study seeks to answer is whether ICPs, which can be tuned to the frequency spectrum between 1 - 6 GHz, have the potential to replace the current EMI shielding for mobile phones and Wi-Fi devices. Evidence that ICPs can enhance or replace the current shielding materials would promote the reduction or elimination of metals and carbon shielding materials in a new generation of mobile phones and Wi-Fi devices.

That question will be addressed by conducting a literature review, and undertaking simple experiments and computer modelling for a small sample of commercially available ICPs to see whether it is possible to use the ICPs rather than materials like aluminium/carbon in Wi-Fi devices and mobile phones. Given the cost and time constraints on this study, this requires selection and evaluation of suitable, affordable and readily available ICP materials from the range of now commercially available ICPs discussed in the recent literature in the Wi-Fi band between (1-6 GHz).

This thesis will explicitly address a number of subquestions (SQs) relating to the ability of ICPs to shield and alter the transmission losses of the Electromagnetic Radiation (ER) at the main desired Wi-Fi microwave frequency.

SQ1. Can simple experiments or simulations demonstrate whether ICPs can perform EMR shielding at least as well as the current forms of shielding in use?

Addressing this question requires:

- setting up experiments to measure the transmission loss of the ICP shielding devices and compare the ICP shielding devices with currently used conducting metals and microcarbon shielding devices. (Meaningful comparison of realistic simulation results requires that results obtained using samples of new polymer material be compared with the results with the current metal and carbon samples of the same size,
- exploring the relationship between the results obtained from the standard assessment methods requiring use of an expensive equipment and simpler experimental methods,
- using current affordable and commercially available simulation methods to make the assessment of the shielding potential of currently available and new ICPs simpler, speedier, more cost effective and more readily available, and
- exploring and comparing simple simulation methods and more complex simulation methods.

SQ2. Which materials and forms (solid, liquid, gel) of ICPs are most effective as EMR shielding?

Addressing this question requires determining whether liquid or solid forms of the selected ICPs are best suited for use in experiments assessing whether their shielding properties are comparable with the currently used conducting metals and microcarbon shielding devices.

SQ3. What other advantages might the ICPs confer?

Given the cost and time constraints on this study, work to address this question will be limited to:

- reviewing literature to identify some additional advantages that may accrue from use of ICPs,
- doing a few simple laboratory experiments relating to antibacterial properties of selected ICPs, and
- identifying further fruitful avenues of research relating to the shielding potential and other advantages of currently available and new ICPs.

Significance of this study

This study investigating whether ICPs in EMI shielding devices could offer lesser or comparable transmission losses than the materials currently in use provides a firm base for, more in-depth research regarding the future use of ICPs in shielding devices for mobile phones and Wi-Fi devices. Those new materials have the potential to perform as well or better than those currently used in EMI shielding devices, while better addressing the current cost, manufacturing, environmental and health concerns.

Interest in this application of ICPs was evident when the researcher reported some of the study's findings at the conferences listed below:

- W. Al-Shabib, S. W. Lachowicz, Modelling of intrinsic conducting polymer for Wi-Fi electromagnetic interference shielding Science and Information Conference (SAI), 2013 Publication Year: 2013, Page(s): 836 – 838 http://ieeeexplore.info/search/searchresult.jsp?newsearch=true&queryText=Al-shabib&.x=35&.y=2 , London, UK
- W. Al-Shabib, S. W. Lachowicz, Modelling of polyaniline for Wi-Fi Electromagnetic Interference shielding, Modeling, Simulation and Applied Optimization (ICMSAO), 2013, 5th International Conference on Digital Object Identifier: 10.1109/ICMSAO.2013.6552654 Publication Year: 2013, Page(s): 1 – 3
- W. Al-Shabib, S.W. Lachowicz, International Symposium and Exhibition on Electromagnetic Compatibility: APEMC 2013. Barton, A.C.T, Engineers

Australia, 22 May 2013: pages: 260-261, Intrinsic conducting polymers for Wi-Fi electromagnetic interference, Engineers Australia, Melbourne, EMC Australia branch, ISBN: 9781922107022.

- W. Al-Shabib, S.W. Lachowicz, O. Bass, Applications of Intrinsic Conducting Polymer for Wi-Fi Electromagnetic radiation environment pollution reduction, Abstract and Poster in the Science for the Environment 2013 Conference, AARUS University, AARUS, http://dce-conference.au.dk/scientific-content/abstracts/green-economy , Denmark.
- W.Al-Shabib, "Where Research Minds Meet " Abstract and Poster in the Health and Well being Symposium – organised by Dr Darren Gibson on 18th September 2013, ECU, Joondalup, Australia
- W.Al-Shabib, H. Daryoush, Z. Xie, X. Zhao, Identifying smart conducting materials for Wi-Fi electromagnetic interference shielding, International Zurich Symposium on Electromagnetic Compatibility - EMC Asia, 2012, DOI: 10.1109/APEMC.2012.6237899.

Thesis outline

The thesis is divided into the eight chapters outlined below.

Chapter 1 has provided the background to this study and introduced the aims, objectives and the significance of this research.

Chapter 2 reviews the literature, to identify:

- the frequencies of interest for electromagnetic shielding,
- current EMI shielding materials and the properties needed for an effective EMI shielding material,
- evidence that ICPs are worth investigating for use in EMI shielding devices that absorb rather than reflect the unwanted EMR,
- methods that could be used to evaluate the suitability of ICP materials for use in EMI shielding devices,
- the key ICPs to use in both the laboratory experiments and in simulations intended to realistically model the expected transmission loss, and
- metals and microcarbon shielding devices which could be compared with ICPs through laboratory experiments and simulations.

Chapter 3 is Methodology, which outlines:

- the selection and acquisition/preparation of ICPs to use in both the laboratory experiments and in simulations intended to realistically model the expected transmission loss,
- the selection and acquisition of the metals and microcarbon shielding devices to be compared with those ICPs through laboratory experiments),
- the selection of experimental methods to compare the performance of ICPs and metals and microcarbon shielding devices,
- the design and construction of the selected shielding devices and equipment to be used in the experiments and in simulation models to quantitatively assess each shielding device,
- the selection of modelling methods, and
- comparison of experimental and simulation results.

Chapter 4 presents the results of narrowband experiments and wideband experiments to assess transmission loss coefficients for each shielding device and assess the benefits of using ICPs to replace the current materials used to provide EMI shielding for mobile phones and Wi-Fi devices. It discusses the significance of the measurement methods used.

Chapter 5 presents the results of:

- constructing simulation models to assess the transmission loss and generate the necessary data for comparing the modelling and experimental results,
- developing computational models for both the narrowband and wideband experiments to characterise the shielding devices and obtain the simulated transmission loss properties of each shielding device created to enable the ICPs to be compared with other materials used for EMI shielding, and
- comparing the computational shielding model results with the experimental results.

Chapter 6 compares the experimental results with the verified simulation results.

Chapter 7 presents the results of laboratory experiments investigating the impact of the ICPs and other materials currently used in the mobile phone industry on the

culturing of a common bacteria. It also canvasses scope for further work on the environmental and health impacts of increased use of ICPS.

Chapter 8 draws conclusions and discusses scope for further work to enhance the development and application of ICP-based shielding devices for mobile phone and Wi-Fi devices.

Conclusion

This chapter has provided the background to this study and introduced the study's aims and research questions and explained the significance of this research. The next chapter reviews the literature relevant to the research questions this chapter has outlined.

Chapter 2 LITERATURE REVIEW

Introduction

This chapter reviews the literature relevant to the research questions outlined in the previous chapter. It explores:

- the frequencies of interest for electromagnetic shielding,
- current EMI shielding materials and the properties needed for an effective EMI shielding material,
- why ICPs are worth investigating for use in EMI shielding devices,
- methods that could be used to evaluate the suitability of ICP materials for use in EMI shielding devices,
- the key ICPs to use in both the laboratory experiments and in simulations intended to realistically model the expected transmission loss, and
- metals and microcarbon shielding devices which could be compared with ICPs through laboratory experiments and simulations.

EMI shielding properties

EMI shielding or the ability of a device to protect against unwanted frequencies, relies on electrical and mechanical properties such as conductivity, permittivity impedance, heat and chemical resistance, insulation, dielectric dissipation and moisture absorption. The material properties most relevant to its response to microwave frequencies are permittivity and conductivity, as permeability is not influential in the frequency range 1 - 6 GHz. Absolute permittivity is the measure of the material's response impedance in a vacuum to the electromagnetic field impedance on that frequency.

Published results for current materials commonly used in the EMI shielding include air, low-density polyethylene (LDPE) sheet with thickness of 1.5 mm, PET with thickness of 0.18 mm, aluminium foil with thickness of 0.015mm, and 15% weight VGCNF liquid crystal polymer (LCP) sheet with thickness of 1.25 mm. In general, highly conductive materials are considered suitable for EMI shielding.

Table 2-1. Comparison of electrical conductivity

]

Material	Conductivity (s/m)
Copper	$6.4x10^5$
Steel	$6.3x10^5$
Aluminum	$4.0x10^4$
Stainless steel	$1.8x10^4$
Graphite	$0.05.x10^4$

Electric conductivity depicts the relationship between the current density and the electric field strength. There are three types of electric conductivities, Dc conductivity, AC conductivity (and semiconductor conductivity. Table 2-1 shows the dc conductivity of 5 types of common shielding materials. The AC conductivity or the unidirectional flow of electric charge is the flow of charge that depends on the frequency of the electromagnetic radiation, while the semiconductor conductivity varies under different voltages and applied current [17].

The electric conductivity of the materials is also EM frequency dependent; Luo and Chung [2][18] [19][[20][21] show that graphite will increase its conductivity at 1-2 GHz much more than that in Table-2.1 at a dc conductivity to provide a higher EMI shielding than copper and that a polymer with nanotube carbon can also provide excellent EMI shielding at higher frequencies. At microwave frequencies, the material will, however, have capacitance-dominated impedance as the microwave frequency increase the capacitance dominated impedance decrease. [22]
Chung [145] used the skin depth to show that nanocarbon composite is an effective shielding device, especially after electroplating with nickel.
By contrast, all neat polymer materials are insulators, they do not reflect or absorb EM radiation. Polymers and rubbers are non-conducting materials, transparent to EMR. Light-weight conjugated polymer materials with electrical conductivity comparable to that metals can, however, be produced from non-conductive polymer materials via the process of doping, where a polymer is made to accept or donate electron or transfer charges [23]. Unlike metals, which reflect all EMR frequencies, these conductive polymers can be tuned to the mobile phone frequency to limit outside interference and incoming radiation. EMI shielding performance of metals

The high reflection loss and low absorption loss of aluminium give its high shielding effectiveness and stability. Depending on the frequency and network analyser, the incident electromagnetic energy, and type of materials mixed with the aluminium foil, can shield microwave frequencies from 40dB to more than 80dB.

The website (www.chomerics.com) of Chomerics, a company specialising in mobile phone shielding, lists two materials which reduce the unwanted signals to a mobile phone at wideband frequencies. One identified as CHO-SEAL 1310 is all metal, consisting of silver coated with copper [24], while the other identified as CHO-SEAL S6304 is pure silver or hybrid coatings [25] as shown in figure 2-1. In mobile phones, these two types of CHO-SEAL provide more than 60 dB EMI shielding attenuation from 200 MHz to 10 GHz.

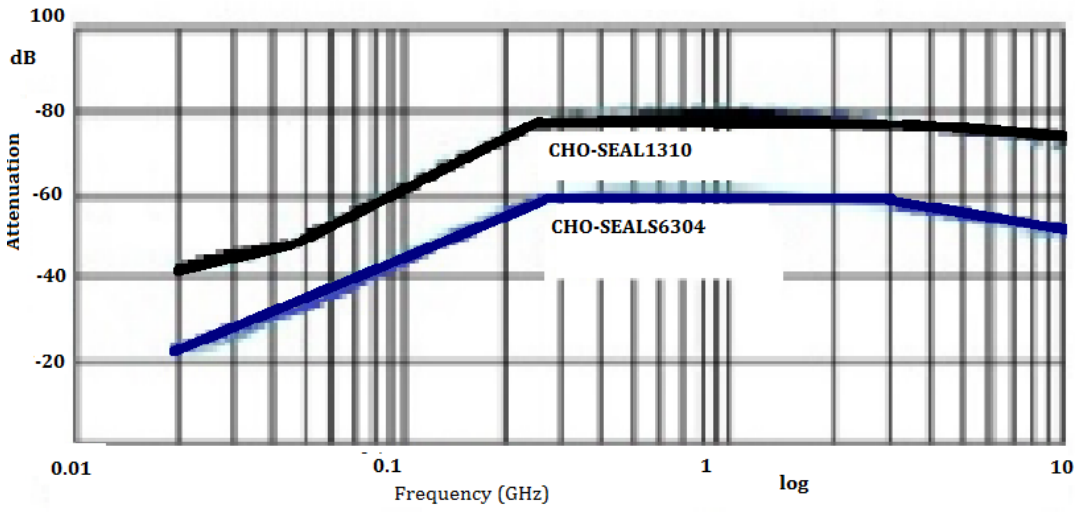

Figure 2-1 Current shielding materials that are used in mobile phone

While metals appear to be ideal materials for EMI shielding, they have several disadvantages including high cost, high reflection, heavy weight, susceptibility to corrosion, and a tendency to crack with use due to their brittle nature. [21][26] Corrosion of metal-based conductors is the important factor, which leads to a non-linear effect on the receiver and this affects the EMI shielding specifications. The corrosion on the transmitters and receivers creates a rusty bolt effect that has been the cause of intermodulation products since it was researched in the 1970s. [150]

EMI shielding performance of composite polymers

One category of conductive polymers are composite polymers, which are polymers of non-conductive material coated with conductive metals. This coating is produced by manually or robotically spraying copper, nickel or zinc paints onto non-conductive material. Electrolytic plating and vacuum metal techniques are required to make the minerals adhere to the polymer.

The many advantages of using composite polymers in EMI shielding relate to cost reduction, weight reduction, ease of production, ability to improve the device in terms of colour, surface softness and the product shape complexity and because polymer materials are more acceptable than other metals. Mobile phones, laptop computers and other wireless networks (LAN) use the EMI shielding method despite its disadvantages in terms of flexibility, heavy weight, corrosion and difficulty in varying the tuning of both the shielding efficiency and frequency spectrum. [151] The novel metal SnO_2 Nanowires (NWs) [34], was studied because the nanowires differs from normal wires because electrons in nanowires are quantum and therefore the electrons occupy different energy levels than the energy level of bulk materials and can be used to enhance the microwave absorption properties, of special materials rather than its reflective properties. Their research measured the complex permittivity and permeability of the SnO2 NWs/paraffin in a frequency range of 0.1 – 18 GHz [28].

EMI shielding performance of carbon nanotube (CNT) and polymer

The second generation shielding devices are the non-metal Carbon Nanotubes (CNTs) devices, which many researchers prefer for EM shielding applications. CNTs have a much larger possible length-to-diameter ratio than polymers, and they exhibit very high strength and flexibility, as well as good conductivity. The CNT wire glue, used to make solder-free connections and to support the latest advances in nano-carbon technology, is used as 0.25 mm as a coating on the glass substrate.

A low volume fraction of Carbon Nanotube (CNT) in a non-conductive polymer provides conductivity without changing the polymer properties. CNT ranks among the strongest material known, acts as a semiconductor or conductor depending on the way the original sheet of graphene is rolled. CNT has excellent applications in electronic devices and sensors, and it is used for fuel cells and batteries.

Carbon Nanotube (CNT) and other conductive fillers in non-conducting polymers have been investigated for EMI shielding. By comparison with the metal commonly used in EMI shielding, CNT has the advantages of low cost [29], low weight, high-performance and thinness. CNT can also be used with a polymer binder layer to enhance performance [30], increase adhesion, abrasion resistance, and provide flexible broad range conductivity of (10-10^7 S/cm). Such an approach provides uniform and linear conductance [32], excellent transparency [33], and good adhesion durability, and good chemical resistance, ease of patterning, outstanding microwave, and shielding efficiency for electromagnetic interference applications. CNT does, however, have some disadvantages. All three of the main methods of synthesising CNT, namely arc discharge, laser ablation [34], chemical vapour deposition, are very expensive [35]. It is also difficult to controlling the dopant amount and difficult to synthesise particular types and shapes of nanotube, especially high quality, very long (1mm or more) CNT [36][37].

EMI shielding performance of graphene-polymer composites

Another form of electromagnetic radiation shielding uses graphene and polymer. According to [147] a high Shielding Effectiveness (SE) can be obtained using less than 0.1 weight % loading of grapheme. As Graphene is an atomic-scale honeycomb lattice made of carbon atoms, it contains less carbon. However this offers the same disadvantages as the carbon nanotube described in the previous section.

Why ICPs are worth investigating for use in EMI shielding devices

The third generation of shielding materials is a selected novel group based on 100% stable polymers called Intrinsic Conducting Polymers (ICPs). The electronics industry

already makes use of this type of conducting polymer in applications such as (LED)[39], plastic wires [40], signal processing [41], batteries [42], solar conversion [43], optical devices [44], displays and photovoltaic cells[45].

The three types of these materials that can be used to shield a mobile phone from EMR are:

- Composite Polymers, made conductive by the addition of nanofibres (carbon black, metals),
- Doped Intrinsic Conducting Polymers (ICPs), and
- ICPs made conductive by an electrolytic process, in which charge is transported by dissolved ions using ionic conductive polymers. That type works on a different principle from the normal electronic conductivity of metals.

Each of the categories listed above will now be discussed in turn.

Intrinsic Conducting Polymers (ICPs)

The main ICPs materials used in the electronics industry are polythiophene, polyacetylene, Polypyrrole (PPy), polyaniline (PAni) and Poly(3-4-ethylenedioxythiophene) (PEDOT:PSS).

These ICPs have three main applications [46] to date:

- as conductors to replace copper-based electronic circuits [47],
- as active components in applications which require sensing [48]. For example in a gas hazardous environment. Also windows and mirrors that become reflective when an electric current is applied, [49], and
- in antistatic coating applied to electronics components [50]. The (PEDOT-PSS) product Clevios P commercialised by Bayer AG laboratory has been extensively used as an antistatic coating. [141][148]

The many advantages of using ICPs include:

- ability to adjust and even reverse the amount of doping and hence the conductivity of the polymer,

- the ICP synthesis can be a very easy and inexpensive process. ICPs can be prepared by either an aqueous two-phase system [51] or liquid-liquid extraction. According to [51], the polymerization process reportedly takes less than 1 hour, but its conductivity reached 2.76 S cm - 1 at 25 °C,
- ICPs have good electromagnetic properties, both their permittivity and dielectric loss decrease with increase in frequency,
- ICPs exhibit a dominant shielding characteristic of absorption rather reflection like metals [52], and
- ICPs are environmentally stable that depends on the rates of renewable resource for manufacturing and not mining, also pollution creation, and there is little non-renewable resource used in the manufacturing that can keep manufacturing ICPs indefinitely. The resources for metals and carbon cannot be continued indefinitely therefore the current shielding products are not sustainable.
- ICPs are highly resistant to heat [28].
- because ICPs resist corrosion, ICP materials are cheaper to maintain than metals.

The disadvantages of using ICPs to provide an electromagnetic shielding device are:

- their unstable conductivity in room temperature, particularly for doped ICP materials [54][53],
- some ICP materials are extremely sensitive to water vapor and air in controlled spaces [56],
- ICP materials are not soluble in ordinary solvents, are difficult to melt and soften and cannot be treated like other thermoplastic polymers,
- it is commercially difficult to find any high conductivity ICP that does not require use of metals or CNT to increase its conductivity,
- poor mechanical properties mean other metals or CNT are required to enhance the mechanical properties of the ICPs,
- ICPs are sensitive to changing environmental conditions and can change their colour and conductivity in response to environmental conditions, and
- ICP materials have not been used for EM shielding in mobile phones.

The key ICPs to assess for use in EMI shielding devices

While a wide variety of ICPs have potential value for use in EMI shielding, they are not all equally suitable. Doped polyacetylene for example has a very high level of conductivity, but is so unstable when exposed to air and vapour that it has no potential for use as an EM shielding device. The properties, current uses and of some specific ICPs with potential for use in EMI shielding will now be considered in turn.

Polyaniline (PAni)

The ICP material that appears best suited to the third-generation of EM shielding devices is Polyaniline (PAni), which can be made to conduct electric currents without the addition of conductive (minerals or carbon) substances and therefore can be classified as an ICP. PAni comes in different forms depending on the level of dopent used.

A method for preparation of PAni in an organic medium could specifically involve the synthesis of poly-2, 6-di (thiophen-2-yl) aniline (PDOTA), poly-aniline/2,6-di-(tion-2-yl) aniline (1:1) (CAD2), poly-2, 5-dimethoxyaniline/2, 6-di(thiophen-2-yl)aniline (1:1) (COO), poly-N1-(2,6-di(thiophen-2-yl)phenyl)benzene-1,4-diamine (PAFDOTA) and poly-2,6-dibromoaniline (PDOBA)[16]. One type of PAni material is a non-conductive powder with the properties summarised in the table below.

Table 2-2 Key properties of PAni

Molecular weight	Average molecular weight > 15,000
Particle size	3-100 m
Surface area	5-20 m***2***/g
Conductivity	2-4 S/cm
Melting point	> 300°C (lit)
Density	1.36 g/mL at 25°C
Bulk density	18.8 lb/cu.ft.

Due to its ability to mix with both organic and inorganic molecular components, PAni has been widely researched [58]. Looking specifically at PAni polymer blends shows:

- PAni is the most environmentally stable of the ICPs with regard to temperature, humidity and force,
- the materials for making PAni are readily available in any chemical laboratory. The electrochemical polymerisation of thiophene (to produce a conducting polymer when it is oxidised) is a common method for synthesis of PAni,
- a range of metal-catalysed coupling reactions can be used to produce PAni.
- PAni is available from several reliable chemical manufacturers including Sigma-Aldrich, Ormecon, Fibron, Eeonyx and Panipol [42,59],
- PAni can be fabricated with other polymers to produce a structure with good mechanical properties (e. g. strength and flexibility) and can be doped with materials that form a conductive network inside the polymer [60]. PAni nanofibre can for example be synthesised by using electrochemical methods [61],
- PAni has already gained it wide commercial application LEDs, and rechargeable batteries due to its special mechanism for accepting doping that changes its conductive properties [62],
- PAni polymer blends may be made with conductivity between 10^{-11} and 10^{-4} S/m High specific conductivity at high volume fraction saturation concentration, therefore good shielding against electromagnetic interference (EMI),[63]
- PAni is good for very high frequencies such as 2 - 8 GHz, the magnetic field are not effective as permeability is very low (near 1). This will give the

freedom to use any metal material, [63] and therefore the focus of this research is on the electric field.

- PAni was reported to form EM shielding with carbon nanotubes (CN),[64] and
- Electro-polymerization can be used to apply a thin film (10nm up to 100 nm) of PAni.[65]

A conducting film was produced from PANI with $SinO_2$. [66] Another conducting film was made by using a hybrid of dodecylbenzene sulfonic acid-doped polyaniline (DBSA-PANI) and 3-glycidoxypropyltrimethoxysilane (GPTMS) through sol–gel route [8]. As they reported in [146], for PAni blends with room-temperature conductivities in excess of 1,000 S/cm, resistivity decreases monotonically as the temperature is lowered down to 5K. This makes this ICP material a good replacement for metal.

A PAni material synthesised by conventional oxidative polymerisation was reported [16] as having a permittivity and conductivity useful in electromagnetic shielding. Further research is still ongoing on different blending and doping methods. The study of the dielectric properties of polyaniline nano ferrite (PANI-Fe2O3) found it possessed a conductivity of 2.5 S/cm. These composites were prepared using chemical oxidative polymerization [68].

Those researchers investigated the EMI shielding performance of PAni as a film blended with polystyrene by testing for EMI shielding performance for blends doped with different percentages of PAni. They found the best EMI shielding effectiveness (more than 58.59 dB) was achieved with a 50% loading of PAni. PAni shielding effectiveness was reported to be more than 60dB when PAni was used with ABS (Acrylonitrile Butadiene Styrene).[51][70]

The EMI shielding level was reported to change when the material is doped with benzene sulfonic acid or other protonic acid (fatty acid). Changing the relative amount of PAni changes the frequency-dependent parameter, real permittivity,

imaginary permittivity, tan and the A.C conductivity and those parameters as shown in Figure 2-1.

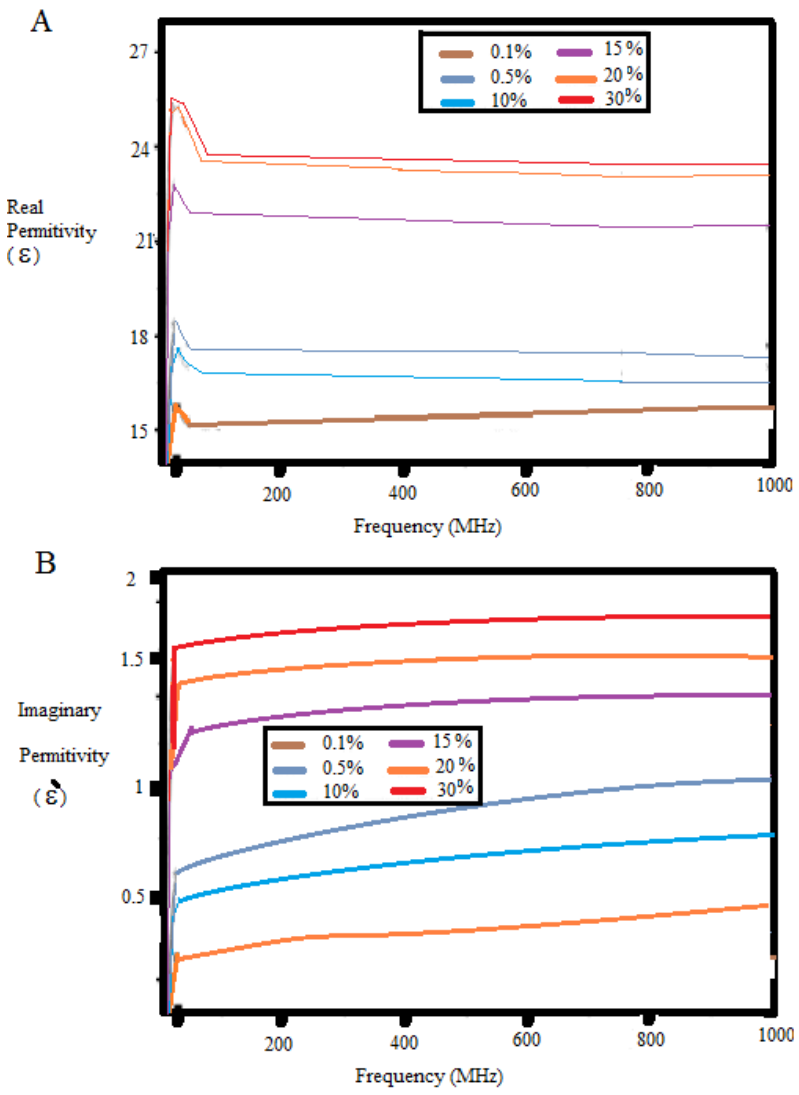

Figure 2-2. Variation of real and imaginary permittivity with frequency

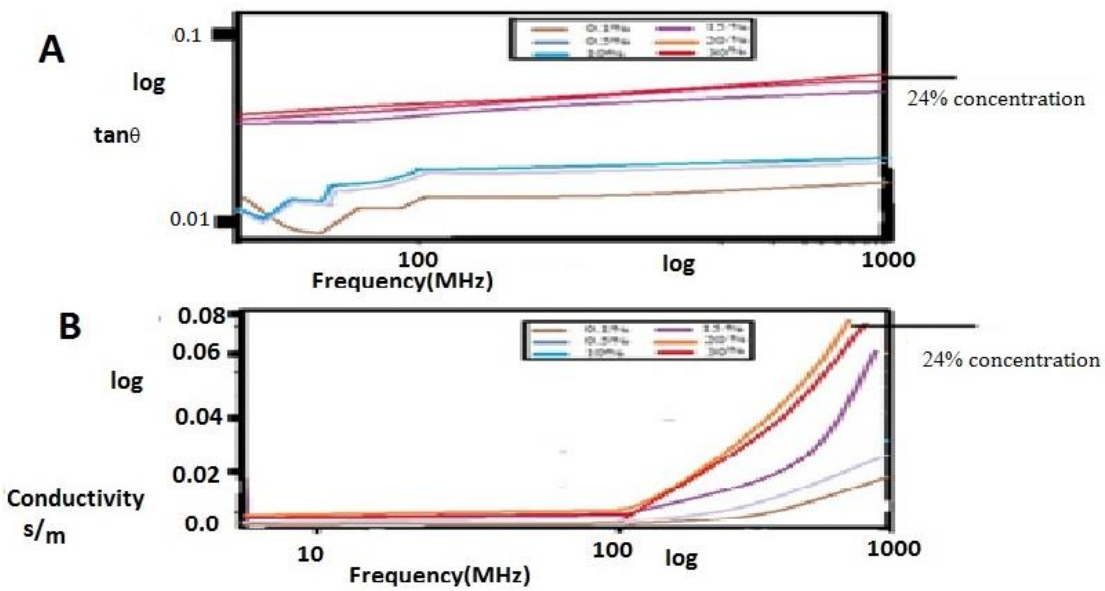

Figure 2-3. Variation of tan θ and AC conductivity with frequency (Polymer Journal (2010) 42, pp 546-554

The Results in figure 2-2 and figure 2-3 show PAni Composites with a concentration of more than 24% produce a polymer material that reduces the EM transmission that will make the polymer suitable for EMI shielding. For example the undoped PAni has a conductivity of 6.28×10^{-9} S/m, while conductivities of 4.60×10^{-5} S/m can be achieved by doping to 4% and $2.3\text{x}10^{-3}$ while trying to reach a target of $3.50\times10^{+7}$S/m at 20° for aluminium and depends heavily on the temperature coefficient. [149]

Poly(3-4-ethylenedioxythiophene) (PEDOT:PSS)

PEDOT:PSS has very good thermal stability, which can be used as a liquid solution [71] and has a high transparency in the visible frequency range [153]. It is available commercially from Heraeus and AGFA [72].

The benefits of using PEDOT in the industry are excellent stability [144], large area processing, low cost [73], flexibility in using spin coater or dip coating. A team at the Australian Centre of Excellence for Electromaterials Science at Monash University in Melbourne reported that PEDOT:PSS can be used as cathode for fuel cells that

convert hydrogen and oxygen. A spin coater of Laurell WS-650-23NPP was used to try create a shielding device using the spin coating method.

Polypyrrole (PPy)

Polypyrrole (PPy) has been used in a vast range of applications which includes biosensors[74][57], gas sensors [158], wires, microactuators, antielectrostatic coatings, solid electrolytic capacitors, electrochromic windows and displays, packaging, polymeric batteries, electronic devices, and functional membranes. PPy is already used in a vast range of applications which includes bio-sensors [75] [76], gas sensors [77], wires [78], micro-actuators [79], anti-electrostatic coatings [59], solid electrolytic capacitor [80], electrochemical windows and displays, packaging, polymeric batteries, and electronic devices. PPy is also used for radar-absorbing materials (RAM) [28], camouflage netting [81], antennas and functional membranes. These diverse applications of PPy suggest PPy is worth investigating as an EMI shielding device

Like PAni, Polypyrrole (PPy) also has good environmental stability that depends on the rates of renewable resources for manufacturing and not mining. There is little non-renewable resources used in the manufacturing industry that can keep manufacturing PPy and PAni indefinitely, they are easy to produce from chemical compounds through chemical reaction, low costs of production [28] and higher conductivity compared to the rest of ICPs and have the great potential to replace metals and carbon. [82].
PPy has a promising future in EM shielding because of its high shielding effectiveness (SE), good mechanical properties, ability to withstand harmful external environment influences (e.g. oxidation, corrosion), durability, and homogeneity.

While both PAni and PEDS:PSS materials are available in liquid form, it is difficult to obtain liquid PPy. PPy can, however, be coated on an organic polymer such as polyester. The typical substrate for coating PPy includes woven and nonwoven material, felts and knits of polyester, nylon, glass, quartz, spandex, polyolens, and

aramids. · Conducting fabrics can provide an absorption dominant interaction with the microwave radiation. The ability to use a nonwoven fabric to form a shield with PPy [28] [83] enhances the attractiveness of using PPy in EM shielding devices.

EeonTex produce a PPy material by treating a conductive textile such as the polyester fibres with a PPy material in a unique aqueous process. EeonTex fabrics can be custom-made, designed for the desired electrical resistance, thickness, porosity, strength, and stretchability. Depending on the particular base fabric, EeonTex fabrics can be made to have surface resistivity between 10 ohm/sq and 10 billion ohm/sq. A PPy-coated textile foam sourced from Eeonyx Corporation [84] offers many advantages including flexibility, adaptability to different shapes, light weight and low cost. However, the major advantages are that it can be used with metal flakes and carbon fillers. [85]

The data below was supplied by EeonTex for EeonFelt — F/PF-PI-PV-10/100[3] which is a polyester felt coated with PPy. This ICP material has enhanced stability and retardation, able to eliminate Si from dust SiO_2 [86][143], clear electrostatic charges [87], and has a variety of other applications. The surface resistivity is between 3 and 40/sq

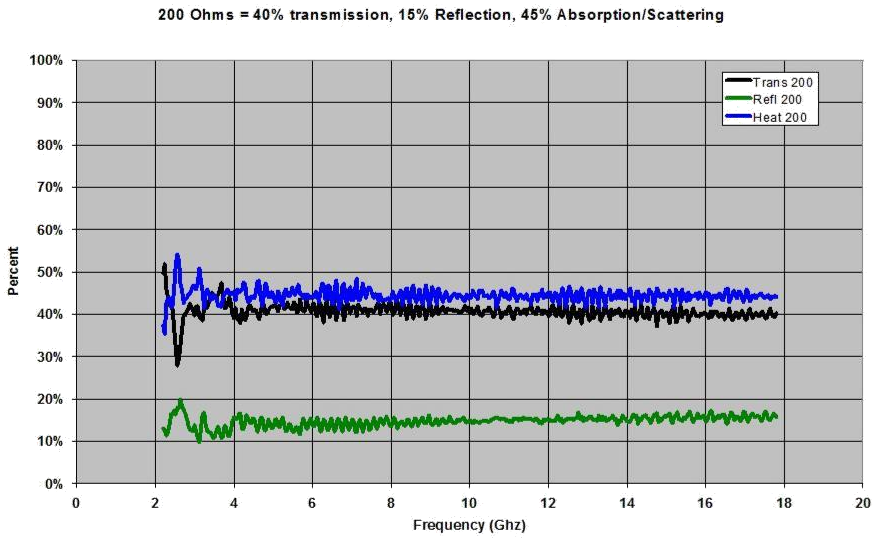

Figure 2-4. Transmission characteristics of PPY 200 Ω.m^2 of nonwoven felt (EeonTex PPy nonwoven shielding device data)

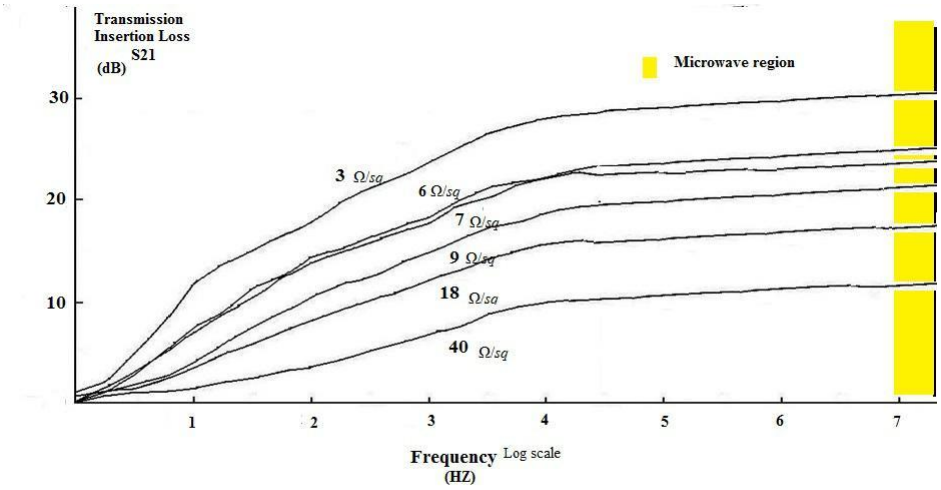

Figure 2-5. Transmission loss vs frequency for various surface resistivity between 3 to 40 Ω/sq

The data supplied for the PPY-coated fibre shows this type of nonwoven fabric ICP material can provide a sufficient level of shielding to warrant comparison with metal and carbon materials and stability at the desired microwave frequencies of (1-6) GHz.

Standards for testing shielding devices

Many methods and standards are currently used in the testing of shielding devices. The type of shielding device, the material and their applications influence the test to be used. The existing standards including ASTM D4935-99, ASTM ES7-83, MIL-STD-188-125A, IEEE-STD-299-1991, MIL-STD-461C, and MIL-STD-462 characterise the scattering parameter (S_{21}) of shielding devices. As the current testing methods have limited dynamic range and relatively large specimen dimensions, these standards may be impractical and inadequate for testing new materials for use in EMI shielding.

As newer forms of shielding devices may require materials that are rare or expensive at the time of exploratory testing, the specimen size required for exploratory testing of the transmission loss property needs to be kept as small as possible. Using the ASTM D4935-99 standard coaxial holder to measure SE is regarded as convenient because it requires relatively small specimens required for testing in unlike the military standards, which require 46cm square samples [88]. The ASTM D4935-99 standard test device is a flanged circular coaxial transmission line, with internal conical shape that secures the shielding device and forms a capacitor load between the transmitter and receiver. Unfortunately, it has a complex shape and is difficult to manufacture.

Measuring and comparing EMI shielding effectiveness

The two common ways to measure the material's shielding are:

- Shielding Effectiveness (SE) [89], and
- Scattering Parameters (S-Parameters)[90].

Shielding Effectiveness (SE) is the ratio of the transmitted Electrical Field (E_t) or Magnetic Field (H) after hitting the shield, to the incident Electric Field (E_i) before the attenuation of the electric or/and magnetic field due to the reflection and absorption of the electric field or magnetic field.

The rations are shown in the following equations:

SE=20.log(E_t/E_i) for electric field or

SE =20.log(H_t/H_i) for magnetic field

Where E and H are the electric and magnetic fields and the subscripts (t) and (i) refer (t) the transmitted and (i)for incident waves.

As the electromagnetic wave shielding for the electric wave E_i hitting the material in Figure 2-6

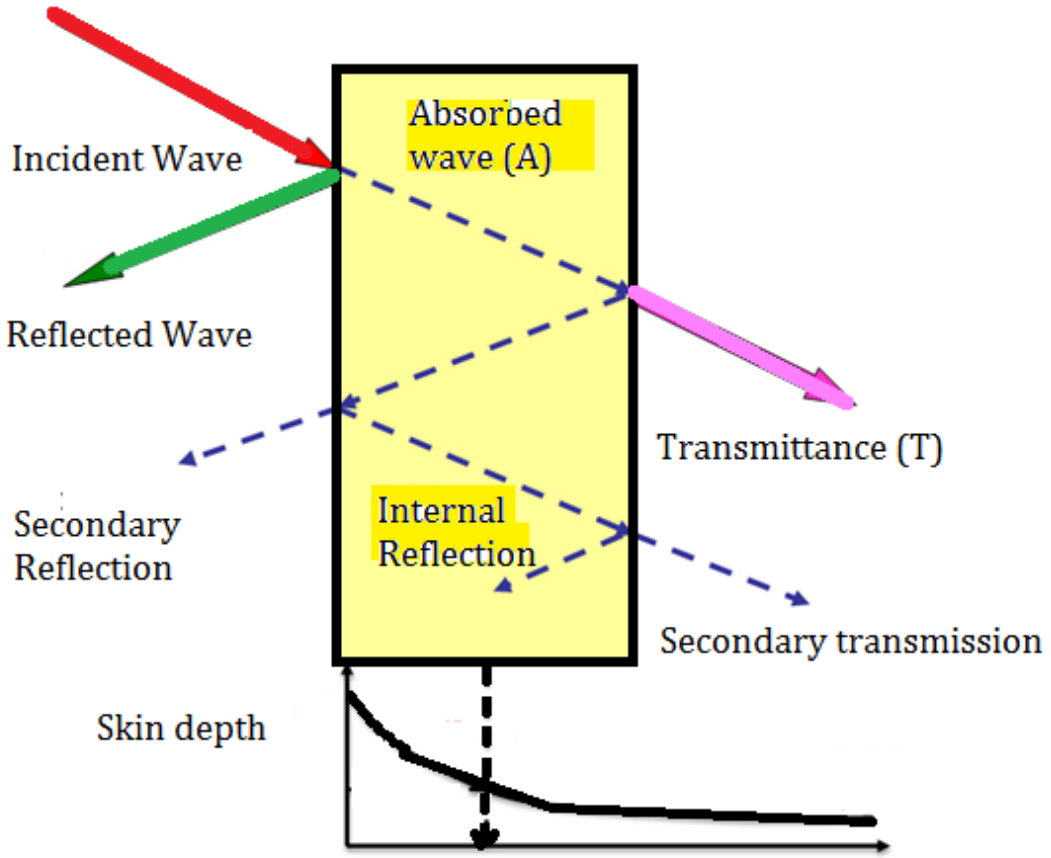

Figure 2.6 Shielding Effectiveness (SE)

Figure 2.6 shows the Shielding Effectiveness (SE) that has three components. Those three components are shown in three arrows coloured in pink, green and red. Those components indicate the amount of absorption E_A which is the amount of absorption Absorption(A) , E_r that is the Reflection(R) and E_t is the amount of electric field transmitted (T) , the shielding effectiveness (SE) is the ratio of the RF energy incident on E_i one side of the shield to the RF energy emerged from the other side of the shield E_t expressed in decibels (dB).

For an infinitely good conductor, the shielding effectiveness will indicate the two terms, of the Absorption loss and the Reflection loss. In this thesis the main focus is on the ratio of the RF energy incident on the shielding device to RF energy transmitted from the shielding device.

Calculates the plane wave shielding effectiveness of different conductors using the equation [160]:

$$S.E = \frac{\eta_0}{4\eta_{Device}} + 20\log e^{d/\delta} = E_r(dB) + E_A(dB)$$

Where η is intrinsic impedance, d is the thickness of the shielding device and δ is the conductivity of the shielding device

The above equation is only suitable for very thin thicknesses that are less than the wavelength, the wavelength we are dealing with is around 12cm.

Although the SE analysis is an easier way to compare shielding devices but in ICPs shielding devices the conductivity, thickness and the skin depth are of a different nature. It is concluded that another analysis that is more appropriate to group all the shielding devices under one test.

The skin depth in figure 2-6 relies on the conductor, dielectric properties of the material that is considered in the simulation software as part of Maxwell's equations.

$$\delta = \sqrt{2\rho / 2\pi f \mu_R \mu_0}$$

Where δ is skin depth *p* is resistivity (Ω-metres) μ is magnetic permeability = μ_0. μ_r, f is the frequency (Hz),π is 22/7, μ_0 is 4 π.10^{-7} $\Omega^{-1}m^{-1}$, μ_R varies depending on the materials type. The skin depth is used in the Maxwell simulation software but the above equation, various spread sheets available with tables of current bulk materials on (http://www.rfcafe.com/references/calculators/skin-depth-calculator.htm), those spread sheets are updated regularly and therefore skin depth analysis can be used to make a simple spread sheet model to compare all types of materials.

In the frequency range 1GHz to 6GHz, transmission line will suffer from the skin depth effect and therefore waveguide is used where the dominant field can be controlled and made to have the electric field as a dominant mode [91] and [142].

The Absorption loss (A) is affected by the frequency, conductivity and thickness of the material. The Absorption loss (A) is directly proportional to the thickness of the shield expressed in skin depths [21] and it is linked to S_{12} and S_{21}.

The reflection loss (R), is the attenuation due to the reflection of the electromagnetic wave at the interfaces of the material, the value of R is related to S_{11} and S_{22}. The reflection loss is independent of the thickness of the material, but it is related to the intrinsic impedance inside the material and the intrinsic impedance of free space [92], while the absorption loss is related to the thickness of the conducting material and that is directly related to the skin depths.

The skin depth governs the minimum thickness of shielding devices for metal. Figure 2-7 below shows the variation of minimum thickness that is required for aluminium and copper as the frequency of the electromagnetic radiation increases, the thickness of the shielding devices decreases and a very thin layer of shielding metal are needed in the experiments.

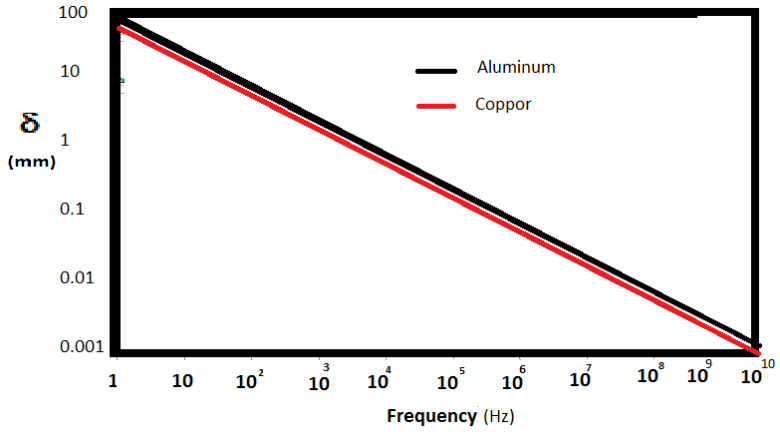

Figure 2-7 the variation of skin depth with the frequency

The scattering parameters are of more significance for any investigation when using intrinsic conducting polymers without the addition of any high conductive material. Scattering Parameters (S) show the response of a linear system. The S parameters of

one system can be compared to the response of another system or can be cascaded with another system and the changes to the response of the two systems.
The S parameters calculation is a great tool to be applied to passive devices only.
A full mathematical excel tool for detailed calculation of s- parameters can be found in http://www.microwaves101.com/encyclopedia/Sparameterspreadsheet.cfm and that provides a detailed analytical spreadsheet tool for calculating all the S-parameters.

Vector Network Analyser equipment (VNA) can be used to form a mathematical matrix showing how the EM wave propagates through a multi-port system. The S parameters are values in a matrix that accurately describe the values of a device that is used as a box without looking into what the contents of the box or its material properties as in the SE value that take into account the material properties of the whole system. The values of the S parameters are used magnitudes for a given frequency and this value relates the output voltage to the input voltage.

Electromagnetic shielding testing methods

The commonly available methods for testing the shielding of EMI interference and comparing effectiveness of the new conducting materials with the current materials are:

- flanged coaxial cable method [92],
- Faraday cage method [7],
- anechoic chamber [93], and
- OEMI method.[94].

Each of these methods will now be discussed in more detail.

Flanged coaxial cable method

As shown in figure 2-8 below, the flanged coaxial cable method uses a two port device to measure the shielding effectiveness of a thin material sheet. The flanged coaxial cable methods are used first without sample material under test [157] and

then the material is inserted and the reduction of the signal is shown on the display. The VNA performs the measurement at specific frequencies.

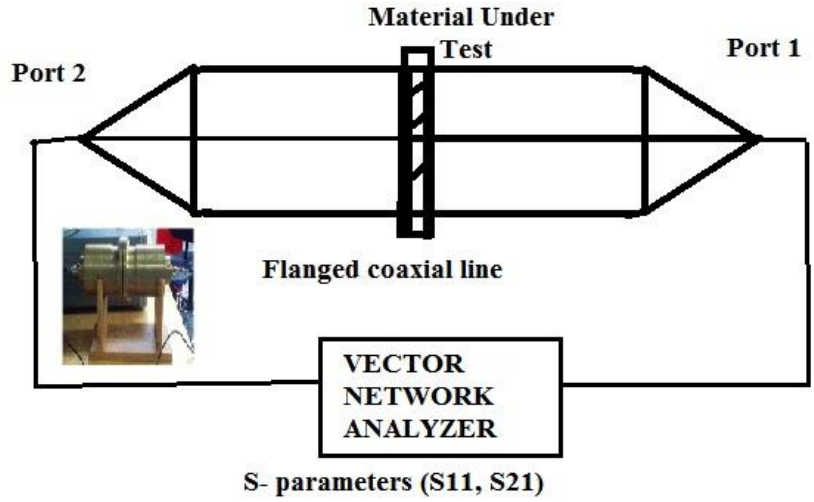

Figure 2-8. Flanged coaxial cable method

The major advantages of the flanged coaxial cable method are:

- that the coaxial fixture is a standard device,
- only a small sample of the test material is required,
- the SE values obtained are similar in different parts of the world,
- the measured SE values are sorted into SE for reflection and SE for transmitted components,
- this method has the higher dynamic range for SE values than other methods, and
- the method permits evaluation of both the near field and far field shielding, and the results are repeatable for the material ranking in the shielding tables.

Disadvantages of the flanged coaxial cable method include:

- use of this method is mainly limited to the United States,
- method requires expensive military grade equipment, and
- results may not be representative of real-size object in real world situations.

Faraday cage method

The Faraday cage method can be used to compare the measurements of various test samples to check their shielding capabilities. [38] In this method, an external electrical field is propagated through a cage or box made of good conductive material. The charges along the surface rearrange themselves outside the box, while the field inside cancels itself.

In this method, the test sample is placed on one side of metal box fitted with an internal receiving antenna. A transmitting antenna is placed outside the box. The network analyser transmits and receives the signals by the antenna, and is then stored as data files that can be analysed for the shielding quality of the sample.

The major advantages of the Faraday Cage method are that it is:

- cheap and easy to construct, and
- good for small to medium-size test samples.

The disadvantages of Faraday cage method include:

- difficulty of achieving a good electrical contact between test specimens and the shielded box [95],
- the method has a limited range of frequency of about 500 MHz, and
- the results from different laboratories show poor correlation [96].

Anechoic chamber

An anechoic chamber is a special chamber designed for a specific range of frequencies and these chambers vary in size [97]. Anechoic chambers [155] are designed to test the antenna and other devices, and shielding material without interference from outside the chamber's electromagnetic radiation or reflections from inside the chamber [93]. This method has been used to test, and to gauge the level of EMI.

The major advantages of the anechoic chamber method are:

- the testing of devices or shielding materials yields shielding parameters that conform to Australian Communications and Media Authority (ACMA) standards, and
- this method of testing has been used to clarify the doubts about the disadvantages of the other methods and to give assurance that the results are reliable and reproducible.

The disadvantages of the anechoic chamber method include:

- expense of constructing and using the anechoic chamber,
- scarcity of anechoic chambers (Curtin University hosts the only such facility in Western Australia),
- difficulties often encountered in gaining permission to access these rare facilities,
- difficulty moving test samples to the anechoic chamber facility,
- difficulty repositioning test samples or network analysers within the anechoic chamber, and
- limitations on the size of the samples that can be tested within the anechoic chamber.

Open EMI method

An Open EMI (OEMI) method is enabling comparison of EMI shielding systems and was reported in [98]. This method was used to evaluate clothing fabrics that served as radiation detecting devices.

This method tests the overall shielding system and compares it to another shielding device. Rather than isolating the device from the electromagnetic radiation, this method measures the actual electromagnetic radiation that a device encounters, measures the amount of transmission attenuated by the shielding device, estimates the amount of reduction of the original electromagnetic radiation and then measures the device's response to a controlled source of EMR.

The open to EMI experiment can be conducted in an ordinary communication laboratory by placing a device under test in the middle of an aluminium screen

190cm (height) x 115cm (wide) that was available in the communications laboratory. The Vector Network Analyser (VNA) at the centre of the experiment measures the transmission loss of the Shielding Device Under Test (SDUT) with the unique scattering parameters S_{21}, S_{12} and reflection loss parameters S_{11}, S_{22}. The forward scattered $S_{11}(t)$, and back $S_{21}(t)$ scattered time-domain profiles are uniquely related to the intrinsic properties of the material tested. The appropriate interpretation of the parameters S_{21} (t) and S_{11} (t) relates to the desired frequency.

The VNA generates the S-parameters measurement results in the form of the S parameters versus frequency data files. These S-parameters measurements determine how well the SDUT reduces the EM radiations compared to S-parameters measurements when the SDUT is removed. The calibration provides equal transmission S_{21}, and reflection S_{12} parameters should not differ significantly.

This method requires its users to:

- set the frequency range, and set the number of data points across the frequency range that S_{21} is experimentally measured,
- measure the area on the aluminum screen that the SDUT occupies, and
- calibrate the VNA in order to eliminate the losses in the coaxial cables and also perform standard calibration for reflection and transmission parameters for the two-port VNA.

The major advantages of this OEMI method are:

- enables non-contact measurement of the shielding device transmission loss in a real-world EM-polluted environment,
- suitable for making microwave frequency measurements
- simple to operate and interpret,
- very cost-effective compared to the expensive anechoic chamber or coaxial methods, and
- accuracy can be improved by taking advantage of ongoing developments in network analysis equipment to enable isolation of unwanted radiation and selection of desired frequencies.

The major disadvantages of open EM method are that it:

- has rarely been used,
- requires preparation of measurable shielding devices from materials to be tested,
- needs the shielding device under test (SDUT) to be placed in a tightly EM sealed space inside the hole of a large, flat aluminum screen,
- needs care to minimise EM reflection on the edges of the SDUT's border with the aluminum screen as well as the multiple reflections between antenna and surface of SDUT, and the diffraction effects at the edges of the SDUT, and
- needs to have its results validated in terms of more widely used method(s) such as use of anechoic chamber.

Computer modelling of electromagnetic shielding systems

Computer modelling is an essential tool for characterisation and designing of electromagnetic shielding system in order to comply with electromagnetic compatibility requirements [99]. There are already many analytical modeling tools including web-based calculators and apps for solving EMC design problems. The EM computer modelling techniques can be divided into three categories:

- lumped circuit modelling,
- transmission mine modelling, and
- modelling using full wave Maxwell's equations.

Each of these computer modelling techniques will now be discussed in turn.

Lumped circuit modelling

In this modelling method, discrete components (resistor, capacitor and inductance) are used to form an equivalent circuit. This type of modelling suffers from the increase of the resistance with the frequency and it is mainly suitable for 1D modelling [100].

Transmission line modelling

Transmission lines carry microwave frequencies signals to different places. Transmission lines can be used to model and calculate impedance and other

propagation characteristics. The model analyses transmission attenuation in terms of lumped circuit components such as impedance, inductance and capacitance [101]. Using different frequencies and different lengths for a transmission line enables derivation of an equation describing the wave propagation within the transmission line.

In transmission line modelling, increasing the frequency [102] produces a huge increase in the resistance of the conductors. This tends to increase the attenuation of the transmitted signal along the transmission line. This skin effect [103] starts to increase the resistance of any thin conducting layers within the square root of the frequency.

This old and established method is only suitable for 2D simulations. It does not rely on the properties of the object under test.

Modelling with full wave Maxwell's equations

All software modelling of microwave transmission [104] uses full wave Maxwell's equations. The various modelling methods based Maxwell's equations differ only in the extent to which they simplify calculations undertaken and the interpretation of the results obtained. The extent of these simplifications affects the price of the modelling package, the time to solve the equations, the desired dimensions of the model, the bandwidth that is needed to be simulated.

Other issues relevant to EMI shielding materials

In addition to the concerns about the performance of mobile phones and other Wi-FI devices, there are four other key concerns arising from the increased use of current shielding devices:

- concerns about environmental disposal of current mobile phones that contain dangerous materials,
- concerns about the extensive use of chemicals that are used and mining excavations of current shielding devices,

- concerns about human health problems linked to increased exposure to electromagnetic emissions, given that Wi-Fi and mobile phone devices are increasing in speed and design complexity and more people are routinely using those devices throughout their day-to-day activities, and
- concerns about the heightened risk of spreading bacterial infections through contaminated mobile phones and other Wi-Fi devices. The growing human dependence on and attachment to these devices increases the risk of the devices becoming contaminated by harmful bacteria that can remain infective for many hours.

Environmental concerns

Concerns about safe and appropriate disposal of shielding materials relate to long term environmental effects [105][106][143], cost and future availability. There are also persistent concerns relating to the environmental and social impacts created by the extraction of the metals now in use and the production and their disposal of mobile phones and Wi-Fi devices [107][108]. The mining of those metals incurs significant economic, environmental and social costs such as environmental damage from mining, quarrying and processing, transport and waste disposal operations. Those operations can all damage habitats, use scarce water, create noise and pollute air, land and water with toxic chemicals. Social impacts can include damage to the social fabric resulting from miners being required to live away from their families while engaged in their mining work.

Within a mobile phone, the key areas that contain dangerous materials are:

1. the covers and keypads, that contain metals like chromium, brominate in the protective chemical coating to protect the cover
2. the LED screen, which contains liquid crystals (mercury),
3. circuit board, which contains lead and mercury,
4. batteries, which contains cadmium, nickel and lithium.

EU countries have banned at least 6 materials (lead, cadmium, mercury, hexavalent chromium, Polybrominated biphenyls (PBB) and Polybrominated diphenyl ethers (PBDE). Another EU regulation called Waste Electric and Electronics Equipment

(WEEE) directive that has been introduced is to make it compulsory for the producers of mobile phones to return the phone and discard safely all waste materials that they produce.[109] The objective of those directives is to make the design of electronics devices environmentally friendly. Leading makers in EU countries, including Motorola, LG, Sony Ericsson and Philips, have all implemented eco-design aspects. EU Restriction of Hazardous Substances (RoHS) directive has been extended into the companies production lines, including reducing the amount of hazardous substances used in their products.

The current mobile phone shielding materials contains approximately 40% metal plastic composites and/or 40% nanocarbon plus polymers in composites. Despite manufacturers of mobile phones implementing environmentally-friendly designs, [110], the life cycle of the current mobile phone produces environmental impacts relating to the materials and energy used in manufacturing and processing the mobile phone. Disposal of mobile phones can release dangerous chemicals into the groundwater systems and soils. Although each mobile phone contains only a very tiny amount of toxic chemicals, disposal of billions of mobile phones can release large amounts of these chemicals.

Concerns regarding human health

Despite a lack of any clear evidence that radiation emitted by mobile phones poses a health hazard for humans, concerns about their impact on human health [111, 112, 113] persist. There are well-reported concerns about prolonged exposure to EM fields and pulses associated with mobile phones, heightening the risk of developing leukaemia, breast cancer and other cancers, of producing neurodegenerative disorders, miscarriages and impaired male fertility [114].

A recent study [115] investigating the influence of the electromagnetic field of mobile phone frequency exposure on health outcomes found half of the children and nearly every adolescent owned a mobile phone, which was used only for short durations per day. Although the measured exposure was far below the current

ICNIRP reference levels, the most reported chronic symptom in phone-using children and adolescents was fatigue [115]. Some multidisciplinary reports investigating the impact of mobile devices on general happiness, mental abilities and behavioural issues, cautioned expectant mothers about using mobile phones during pregnancy [116]. Another study investigating brain tumour risk and mobile phone use in children and adolescents strongly recommended monitoring for brain tumours.

The strength of these concerns has led companies to develop devices to reduce the harmful radiation such as:

- special earpieces to overcome any need to hold mobile phones close to a human head while in use [117],
- special EM shields claimed to block EM harmful radiations when placed inside the mobile phones, and
- the Aires Shield device made of a silicon-based microprocessor said to neutralise harmful EM radiation from a mobile phone. Its manufacturer claims that EM radiation could cause brain cancer and other mental illnesses.

While the long-standing health concerns highlighted above all relate to long-term health impacts, there is also growing interest in investigating key short-term health impacts of using mobile devices. Concerns about heightened risk of spreading bacterial infections through contaminated mobile phones and other Wi-Fi devices parallel concerns about increasing bacterial resistance to antibiotics. [118]

The average human body contains about ten times more bacterial cells than the amount of human cells and most of these bacteria are beneficial to human health. Pathogenic bacteria can, however, cause incredible damage to a human body and may even result in human death. Different strains of a single species of bacteria can also have quite different effects on human health.

The much-studied bacterial species *Escherichia coli (E. coli)* commonly found in faeces has one particularly virulent strain. The enterohemorrhagic stereotype of this bacterium known as *Escherichia coli* O157 or *E. coli* O157 causes illness, typically

through consumption of food contaminated by unwashed hands. Infection by this strain of E. coli may lead to diarrhoea, and later may result into kidney failure. [119]

Transfer of the *E. coli* bacteria by touch to much-used mobile phones that do not receive regular cleaning can facilitate the spread of diarrhoea, extreme abdominal cramping and pain, nausea and vomiting, and in extreme cases, death. In 2011, researchers from the London School of Hygiene & Tropical Medicine and Queen Mary, [120] University of London reported that 15% of mobile phones tested in the U.K. had traces of *E. coli* bacteria from faecal matter. The hands and mobile phone samples were collected from 12 cities in Britain. In each city, 390 samples were taken from mobile phones and hands. Then the samples were analysed in the laboratory to identify the bacteria and other germs. The findings showed that despite 95% of people washing their hands with soap, 92% of mobile phones and 82% of hands had bacteria on them, and moreover 16% of hands and 16% of mobile phones were found to harbor the dangerous *E. coli* bacteria that causes infection and diarrhoea. The people who had bacteria on their hands were three times as likely to have bacteria on their mobile phones [120]. The outer shielding of a mobile phone is particularly conducive to bacteria growth because the mobile phone heats up as it is used. As infrequent cleaning of mobile phones heightens the risk of bacterial contamination. Health authorities now need to consider publishing policies and guidance to address the hygiene of mobile phones [121] especially in hospitals [122].

Conclusion

This chapter reviewed the literature relevant to the research questions outlined in the previous chapter. The next chapter outlines the methodology selected to address those research questions.

Chapter 3. Methodology

Introduction

In the light of the literature reviewed in the previous chapter, this chapter outlines the methodology selected to address the research questions stated in Chapter 1.

Choice of materials

As the previous chapter has shown, a wide variety of ICPs have potential to be used for EMI shielding for communication. The requirement for communication shielding devices is to reduce the EMR energy that reflect away by try to get devices that absorb the EMR energy rather than reflecting it.

Given the time and financial constraints on this study, it was necessary to limit the investigation of Intrinsic Conducting Polymer (ICP) materials to those the literature review had revealed to be:

- affordable,
- accessible within the time allocated for the study,
- suitable for investigation with low-cost methods that could for the most part be conducted using facilities available to the researcher at Edith Cowan University (ECU),
- suitable for testing in form (liquid, gel, coating, foam) as a shielding device in terms of stability, conductivity and thermal sensitivity, and
- able to be tested and modelled in ways comparable to the metals and carbon nanotubes already used in the EMI shielding of mobile phones and other Wi-Fi devices,

PPY

Felt shielding devices do not require any additional coating. The one meter square of PPY material acquired for this project had a uniform coated surface, a resistance surface resistivity of 200Ω/sq band with transmission loss (S_{21}) percentage loss is as shown in figure 2.4. The suitability of the supplied PPY nonwoven microfibre was

investigated using two methods, the Shielding Effectiveness (SE) parameters or transmission loss (S_{21}) method.

Preparation/acquisition of PAni

As noted in the previous chapter, doping can be used to produce a more conductive, doped form of PAni. When this researcher did initially attempt to using the limited laboratory facilities available convert the inexpensive powder form of PAni into a more conductive, doped form, the result proved so unsatisfactory. The doped PAni powder had low conductivity, which was not maintained after the liquid dried. Work on the powder form was abandoned in favour of liquid forms of PAni.

PAni can be used from two sources, Polyaniline (PAni) salt and Polyaniline base that was purchased from Sigma-Aldrich Pty. Ltd. The PAni salt was a ready-made solution mixture of polyaniline emeraldine base (different powder weight) plus 2% Xylenes and the PAni base powder polyaniline was an emeraldine base dissolved in different types of solvents. Two solvents used for doped polyaniline powder, were 1-Methyl-2-pyrrolidinone [123], and nitric acid to dissolve the powder.

This researcher purchased a small quantity of a very expensive form of PAni doped with BSA (benzene sulfonic acid) (product number 650013) from Sigma Aldrich. The other form of liquid PAni acquired was polyaniline salt already dispersed in xylene (2-5 wt %).

Selecting a coating method for PAni and PEDOT:PSS

A clear choice had to be made as to whether to use spin coat or dip coat for making shielding device from liquid. Initial consideration of factors such as cost, need for specialised equipment, ease of use, control of the coating thickness and process, consistency of the coatings suggested spin coating would be the preferred coating method. A choice of shielding devices on glass substrates, were suitable for spin or dip coat. The dip coat is an easier method and does not require expensive spin

coating machine however the thickness cannot be accurately controlled and measured.

Spin coating liquid shielding devices

Spin coating a glass substrate involves spreading it with a thin layer of an ICP in liquid form and then repeating the process as required to increase the thickness of the coating. A PAni shielding device can be made using a controlled spin coating method [124] to create thicknesses, enabling investigation of the relationship between the thickness of the coating and the transmission, absorption and reflection parameters. The purpose of this step is to provide a layer of the conductive PAni or PEDOT:PSS material so that its electromagnetic shielding transmission loss (S_{21}) could be tested.

As the spin coating method is preferred for measurement of thin layer shielding device S-parameters, the researcher attempted to use spin coating to make shielding devices using liquid versions of PAni and PEDOT:PSS. A spin coating device made by Laurell (model WS-6505) was used to coat substrates with liquid PAni and liquid PEDOT:PSS. The process involved cleaning a glass slide, positioning the cleaned slide in the centre of the spin coater, then using a pipette to apply a drop of either of PAni or PEDOT:PSS to the centre of substrate holder. The substrate holder was then rotated at 500 rpm for 60 seconds and substrate sample dried inside a vacuum chamber.

Attempting to produce a more conductive, doped form of PAni using the limited laboratory facilities available created significant problems relating to:

- agglomeration, preventing a smooth coating,
- difficulty achieving a proper dispersion with the solvent, and
- inconsistent conductivity of the coating.

Working with PAni in a liquid form eliminated the problems of dispersion and agglomeration. The initial glass substrate slide made as a shielding device was

76.2 x 25.4 mm with a 1mm thickness and was coated with a thin layer of PAni and PEDOT:PSS. Although the spin coating process was a success, the transmission loss results for this size of device were not encouraging, because of its small size of less than one wavelength and a larger substrate was impossible to achieve.

The glass substrate was then enlarged to the available glass substrate of 15cm x 15 cm x 3mm, but the spin coater could not hold a glass substrate of this size. The spin coating machine therefore needed to be large enough to take a 15cm x 15 cm glass substrate and any spin coating processor suitable for this task would have a diameter up to 300mm or a 230mm square substrate capability.

Unfortunately the spin coating process is designed for small slides, larger size spin coaters are not readily available devices. To overcome difficulties experienced with spin coating, the researcher switched to producing shielding devices dip coated with PAni or PEDOT:PSS.

Dip coating

Dip coating is a simple and inexpensive process, which involves immersing a substrate into a reservoir of solution for 5 minutes so that the substrate is completely covered with a thin layer on one side, and then withdrawing the substrate from the liquid PAni solution. This coating method relies on a combination of the gravity-induced draining of liquid solution [125] and evaporation of solvent [126].

One distinguishing feature of the dip-coating technique [127] and one that makes it particularly useful with mobile phone or Wi-Fi devices, is its ready adaptability to different shapes (e.g. onto a plate, cylinder, or irregular shaped object). Dip coating does however produce more variable results than spin coating in terms of thickness of the coating and hence the consistency of conductivity.

Measuring the thickness of the dip-coated layer

The thickness of a shielding device with a thin layer of liquid on a substrate can be measured by:

- non-contact methods including Optical Coherence Tomography (OCT) and Ellipsometry, or
- contact methods (microscope, prolometry, and digital Vernier caliper).

Other methods to measure the thickness for a shielding device with a thin layer of liquid on a substrate include laser triangulation, digital holography, Atomic Force Microscopy (AFM) and interferometry. This study sought simple, inexpensive solutions that would be applicable to all the shielding devices and not too time consuming.

Ellipsometry

This is a non-contact optical device that transmits light from a light source and detects that light by a detector and the data from the reflection and the phase are converted into thickness. As the maximum layer for thickness determination is typically about 100 nm, this method is only useful for a thin film and could not be applied to all the shielding devices. This method therefore had to be rejected.

Prolometry

This thickness measurement method is a contact method using a stylus that moves across the surface, measures the original substrate and then moves to the thin layer. As the stylus photometry method requires a reference, it is not suitable for measuring a liquid paint surface. This method therefore had to be rejected

OCT

Optical Coherence Tomography (OCT) is used by opticians in biomedical imaging [80], and in art applications requiring both micrometer accuracy and depth resolution up to a millimeter. All of these methods could be used for accurate

measuring of the thickness of very tiny objects, but are time consuming and expensive. This method therefore had to be rejected.

Microscope method

In this method, a basic confocal microscope is calibrated and the thickness is compared to a slide of known thickness. In more advanced microscopes, a graticule focuses the microscope system on the differences between the two surfaces. This focusing system and the digital scale allow non-contact, highly accurate measurements of differences between the heights of the two surfaces. This method was rejected because of its complexity compared to use of the digital Vernier caliper.

Digital Vernier caliper

The digital Vernier caliper has a series of rectangular plates etched into a copper frame that stretches the length of the bar and is usually covered by a taped scale. Mounted above this in the movable metal jaw, that is a similarly plated slider board. When these rectangular boxes align and misalign, signals sent to an electronic chip within the calliper's case generate the readings on the visual display. As this simple, reliable, well-established method has a measuring range of 0-150 mm, resolution of 0.01 and accuracy of 0:02mm, it was clearly the most appropriate method to use to measure the thickness of the dip-coated layer in all the shielding devices. This method was therefore used for measurement of both the PAni and PEDOT:PSS shielding devices.

Figure 3-1: Digital Vernier caliper

Devices and setups

As no single device or experiment setup could meet all these requirements, the study required:

- a number of different experimental devices and setups, and
- open to EMI and anechoic chamber measurements at narrowband and wideband frequencies, and
- a range of modeling simulations.

In all the experiments undertaken, the ICP-based shielding devices tested differed thicknesses due to the ICP material used for the coating and the method used to achieve the coating method. The SDUTs contained a thin layer of:

- either PAni (dip coated on the surface of the 150mm x 150mm glass substrate,
- or PE-DOT:PSS (0.25mm thickness dip coated on the surface of the 150mm x 150mm glass substrate, or
- or polypropylene fabric coated on a 150mm x 150mm substrate of NW170-PI-20-PV3, a polyester non-woven fabric, containing both natural polyesters and a few biodegradable synthetic polyester.

OEMI calibration procedure

The OEMI method was chosen to measure the S_{21} parameter of the shielding devices coated with PAni, PEDOT:PSS, PPy and compare them to the established materials in the current mobile phone shielding devices. As discussed in Chapter 2, this method places the shielding device under test between two antennas (microwave horns for wideband measurements, and Yagi-Uda antennas for narrowband measurements, that measures the transmission/reflection loss from the shielding device. The narrowband is used to focus measurement around the Wi-Fi frequency of 2.45 GHz, use this initial study for a simple 2D model to simulate the results and also test the speed of the software for meshing and materials properties.

Figure 3-2 shows the procedure that was followed to obtain the S-parameters. The main source that was used to obtain the S_{21} from this procedure is the VNA. Also it is noted that the calibration of the two ports were important in the procedure and was time consumed to reduce all the reflection and unwanted interference. The

outcome of the OEMI procedure is the S_{21}. The experiments focussed on measuring the S-parameters generated as results of the calibration procedure. At first the focus of the narrowband experiment is the Wi-Fi frequency interaction with ICP materials and more specifically on the S_{21} data because the transmission data is the one that penetrates through the shielding device to reach the mobile devices. This transmission loss parameter S_{21} is a measure that can be used to compare different types of ICP devices with the currently available conducting materials used for EMI shielding of mobile phones and Wi-Fi devices.

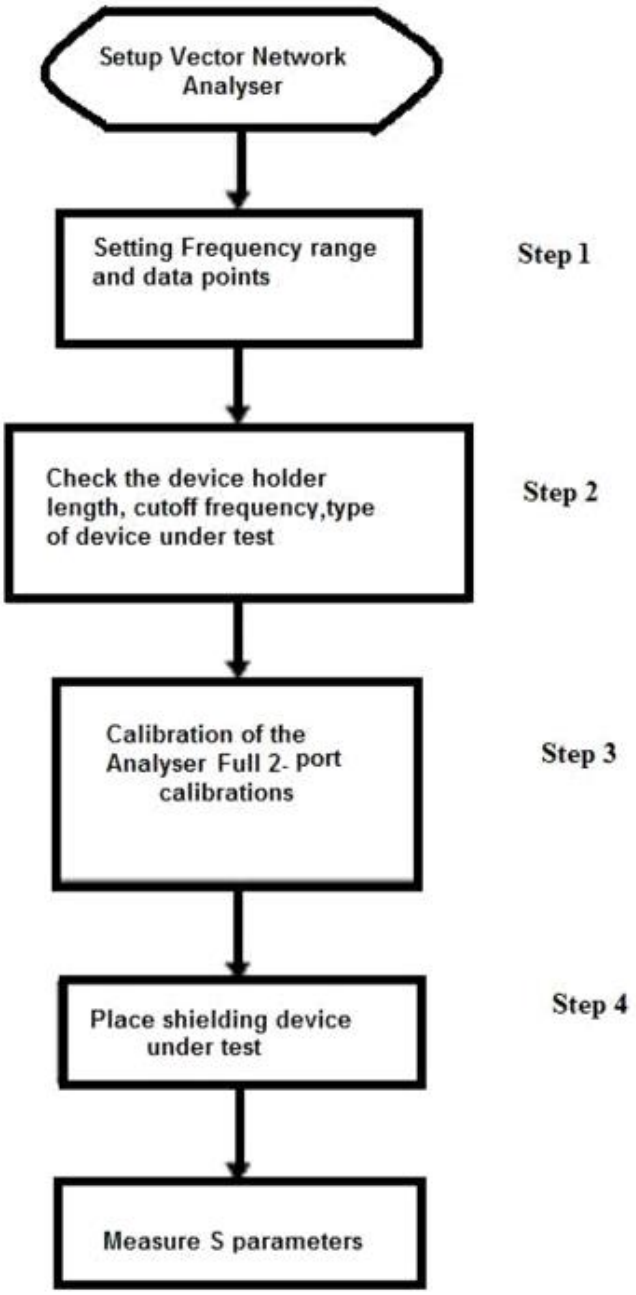

Figure 3-2. OEMI calibration procedure

S-parameter analysis

The S-parameter measure is the outcome of the calibration procedure figure 3.2 and it is a standard analysis that is used in RF and microwave modelling and in all linear operating frequency system modelling. The S-parameters have both a real and imaginary number, the value of S-parameters depend upon the type of material used

in the shielding device, the characteristic impedance of the source, the load used to measure it, and the frequency measurements. If the transmitting and receiving antenna's bandwidth changes, then the S-parameters change accordingly. Likewise, a change in the load or source impedance also impacts on the S-parameters. This S-parameter measure is a simple way to compare an EM shielding device.

The analysis method is governed by the following equation

$$\begin{pmatrix} b1 \\ b2 \end{pmatrix} = \begin{pmatrix} S11 & S12 \\ S21 & S22 \end{pmatrix} x \begin{pmatrix} a1 \\ a2 \end{pmatrix} \qquad \textbf{Equation 3.1}$$

Where:

$S_{11}=b_1/a_1$

$S_{22}=b_2/a_1$

$S_{21}=b_2/a_1$

$S_{12}=b_1/a_2$

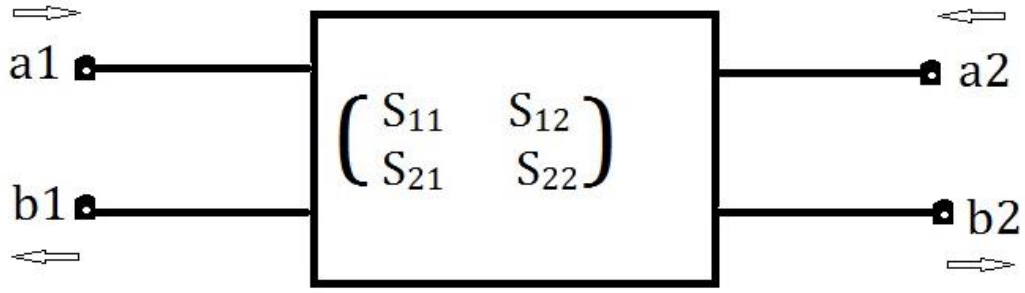

Figure 3-3 General two port characterisation with Z_0 impedance

The (a) and (b) in equation 3.1 of the S parameters measurements are vectors but in this research it was not necessary to keep the angle for the vectors of the S-parameters, and magnitude only S-parameters, was used to simplify the results. It is assumed that the vector network analyser (VNA) generates the magnitude.

S-parameter magnitudes are presented in logarithmic based decibels (dB). Because S-parameters are complex voltage ratios.

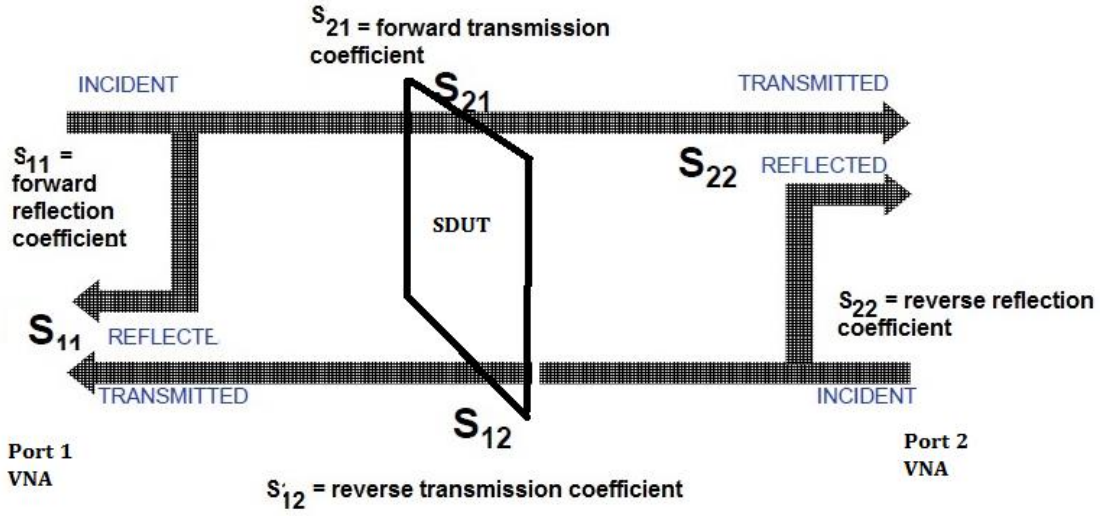

Figure 3-4 S-parameters method

Figure 3-3 shows the two port characterisation of equation 3.1. The incident EM radiation at port 1 is (a***1***) in figure 3-4, incident EM radiation at port 2 is (a***2***) in figure 3-4 , exiting EM radiation from either port 1 is (b***1***) and the incident EM radiation on port 2 is (a***2***) the exiting EM radiation from port 2 is (b***2***). The first step is to terminate port 2 with the characteristic impedance so that b***2*** and a***2*** are zero, and then terminate port 1 with the characteristic impedance so that a***1*** and b***1*** are zero. Reflection coefficient, S***21*** describes the forward transmission coefficient (responding port 1st).

The relevant equation (3-1) assumes a matrix symmetrical about its diagonal. Parameters along the diagonal, S_{11} and S_{22}, of the S-matrix are referred to as reflection coefficients, because they refer to the reflection occurring at a single port. The other diagonal S-parameters, S_{12} and S_{21}, are referred to as transmission coefficients, because they refer to what happens to EM radiation transmitted from port 1 to port 2 and vise versa.

The procedure used to obtain the S_{21} is as follows. The VNA allows computer controlled frequency tracking of both narrowband and the wideband experiments. In 1 second, the VNA transmits a signal to sweep the SDUT with the required frequency range and obtains the important parameter S_{21}. The VNA generates a RF signal that

passes through Port 1, which is connected to the transmitting antenna focused on the SDUT. The SDUT will generally reflect some fraction, b***1***, of the incident wave amplitude, a***1***. The VNA serves to separate and measure both the incident wave amplitude (a***1***) and the reflected wave amplitude (b***1)***.

The coefficients S_{21} and S_{12} are calculated and may have the same value. When the network analyser is a 2-port analyser, $S_{21} = S_{12}$ and changing the input antenna and output antenna ports does not change the transmission properties. The key scattering parameter S_{21} can then be used to compare the EM shielding devices.

OEMI measurements of SDUT

This study used a VNA two ports instrument, Agilest E5071C (9 kHz to 8.5 GHz) to measure the parameters for the SDUT. Prior to making any scattering parameters measurements, the VNA had be calibrated by following the above standard calibration procedure of making short, open and matched circuit termination to eliminate the VNA and other RF radiations in the laboratory.

Two calibration methods were used. The first calibration method used with VNA (EC5071C), was a manual method described in the manufacturer website link (http://cp.literature.agilent.com/litweb/pdf/5989-5478EN.pdf). This type of calibration requires use of the calibration kit 85032F supplied with the VNA in different N type connections, for an open circuit, a short circuit, and a matched 50-ohm load. The calibration kit is used to provide a calibration over open matched load with a very low reflection over a wide bandwidth.

After calibration, the Vector Network Analyser (VNA) model E5071C was used to transmit and receive two types of bands, a narrowband around Wi-Fi frequency 2.45 GHz and wideband between 1-6 GHz, the VNA has a capability for computer controlled frequency tracking of both narrowband and the wideband experiments.

The general setup for an S-parameter test with two ports including the Shielding Device Under Test (SDUT) is used between Port 1 and Port 2 of the VNA is shown in Figure 3-5. The VNA generates a RF signal that passes through into Port 1, which is connected to the transmitting antenna that is focused on the SDUT. The VNA serves to separate and measure the incident wave amplitude, a***1***, and the reflected wave amplitude, b***1.*** The coefficients S_{21} and S_{12} are calculated and may have the same value.

The thickness of the SDUTs differed because of the different materials used and the methods used to coat the device with the ICP. The SDUT is placed on an aluminium screen 2000mm height and 1200 mm width with a square hole in the centre of the screen to hold 150mm x 150mm SDUT.

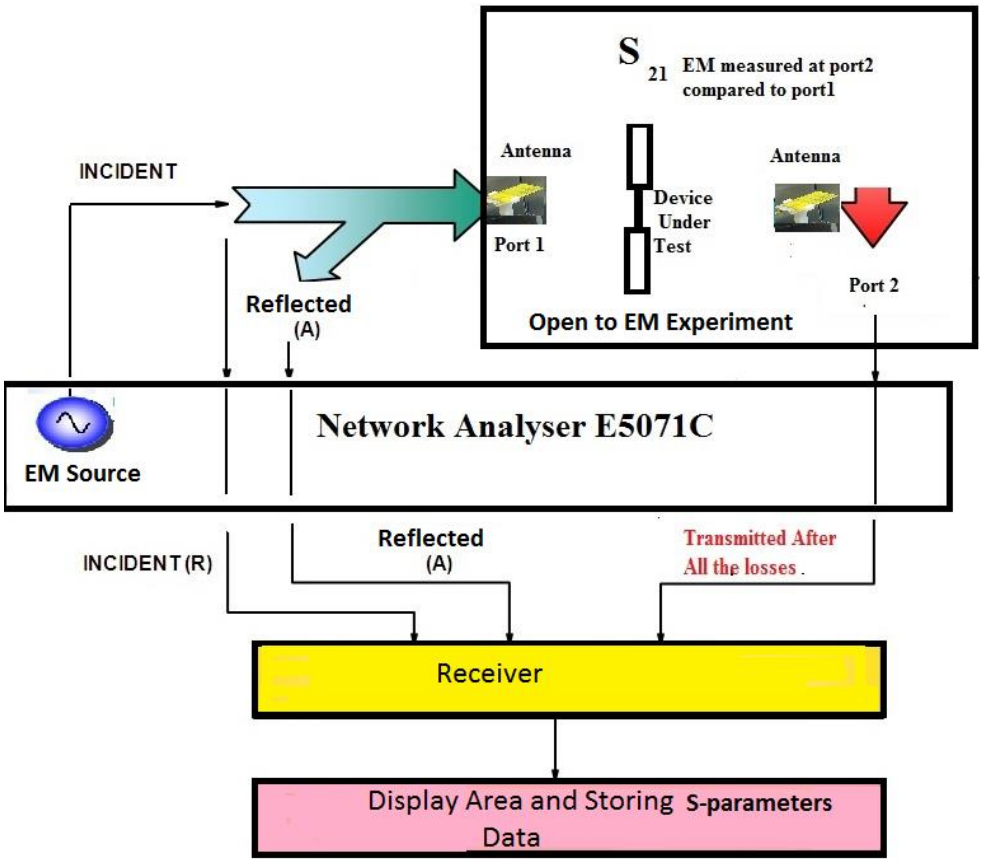

Figure 3-5. Procedure for OEMI measurements of S_{21}

Figure 3-5 show the two antennas that were placed on opposite the aluminium screen connected with coaxial cables to the VNA. One antenna was attached to port 1 and a matching replica receiver antenna to port 2 without the SDUT holder was inserted in the middle of the aluminium screen. The SDUT was placed tightly in the device slot of 150 mm x 150 mm and secured tightly with aluminium tapes to the large aluminium screen, in order to reduce the measurement uncertainty caused by air gaps. Aluminium tape was used to reflect the EM where the SDUT met the aluminium screen. Care was also taken to address the multiple reflections between antenna and surface of SDUT, and the diffraction effects at the edges of the SDUT. Highly conductive aluminium tape was used to cover all the edges.

Each SDUT was tested for two types of frequency bandwidths by using a Vector Network Analyser (VNA) model E5071C to transmit and receive two types of bands, a narrowband range around Wi-Fi frequency 2.45 GHz and a wideband range between 1-6 GHz. The important parameter S_{21} of the EM radiation data is measured for all SDUT materials and compared with the EM radiation data when there is no shielding device in square hole of the aluminium screen. Results of these measurements performed in the OEMI method can be checked with the anechoic chamber method.

To measure the transmission losses S_{21} of the devices at narrowband and wideband frequencies, two experiments set up were created. The first objective of each experiment was to observe the transmission loss (S_{21}) of EM-shielding device created from each of the ICP materials, and compare its S_{21} to metal and carbon shielding devices at the chosen frequency. The value of S_{21} was normalised to the S_{21} *of the reference (no shielding device)* S_{21}**.** The next two sections discuss the commonalities and differences in the experimental setup for narrowband and wideband measurements made using the OEMI method.

Narrowband experimental OEMI set up

These OEMI experiments related to the narrowband of the Wi-Fi frequency of 2.45 GHz. The transmission loss data S_{21} is the one that penetrates through the SDUT to reach the receiving antenna that resembles penetrating a mobile phone device.

The main components of the narrowband experiments are a network analyser (E5071C NA), two balanced feed antenna Yagi-Uda antennas with integrated balun, and an aluminium screen (1900mm X 1150mm) with 150mm X 150mm shielding device holder in the middle, 2 coaxial cables, and the shielding device under test (SDUT).

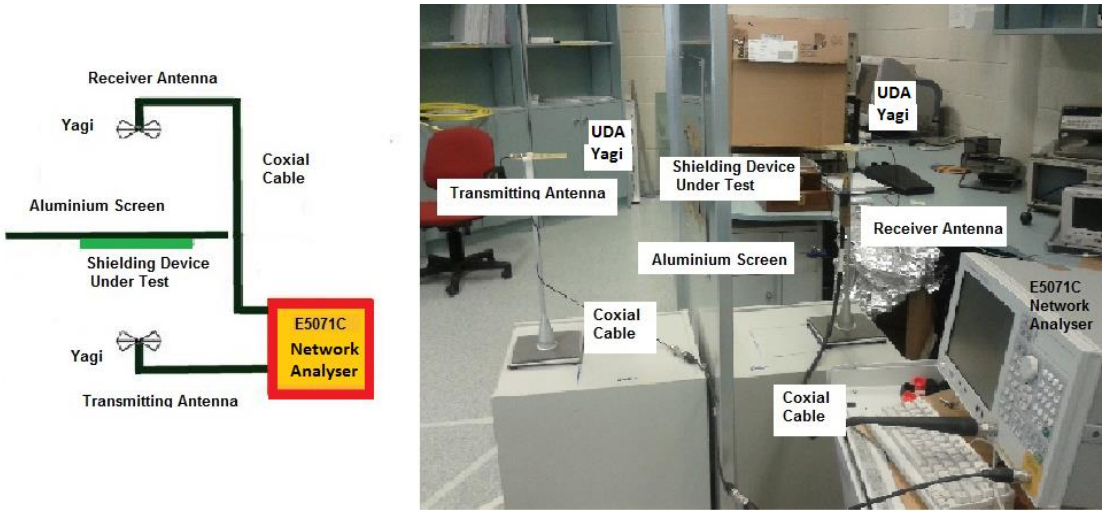

Figure 3-6. Yagi-Uda balanced feed antenna with integrated balun in OEMI experiment

balanced feed antenna Yagi-Uda with integrated balun is commonly used in mobile communications applications such as Bluetooth, Wireless LAN, etc. The Yagi-Uda antennas was selected for this research because of their narrowband width (~6db) and their ability to operate at low power levels over coaxial line or strip-line that resembles mobile phone transmission/reception at 2.45 GHz. A balun patch was attached to the Yagi-Uda antenna on one side with the ground plane on other side of the balun patch.

Wideband experimental OEMI set up

The wideband experiments aimed to measure the transmission loss (S_{21}) and to observe the EM shielding devices of ICP materials in the wideband frequency range of 1-6 GHz and compare them to metal and carbon shielding devices within that frequency range of 1-6 GHz. This (1-6) GHz experiments used horn antennas type LB-1080 M-SF that was supplied by Ainfoin rather than the Yagi-Uda antenna used in the narrowband experiments. The frequency gain plot for the horn antenna is shown in the figure below

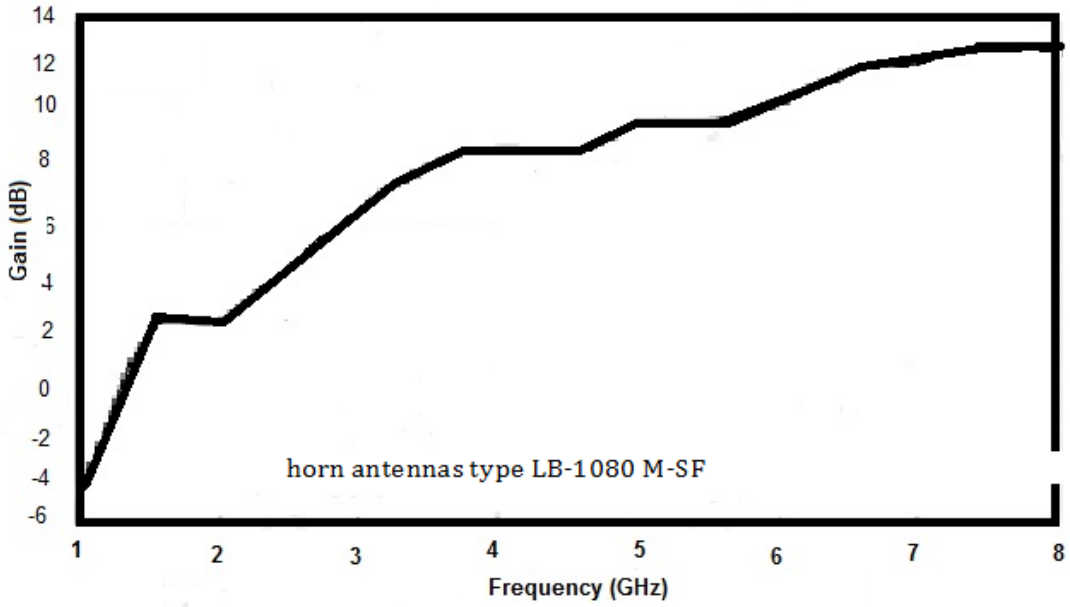

Figure 3-7 frequency gain plot for LB-1080M-SF

The main components of the wideband experiment are network analyser (E5071C NA), two horn antennas, and an aluminium screen (1900mm x 1150mm) with a 150mm x 150mm shielding device holder in the middle, 2 coaxial cables, and the shielding device under test. The setup for the wideband experiments is shown in the figure below.

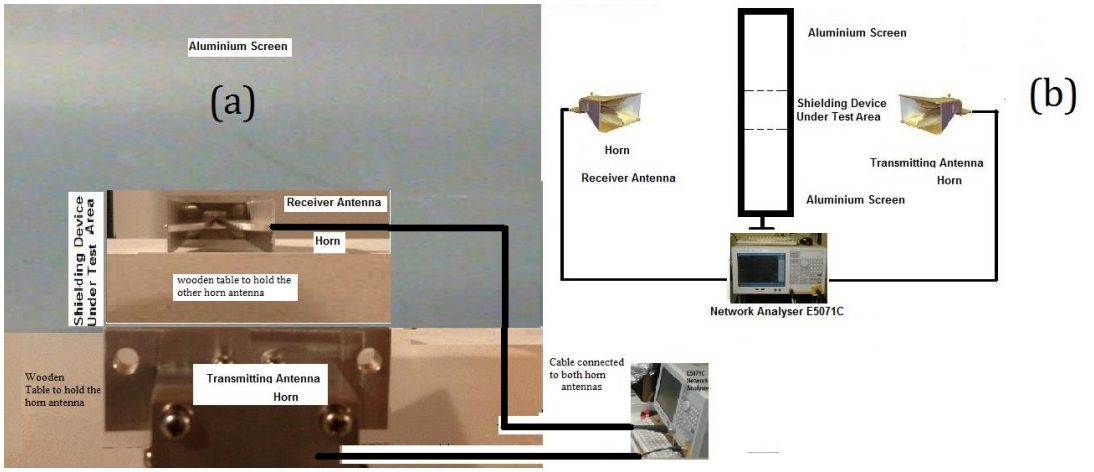

Figure 3-8. Horn antenna 1 to 6 GHz EM shielding set up

Figure 3-8 shows on the left the experimental setup with the aluminum screen separating the two identical horn antennas by a 150mm by 150mm area for testing shielding devices. Figure 3-8(a) is a photo shot of the actual experiment with the SDUT is representing the reference as there is no shielding device in the center between the two identical horn antennas, figure 3-8(b) is the sketch of the experiment.

Validation via the anechoic chamber method

As noted in Chapter 2, the anechoic chamber method is the preferred method for obtaining performance data on shielding devices and measures performance of electromagnetic shielding devices by their transmission loss S_{21}. It is the only method used to certify devices for EM compliance.

This study used the anechoic chamber method to verify whether the transmission loss S_{21} results obtained for the ICPs materials and other materials by the OEMI method obtained from other methods fell within an acceptable margin of error. The researcher checked:

- whether the scattering parameters obtained by the OEMI method were within acceptable error of 10dB of the anechoic chamber method, and
- how closely the scattering parameters of the shielding device correlated with those obtained by the more accurate anechoic chamber method.

The anechoic chamber measurements were conducted at the International Centre for Radio Astronomy Research (ICRAR), a joint venture between Curtin University and The University of WA. Unfortunately, ICRAR refused to allow the researcher to bring the measuring equipment used in the original open EM method setup in the Edith Cowan University laboratory into the anechoic chamber setup in ICRAR. The VNA was substituted for the While the E5071C analyses with the ICRAR VNA (a Rohde & Schwarz R&S ZVL6 operating at (9 kHz to 6 GHz).

PPy shielding device thickness sensitivity experiment setup

A thickness sensitivity experiment was used to investigate whether the reduction of thickness of PPy shielding device could reduce or increase the transmission loss. Because of the importance of thickness those changes at the Wi-Fi frequency of 2.45 GHz, this experiment used a setup similar to that for the narrowband experiment in Figure 3-5 and two thicknesses of the shielding device normalised to the reference transmission loss (without PPy shielding device). A full thickness was used of 25mm first and then half of 25mm was used in the device under test holder.

Simulation methods

The objective in using the simulation methods was to see whether the computer simulations matched the experimentally obtained data obtained for the various shielding devices by the OEMI method experiments in the narrowband and wideband frequency ranges. To simulate the experimental results without using an expensive experimental setups that requires expensive testing equipment and ICP materials, each shielding devices tested was modelled in a computer simulation modelling software.

Use of simulation modelling methods [128] generated a new set of problems not present in the experimental methods. These problems relate to the accuracy of the model, the parameters of the model, and the approximation of the model to the real life situation where all EM radiations are present in the experimental setup of the testing of the shielding device and perhaps most importantly to the processing of instant of real time that is required for modelling the transmission for that area.

An EMI simulation modelling of the EM shielding device during the testing process is therefore not an easy task if high accuracy is the goal. However, the simulation modelling tools can however still be invaluable assets if the model serves to simplify the shielding device testing process, reduce the cost and the time frame needed to finalise the assessment of the new type of shielding devices. In mobile phone and Wi-Fi devices, it is important to recognise the strength of the electric field and the electric field distribution, however it is difficult to calculate and accurately locate the electric field around the shielding device.

A finite element simulation modeling called COMSOL was used to model transmission loss S_{21} for EM shielding devices under test by solving the Maxwell equations [129]. COMSOL is based on the finite-element method, and is able to solve multi-physics problems. COMSOL generates a model of the experiment using electromagnetic solver to Maxwell's equations and the electromagnetic wave, COMSOL uses the finite elements method (FEM) to generate a model of the experiment to approximate the electric field at the chosen frequency domain to display the electric field intensity.

COMSOL Multiphysics is the only FEM method simulation software that uses a finite element code, allowing partial differential equations (PDEs) to be solved in 2D and 3D domains. The Using PDEs solves the explicit mathematical of Maxwell equations without the need to assign elements, and therefore allows to deal with more physics without adding to the solving time.

The COMSOL solver formulation has the advantages of simulating the scattering parameters of the shielding devices. The COMSOL modelling offers the choice of 1D, 2D and 3D Modelling [130] and can be used on various Windows and Mac platforms. The electromagnetic shielding application modes where the governing PDEs are present in several examples and the PDEs can be freely defined. The electromagnetic application module in COMSOL is used. The COMSOL Graphical User Interface (GUI) requires the input of geometry, shielding device material properties and boundary conditions of the experiment.

FEM is the most widespread modelling method that is formed from the optimal solutions used within the calculus of variations. FEM is a method that is primarily based on solving Partial Differential Equations (PDEs)[131]. FEM subdivides space into elements, for example tetrahedral and the electric fields inside these elements are expressed in terms of a number of basic functions, i.e. straight line, polynomials or spline. These expressions are inserted into the functions of these equations, and the variation of the functions is made zero. FEM produces a very sparse matrix equation that can be solved using matrix algebra, in a very fast solution times.

COMSOL is a general simulation method suitable for many multiphysics applications, and has the advantage of modelling a wide band of frequency in one run yielding much faster results than other simulation methods. COMSOL starts in time domain and convert the results to frequency dimension via Fourier transform. The problem with COMSOL is the difficulty in including fine details in the geometry, and the inclusion of the antenna model.

Another simulation software based on FEM solver is HFSS (Ansoft HFSS simulation), which has much better interface, which enables the user to include very fine details in the geometry of simulated structure and antenna model. High Frequency Structural Simulation (HFSS) is the best specialised commercial software for the design of Microstrip Patch Antenna (MPA), Dielectric Resonator Antenna (DRA) & Metamaterial based antennas, especially for three-dimensional (3D) modelling of the antenna. The HFSS simulation technique is suitable for small or moderate objects compared with the operating wavelength. Repeating the simulation modelling with HFSS can serve to validate the COMSOL modelling technique and explore the accuracy of the modelling.

The choice of the method for the model is important, as choosing the wrong type of analysis, can lead to excessive long computing time and errors. The main drawback of this modelling proved to be the lengthy processing time taken to solve the Maxwell equations by the finite elements method.

The model of the EM shielding devices involved two types of modelling, narrowband and wideband:

- the narrowband modelling process was used to model shielding devices that protects systems from interference that normally arises from deliberate transmissions such as radio and TV stations, pager transmitters, cell phones, etc and it is centered around the Wi-Fi frequency 2.45 GHz, and
- the wideband modelling type is used for the protection from the wideband frequency shielding devices [132] from a wideband frequency between 1-6 GHz that includes 2.45GHz.

PAni shielding device temperature sensitivity experiment setup

A temperature sensor experiment was used to investigate whether a PAni shielding device could serve as a temperature sensor. Because of the importance to monitor those changes at the Wi-Fi frequency of 2.45 GHz, this experiment used a setup similar to that for the narrowband experiment in Figure and subjected the shielding device holder to a temperature increase. A hair dryer was held perpendicular at 90 degree on the PAni shielding device for 300 seconds and then at 300mm away from the PAni shielding device to heat the PAni SDUT.

A noncontact infrared thermometer GM550 with the specifications shown in the figure below was used to measure the temperature increase, the response time and the transmission loss S_{21} variation.

Temperature range	-50 -550 Celsius(-58-1022 Fahrenheit)
Accuracy	0 Celsius -380 Celsius (32 Fahrenheit -1022Fahrenheit) Celsius; ± 1.5 Celsius (± 2.7 Fahrenheit)or ± 1.5% -50 Celsius -0 Celsius（-58 Fahrenheit -32 Fahrenheit）； ± 3 Celsius（± 5 Fahrenheit） whichever is greater
Resolution	0.1 Celsius or 0.1 Fahrenheit
Repeatability	1% of reading or 1 Celsius
Response time	500 mSec, 95% response
Spectral reponse	8-14 um
Emissivity	0.95 Preset
Distance to spot size	12:01
Operating temperature	0-40 Celsius(32 Fahrenheit - 104 Fahrenheit)
Operating humidity	10-95%RH non-condensing, Up to 30 Celsius (86 Fahrenheit)
Storage temperature	-20-60 Celsius(-4-140 Fahrenheit)
Power	9V Alkaline or Nicd battery
Typical battery life(Alkaline)	Non-laser mode:22 hrs

Figure 3-9. GM550 specifications

COMSOL 2D modelling

The COMSOL modelling undertaken started with simple 2D narrowband around the Wi-Fi frequency 2.45 GHz. A 2D model displays the real dimensions of two aluminium chambers separated by the SDUT. In the model, a 2D aluminium chamber of size 0.1 m, is separated by a gap between of 0.015 m from another 2D aluminium chamber as shown in the figure below. The 2D modelling is justified here because of the advances in 2D that improved the speed and complexity by reducing the problem into a series of 1D integration equations

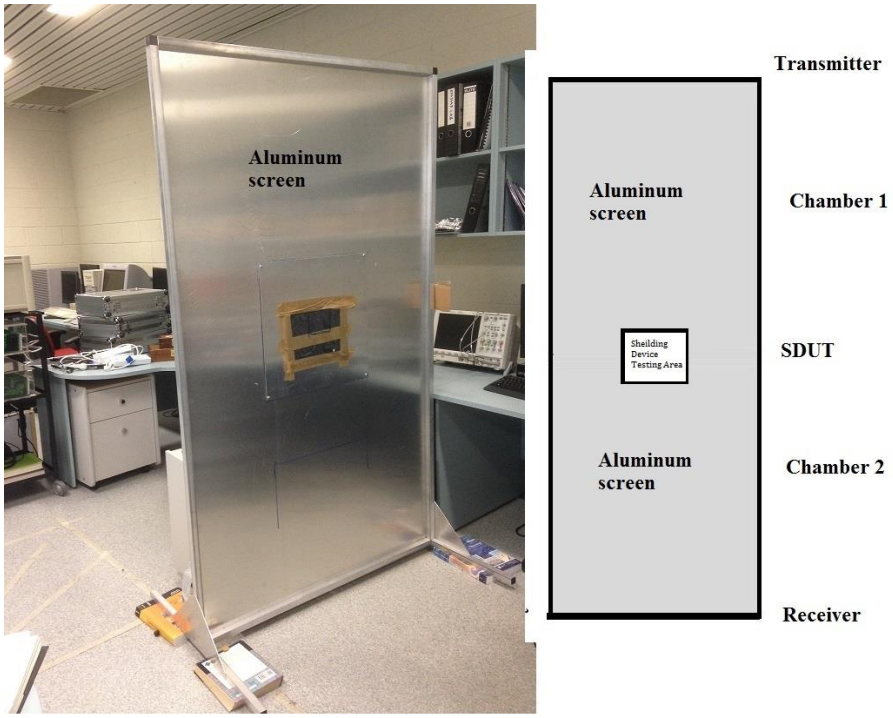

Figure 3-10. 2D Narrowband COMSOL modelling approximation

The figure above shows the approximation of the real life experiment to 2D simulation with the SDUT in the centre of the gap between the two chambers. The main advantage with setting up this model in 2D is that a laptop computer can be used to solve the model much faster and uses less memory than normal PC. The shielding device is then inserted into the gap between the two exterior metal chambers that are adjusted and scaled to simulate the 2D experimental results.

The 2D model allows its users to determine the types of measurements anticipated, and this study focused on the S_{21} transmission loss measurement. The 2D model also allows its users to:

- vary and scale the shielding device under test size according to many factors such as its applications,
- set the frequency range,
- view cross section levels, and
- vary the material properties used in the chambers and the shielding device under test
- more flexible and easier than 3D.

The COMSOL 2D model is divided into 7 parts, namely: RF physics, material properties, the geometry, meshing, frequency range, study of the selected frequency domain and displaying the results. The RF physics is based on equations derived from Maxwell's Equation and Ampere and Faraday's laws, embedded in COMSOL to describe the wave behaviour.

Creating a customised 2D model of the experimental setup was simple. This COMSOL 2D narrowband model depends on the dielectric properties of the material that is used in the SDUT inserted between the transmitter and receiver. The material properties required for the COMSOL model are the electrical conductivity, relative permittivity, relative permeability and the refractive index. This study obtained those materials properties from the manufacturer or from the literature.

The customised 2D model also required specification of the geometry parameters of the experimental setup. The model used represented two rectangular rooms with aluminum walls coupled together by the SDUT. Use of this geometry meant the transmitter transmits the 2.45 GHz frequency as a far distance source, the two chambers acted like two empty metal compartments resembling waveguides. The waveguide materials could be varied from air to different dielectric materials. In this 2D model, the hollow two chambers are in the x and y planes, while the z plane has the electric field. As a single propagating mode of TE_{10} wave is used, only the z-component needs to be solved.

The COMSOL model assumes that the effects of wave propagation delays and the magnetic field are neglected and that the charges in the material that is used in the SDUT is linear. The COMSOL model generates the S-parameter of transmittance loss S_{21} of the shielding device for several frequencies around 2.45 GHz. This customised COMSOL 2D narrowband modeling shown in the figure below was used in the microwave region of 2-3 GHz narrowband or 1-6 GHz wideband.

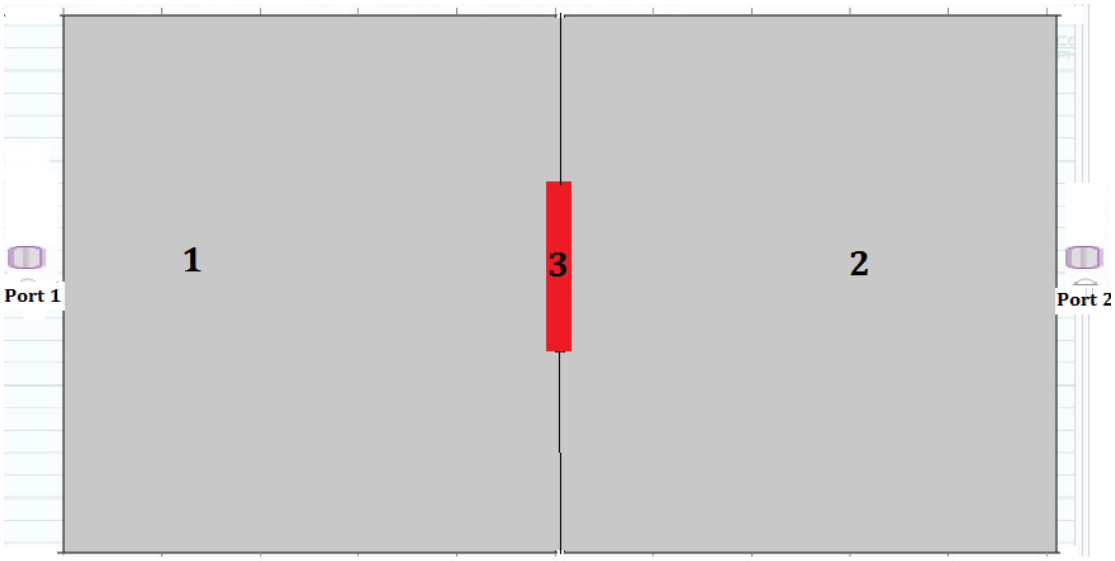

Figure 3-11. 2D narrowband shielding device model

While many types of meshing can be used, this customised 2D model used the the faster standard meshing tool, that can as shown in Figure 3-10,the meshing is varying in details according to the regions.

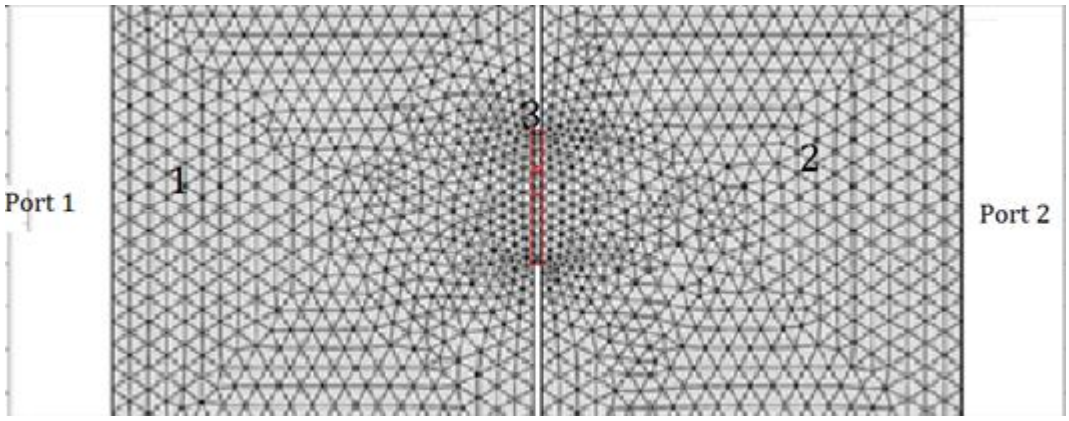

Figure 3-12. Meshing of the 2D model

The Electromagnetic Wave (EW) interface is used to approximate the electric field radiation in the whole the model. The S***21*** parameter, the important parameter corresponding to the transmittance loss, is given by the curve showing the frequency and the amount of attenuation in the path of the plane wave between the transmitter port 1 and receiver port 2 with the electric field in z direction (Ez).

COMSOL 3D modelling

To add another dimension to the 2D model, so that the simulation can better model the experimental results in chapter 4, a 3D model was created using the actual dimensions of the two aluminum compartments separated by the SDUT and taking account of the thickness of the SDUT. Like the COMSOL 2D models, the COMSOL 3D models simulate the electromagnetic wave transmission loses and the EMR distribution between the transmitter and receiver for frequency range for 2-4 frequency range (GHz). This study's use of the COMSOL 2D model focused on the frequency of 2.45 GHz that is in current use, while use of the COMSOL 3D model focused on the wider band of 1-6 GHz that will be used in the future.

As always, the COMSOL model depends on the dielectric properties of the material that is used in the SDUT inserted between the transmitter and receiver. The 3D model allowed the researcher to determine the types of measurements anticipated, vary the device size, set the frequency range, view cross section levels, and vary the material properties that are used in the SDUT and simulate anechoic chamber measurements. The model could accommodate shielding devices thicknesses from 0.05 mm up to 25 mm.

In the customised 3D model, a 3D square aluminum box of size 0.1m is separated by a gap of 0.015m from another 3D aluminum box. Each compartment was made of aluminum with total length and width of 0.1m and width 0.1m in the model. The SDUT is inserted into a gap between the two metal exteriors boxes that is adjusted and scaled to simulate the 3D experimental results. The 3D model in the microwave region of 1-6 GHz acts like two empty metal compartments that resemble waveguides. The waveguide materials can be varied from air to different dielectric materials. In this 3D model, the two hollow boxes are in the x and y plane, while the z plane has the electric field. As a single propagating mode of TE_{10} wave is used, only the z-component needs to be solved.

Validation of the COMSOL simulation via HFSS

COMSOL is a general simulation method for many multiphysics application, and has the advantage of being able to modelling a wide band of frequency in one run and generating the results more quickly than other simulation methods, because it starts in time domain and convert the results to frequency dimension via Fourier transform. The problem with COMSOL is the difficulty of including the details in the geometry, and the inclusion of the antenna model.

Another special software method High Frequency Structural Simulator (HFSS) can be used to address some of the shortcomings of COMSOL and validate the COMSOL computer model in terms of S_{21} transmission lose simulation output. HFSS, a 3D finite element method solver for electromagnetic structures from Ansys, is the best specialised commercial software for the design of Microstrip Patch Antenna (MPA), Dielectric Resonator Antenna (DRA) & Metamaterial based antennas, especially for three-dimensional (3D) modelling of the antenna. This important EM commercial software is used mainly for antenna design, and the design of complex RF electronic circuit elements including filters, transmission lines, and packaging.

HFSS has a much better interface, which enables its user to include very fine details of the geometry of the simulated structure and antenna model. Like COMSOL, HFSS is an FEM-based method. The HFSS simulation technique is suitable for objects of small or moderate size compared with the operating wavelength.

This researcher's objective in repeating the simulation modelling with the Ansoft HFSS simulation was therefore used to validate the above COMSOL modelling technique [156] and become familiar with the accuracy of the modelling. The first validation model was done with 3D chambers that measure S_{21} as the experimental aluminum screen of 2m width.

The first 3D simulation was attempted with no shielding device between the transmitter and the receiver and both the transmitter antenna and the receiving antenna were encapsulated in a waveguide. To reduce the time taken to produce a result, the model was simplified by removing the waveguide around the antennas.

Another model using Horn antennas operating in 1-6 GHz, was used to generate the transmittance loss S_{21} as a function with wideband frequency for 1-6 GHz for comparison with the wideband COMSOL simulation results. Further refinement of the model involved removing the shielding device in the simulation between the transmitting horn antenna and the receiving horn antenna.

Other simulation options considered but not adopted

Parallel computing could have been used to reduce the simulation processing time. Those methods are cheap and available and mainly involve use of transputer arrays and clustered workstations over the local network. In the case of this research project, there was no funding available to reduce the processing time.

Another approach would be to use IVEC supercomputers and cloud computing. Cloud computing is arguably the true future of computing, whether for personal, corporate or military purposes. One technique that can be used with cloud computing is to use is an object-oriented C++ finite element framework for the development of tightly coupled multiphysics solvers from Idaho National Laboratory called MOOSE (Multiphysics Object Oriented Simulation Environment). MOOSE is a generic platform for engineers seeking to understand data in general, and software systems in particular. The major benefit of using MOOSE is that it can be easily coupled to other physics (like heat conduction, chemistry and more) [133].

The input to MOOSE is the experimental data, that contains all the geometry of the objects, material properties and relationships. This data is loaded in MOOSE via importers that can import data from various sources and in various formats. MOOSE uses parallel processing to solve Finite Elements Method (FEM) and numerically approximate the Partial Differential Equations (PDEs) to reduce the simulation time. The advantage of MOOSE is that it eliminates the disadvantage of parallel computing that is the change of the model in the software to segments, without adding to the cost and software alteration time.

Clearly, MOOSE is an open source software that could give a real time modelling of the shielding device [134]. Unfortunately, when this researcher applied to access open source MOOSE subjected to the necessary security clearance, access was denied on the grounds that this researcher was born in Iraq.

Comparing experimental measurements and simulation results

The simulation data points can be considered as (n) pairs of data consisting of two coordinates representing S_{21} and frequency as $(x_i; y_i)$ and i is between (1 to n) for experimental and simulation separately. Those data points can then be plotted by hand as a straight line defined by the equation y = mx + c where m is the slope m and c is the intercept on the y axis. Provided the scatter in the data is small, the line that is drawn is a satisfactory straight line.

By comparison with other mathematical models (logarithmic, polynomials of different degrees, and moving average), linear models are simple and can show the errors between the actual measurements and the simulation model. More modern methods can be used to address any nonlinear errors in this model.

Bacterial experiments

Considerations of time, cost, facilities and expertise limited the scope of the health-related investigations that could be carried out for this study. In acknowledgement of the health concerns relating to mobile devices, this study include a brief experiment investigating the short-term impact of phone shielding materials on the growth of a common species of bacteria. The aim was to investigate whether new ICP shielding devices might be any more effective than current shielding materials in inhibiting the growth of *E. coli* bacteria.

Imanvision Devices Ltd. (Australia) arranged for this experiment to be performed with direct help, supervision and verification from a highly skilled microbiologist technician in a government microbiology laboratory. An experienced qualified microbiologist Dr. Asfar Al-Shbib [135][136], who performed the experiments

comparing the impact of shielding device made of an ICP material with a popular model of a contemporary mobile phone. The ICP material tested was nonwoven PPy, while the mobile phone tested was an iPhone 3 manufactured and marketed by Apple Inc., Cupertino, California.

One of the most common methods of calculating bacteria cell number on the device under test, namely the Surface Viable Count [137](section 1.6), was used to assess bacterial growth. In this method, material contaminated with *E. coli* bacteria is swabbed and diluted in a solution that will not kill the *E. coli* bacteria that is collected, and does not support its growth.

A volume of liquid (or a portion of solid) from the device under test is first diluted 10 fold into buffer and mixed thoroughly. Around 1.0 ml portion of this first dilution is then diluted a further 10 fold, giving a total dilution of 100 fold. This process is repeated until a concentration that is estimated to be about 1000 cells per ml is achieved. Samples of the highest dilutions (lowest bacterial density) are then taken and spread with a sterile glass rod onto a solid medium that will support the growth of the *E. coli* bacteria. Agar with 5% blood is considered an excellent medium for growing *E. coli* bacteria as it provides the nutrients required. While the blood is not a selective medium, it helps the growth of different types of bacteria and fungus.

After aliquots of the diluted solution are deposited on agar to allow growth of colonies, the total number of colony forming units (CFUs) on each agar plate can then be counted [138][139]. When dilution of swabbed sample from the device under test is high enough, individual *E. coli* bacteria cells are deposited on the agar and these then give rise to colonies. By counting each colony, the total number of colony forming units (CFUs) on the plate can be determined. Multiplying this count by the total dilution of the solution yields an estimate for the total number of CFUs in the original sample.

To investigate whether EMI shielding materials impacted the growth of bacteria, colonies of E coli were nurtured in specially prepared Petri dishes under laboratory

conditions. Both of the shielding device materials under test (nonwoven PPy and an iPhone 3) were swabbed and the bacteria removed were then diluted in 5% sheep blood agar. As *E. coli* bacteria produce hemolysins, which break down the red blood cells causing a change of colour, use of sheep blood therefore helps to show the bacteria, aid identification of the type of bacteria. , and assists the counting, comparison of the number of *E. coli* colonies on the growth medium. Three trials were performed for each of the test materials.

Conclusion

In the light of the literature reviewed in the previous chapter, this chapter outlined the methodology selected to address the research questions stated in Chapter 1.

This exploratory research focused on investigating scattering parameters of shielding devices coated with three ICP materials, namely PAni, PEDOT:PSS and PPy. Both PAni and PEDOT:PSS were used in a liquid state while PPy was used as a felt.

Methods chosen to give reliable, reproducible results within the time, budget and equipment and other constraints on this research project and suggest directions and scope for future research.

The next chapter presents and discusses the experimental results relating to the scattering parameters for the ICP-based shielding devices.

Chapter 4. Narrowband and wideband experiments

Introduction

In the light of the literature reviewed in Chapter 2 and the methodology discussed in Chapter 3, this chapter outlines the results of the narrowband and wideband experiments undertaken to address the research questions stated in Chapter 1.

ICP materials based on PPy, PAni and PEDOT:PSS were tested and compared with the current mobile phone materials (copper, aluminum and carbon) by using OEMI experiments to assess the level of transmission loss (attenuation) for the incoming EM radiation at the narrowband of Wi-Fi frequency of 2.4 GHz and at a wideband frequencies of (1-6) GHz. Results obtained by the OEMI method were then validated by repeating the experiments in an anechoic chamber.

A further experiment investigated whether the PAni shielding device could be used as a temperature sensor.

OEMI experimental results

The OEMI experiment setup was used to compare the performance of shielding devices made of PAni, PPy, and PEDOT materials with shielding devices made of aluminium and carbon. The effectiveness of the shielding device in reducing the EM radiation (that is how well the device serves to intercept the EM radiation) is shown by comparison with the baseline reference measured when there is no SDUT. Three methods were used to measure the s-parameters and specially S_{21}.

OEMI experimental results – narrowband

The narrowband results are summarised in the figure below were obtained at 2.45 GHz for all SDUT as shown in Table 4-1 below. Performance of ICP shielding devices made from (PPy, PAni and PEDOT) are compared with those of the current shielding devices made from aluminium and nanocarbon. Figure 4.1 shows the capability of the SDUT to limit the transmission loss S_{21} for metals with thickness between 0.02

mm and 0.5 mm, nanocarbon 0.5 mm and ICPs of PEDOT, PAni and PPy of thickness between 25.4 mm to 0.5 mm. The thin layer of aluminium foil of 0.02 mm is adequate to provide -43 dB, while the thickness of PPy had to be increased to 25.4 mm to provide the same transmission loss. This increase in the thickness of PPy felt demonstrate that PPy has a higher absorption than copper, and thus the electromagnetic energy diffracted around the shield or reaching the receiving antenna after multipath. This increase in thickness of PPy could not be repeated to PAni and PEDOT because the dip coating method provided one layer of thickness and it would have been difficult to control the process of increase thickness. In the case of PPy the shielding device is made of felt and can be increased at a standard thickness.

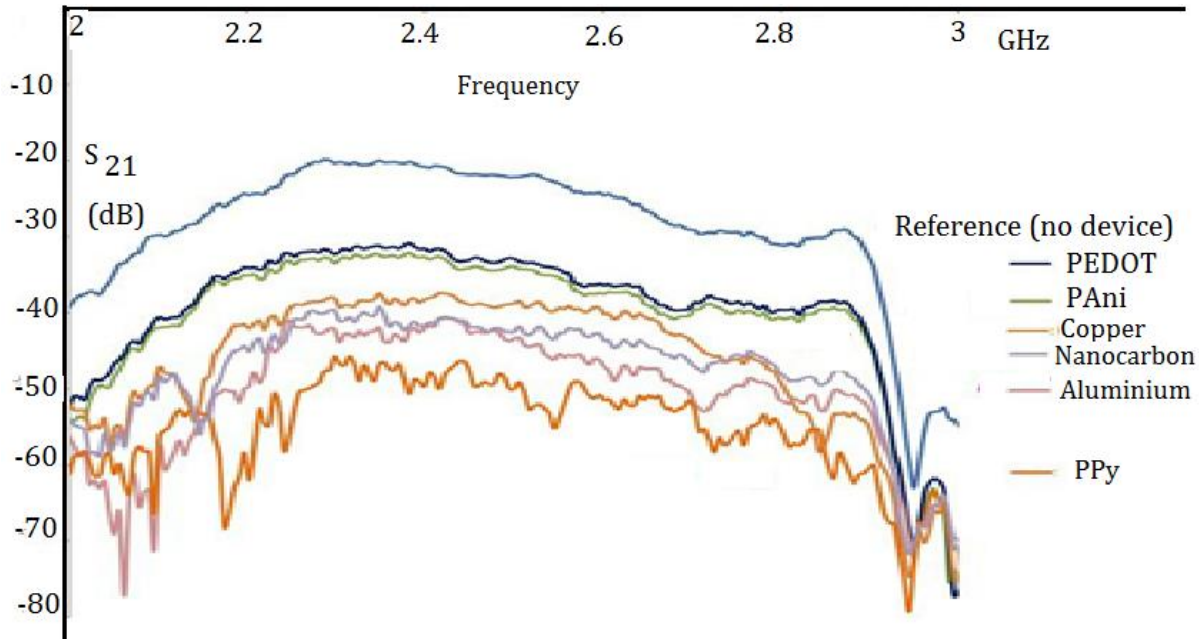

Figure 4-1: Narrowband transmission loss for all the shielding devices

Table 4-1. Extracted narrowband results for S*21* at 2.45 GHz

SDUT (shielding device under test)	**S_{21} (dB)**	**Thickness (mm)Approx.**	**Type**	**Frequency (GHz)**
No SDUT (reference baseline)	-22	0	air	2.45
PEDOT	-35	0.5	Liquid	2.45
PAni	-37	0.5	Liquid	2.45
Copper	-40	0.1	foil	2.45
Carbon (nano)	-43	0.5	Liquid	2.45
Aluminum	-43	0.02	foil	2.45
PPy	-48	25.4	felt	2.45

Experimental results – wideband

The experimental wideband results for all tested shielding devices are shown in the figure and table below.

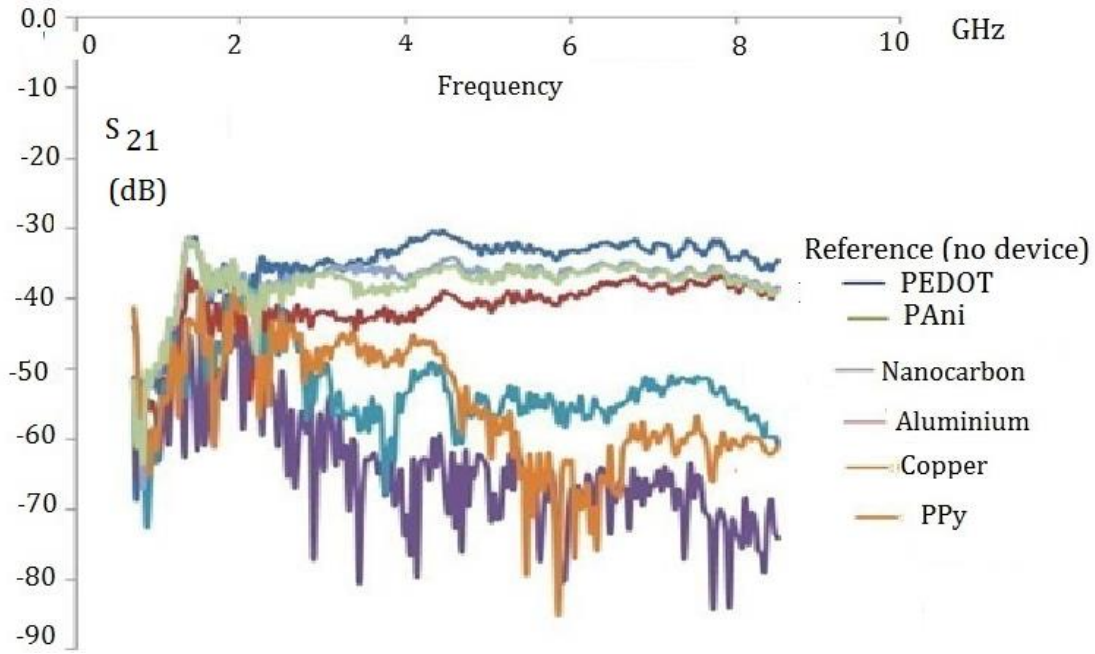

Figure 4-2. Wideband transmission loss S***21*** for all shielding devices

Table 4-2. Wideband results for the same thickness at different frequencies

SDUT (Shielding device under test)	***S21* at 1 GHz (dB)**	***S21* at 2.45 GHz (Wi-Fi frequency) (dB)**	***S21* at 6 GHz (dB)**
No device (Reference baseline)	-32	-32	-32
PEDOT	-35	-35	-35
PAni	-37	-45	-40
PPy	-50	-60	-65
Copper	-45	-47	-60
Aluminium	-50	-55	-55
Carbon (nano)	-50	-50	-55

As the table above shows, the ICP (PEDOT, PAni and PPy) shielding devices provided a different level of attenuation from -3 dB below the reference attenuation to -33 dB, while the conventional and current shielding devices have the same range level of attenuation around -23 dB.

OEMI experimental results – thickness variation of PPy

Reducing the thickness of PPy felt to half of its original size of 25mm at Wi-Fi frequency of 2.45 GHz produced the following results, summarized at an early stage of this research

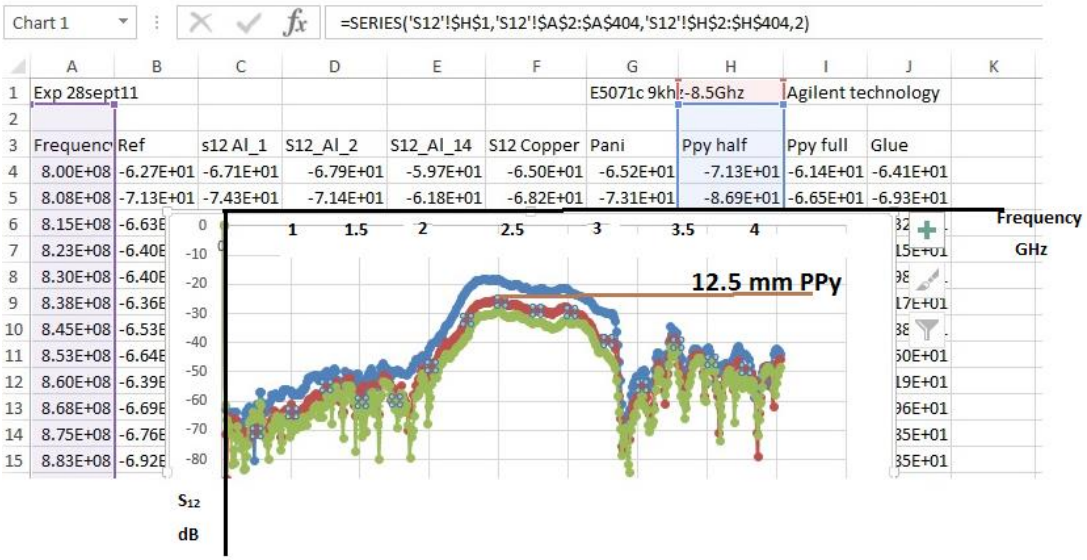

Figure 4-3 PPy shielding device at 12.5 mm of PPy thickness

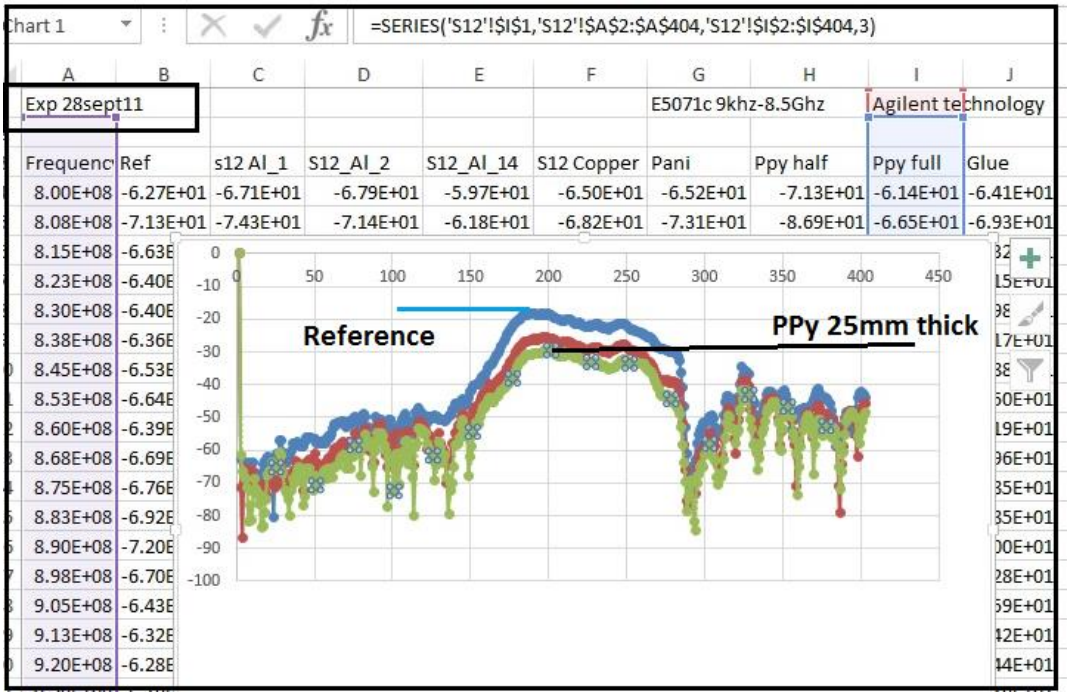

Figure 4-4 transmission loss variation with the change of PPy thickness to 25mm

From figures 4.3 and 4.3 we can show that the shielding devices increases as thickness increases and the transmission loss follows the antennas frequency bandwidth as it shown in figure 4.5.

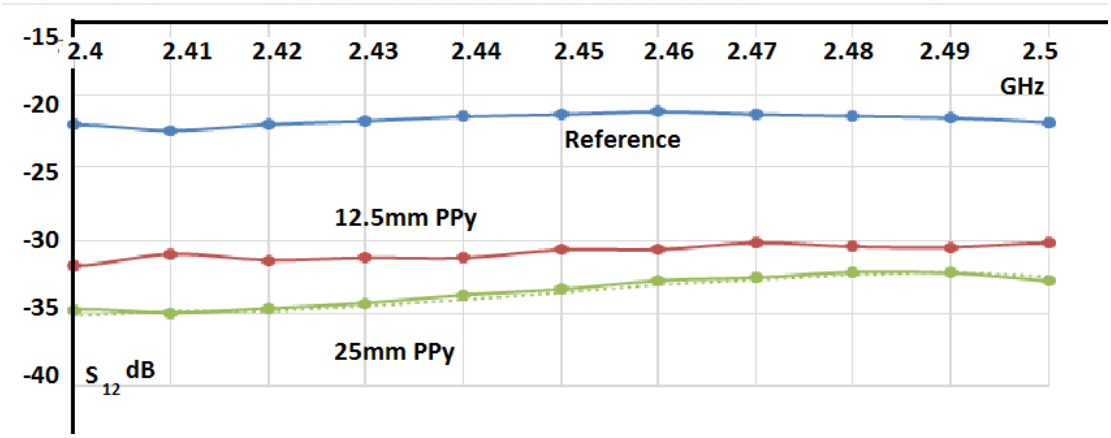

Figure 4.5 the variation of thickness with transmission loss for two thickness

The ICPs materials have a better absorption at the above frequencies of concern and it is controlled by three factors conductivity, permeability and thickness therefore the reflectivity of the ICPs shielding devices at the frequencies of concern is less than metal shielding devices and it depends only on conductivity and permeability

OEMI experimental results – temperature sensitivity of PAni

Varying the temperature from 25C^{o} to 80C^{o} over 300 seconds at the Wi-Fi frequency of 2.45 GHz produced the results summarised in Figure 4-6.

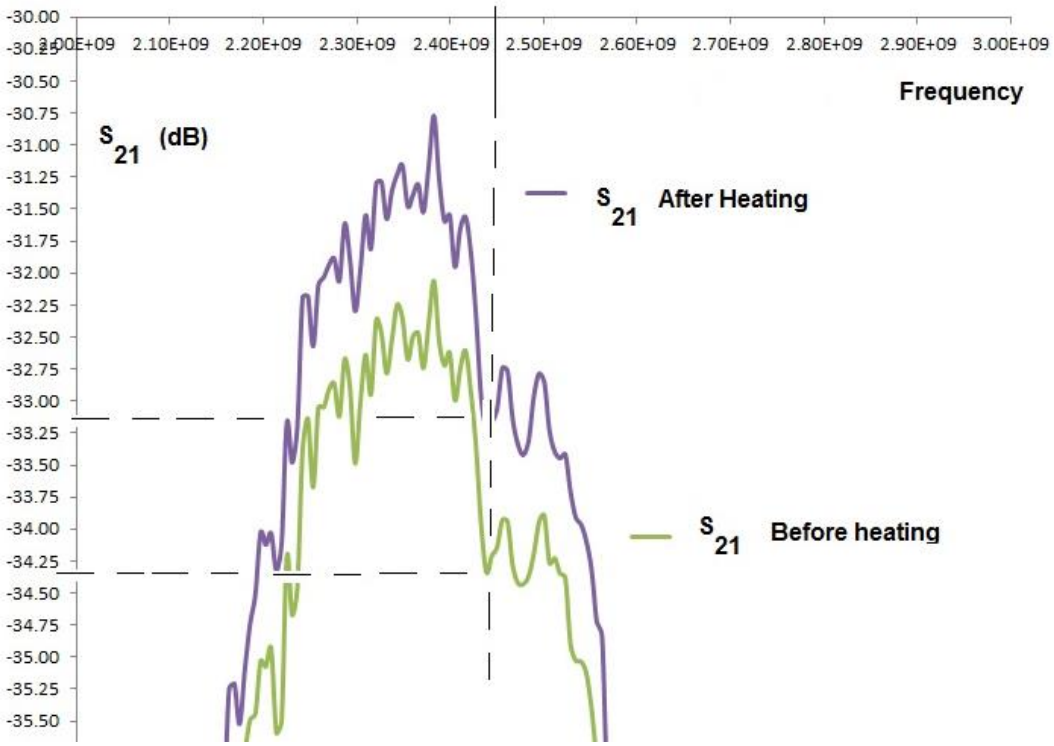

Figure 4-6. Temperature sensitivity of PAni

Results obtained using the narrow band experimental setup show that the transmission loss S_{21} of the PAni shielding device changed with temperature. Measurements were recorded approximately every 60 seconds as temperature increased from 20°C to 80°C, over a 300-second period showed a variation of approximately 1dB in the transmission loss (S_{21}). This is a good start for a variable

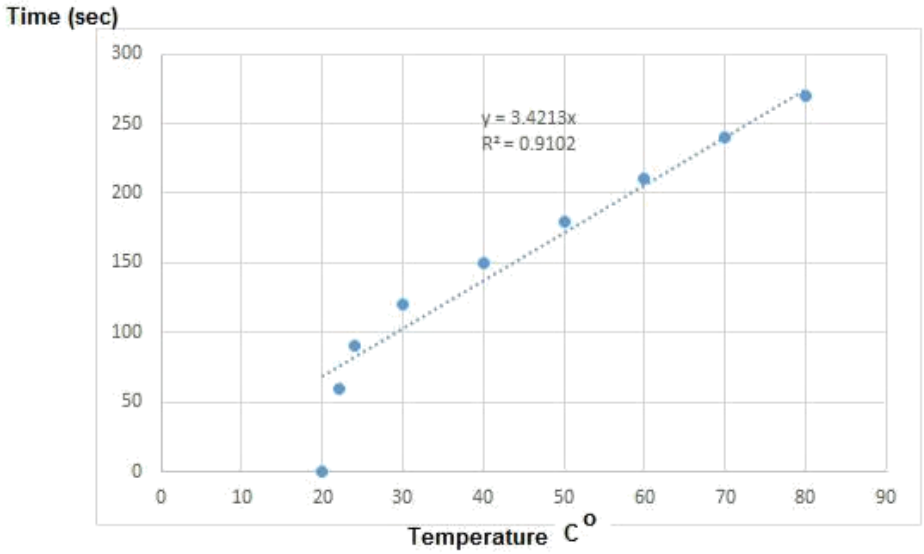

Figure 4-7. Variation of temperature with time for PAni shielding device

Since its transmission S parameter increases with the increase of temperature, the PAni shielding device could be used as a temperature sensor to tune the increase of the transmission without any need to change the shielding device or introduce different type of materials.

Anechoic chamber results

The results for all the shielding devices tested in the anechoic chamber at frequencies of 1, 2.45 and 6 GHz are shown in Table 4-3.

Table 4-3. Results of anechoic chamber tests

SDUT (shielding device under test)	**S_{21} at 1 GHz (dB)**		**S_{21} at 2.45 GHz (dB)**	**S_{21} at 6 GHz (dB)**
No device (Reference)	-35.0		-32.4	-26.1
PEDOT	-35.0		-32.4	-26.1
PAni	-32.4		-34.4	-27.1
PPy	-47.1		-47.5	-48.7
Copper	-46.9		-44.4	-47.5
Aluminium	-47.9		-47.8	-47.7
Carbon (nano)	-48.9		-51.5	-57.5

Validation of the OEMI results for PAni shielding device

The OEMI method results and anechoic chamber results are compared by establishing a maximum error between the two methods for testing the ICPs

shielding devices. This validation for OEMI method is conducted so that there is no doubts that the OEMI method can be used in the future to validate the transmission loss S_{21} results. The whole results for aluminium. Reference, PPy, PEDOT, and PAni is shown in Figure 4-8, the figure shows a red straight line fitting for the anechoic chamber results, those points are compared with the OEMI experimental results.

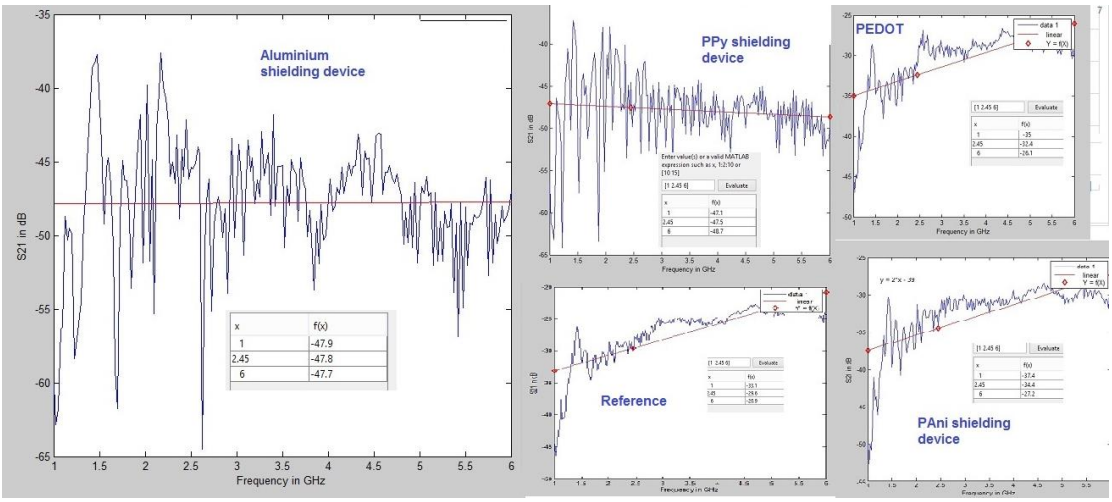

Figure 4-8 anechoic chamber results for aluminium, reference, PEDOT, PPy and PAni with straight line fit

The steps of validation for PAni are:

1. The OEMI result of broadband of PAni shielding device extracted data from the wideband experiments are shown in Figure 4-8. Six data points are selected across the 1-6 GHz bandwidth and a red line is drawn on the anechoic chamber result of PAni figure 4-10. The anechoic chamber result for PAni is used to plot a straight line to show the errors between the experiment red dot point and anechoic chamber method. The straight line is used to generate 6 points across the frequency bandwidth (1-6) using EXCEL to generate a simple linear fit, as shown in Figure 4.11. Figure 4.12 summarise the validation process for PAni shielding devices.

   A linear model is simpler than a quadratic model, and often works just as well for most purposes. In a simple linear fit the variables are independent of each other, if any other fit like quadratic then there is a correlation between x and x^2 and therefore the fit will be unreliable. The linear fit is perfect for making a forecast and that requires a reliable estimate of the parameters.

2. The anechoic chamber results of broadband experiments of PAni shielding device extracted data marked as (B) in Figure 4.6 where analysed by using MATLAB linear fit and the result where imported to EXCEL to compared with OEMI results for error as seen in Figure 4-7.

and the anechoic chamber proved to have an acceptable linear relationship between 2 GHz and 5 GHz, with acceptable small error for the PAni shielding device at 2 GHz as shown in Figure 4-11. The maximum error between the OEMI experiments and the standard anechoic chamber method was about -10 dB.

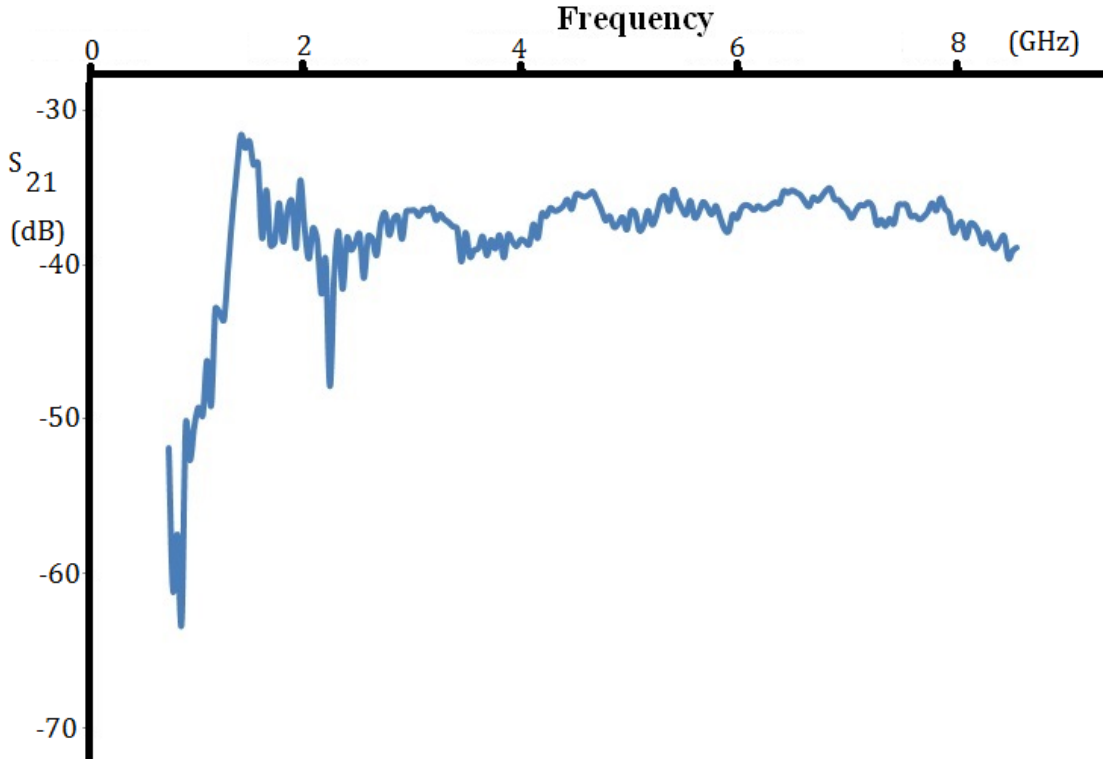

Figure 4-9 PAni S_{21} extracted from the OEMI experiments in figure 4.2

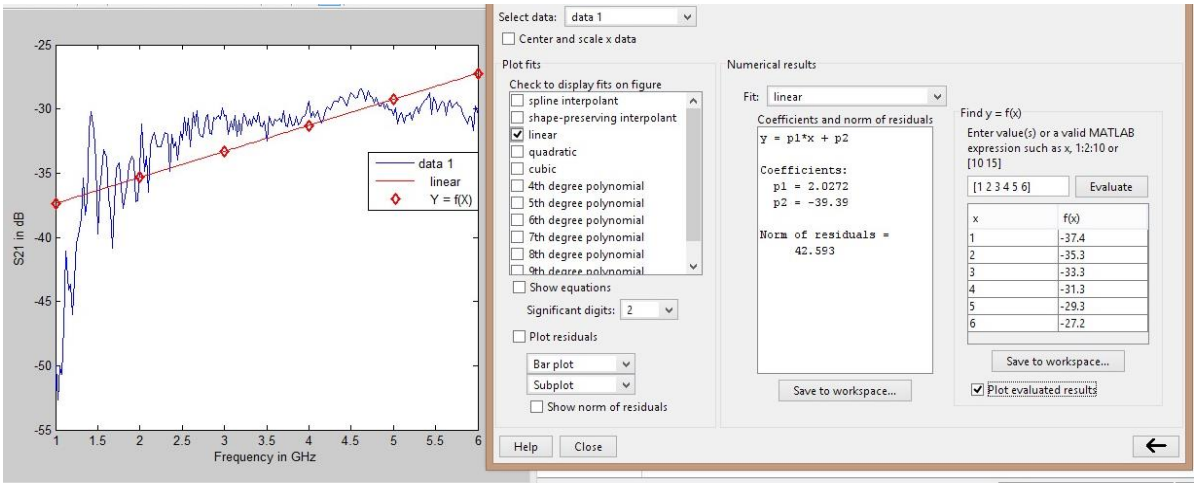

Figure 4-10 Anechoic chamber results for PAni with MATLAB straight line fit and red dots representing the corresponding, OEMI method

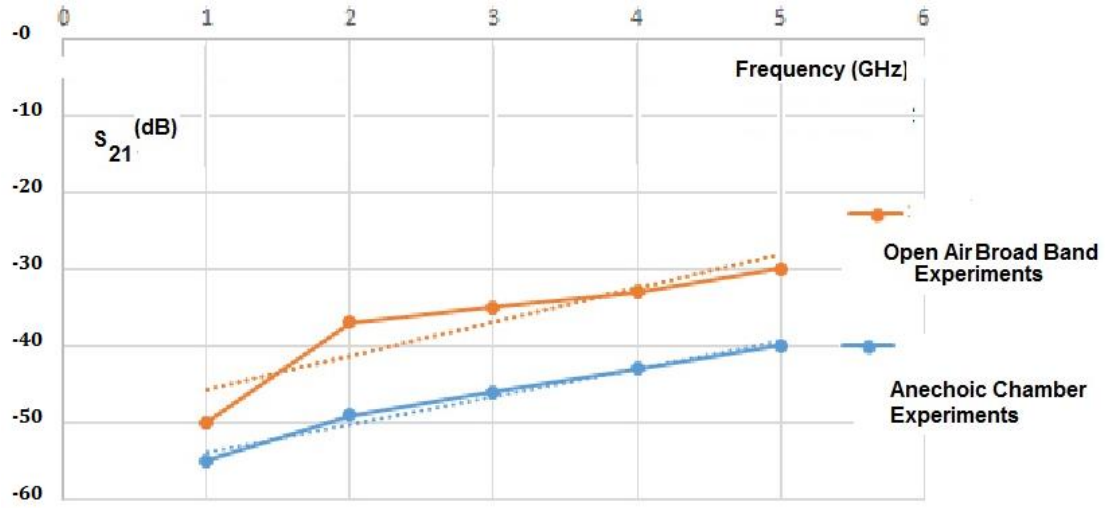

Figure 4-11 the extracted error between PAni anechoic chamber and OEMI experiment

This error shown in figure 4.11 resulted from a combination of the reflection, load matching, diffraction, and other frequency interferences at the time of the experiment.

The whole verification process is summarised in figure 4-12 below, the process was repeated for all the shielding devices that was used in OEMI experiments.

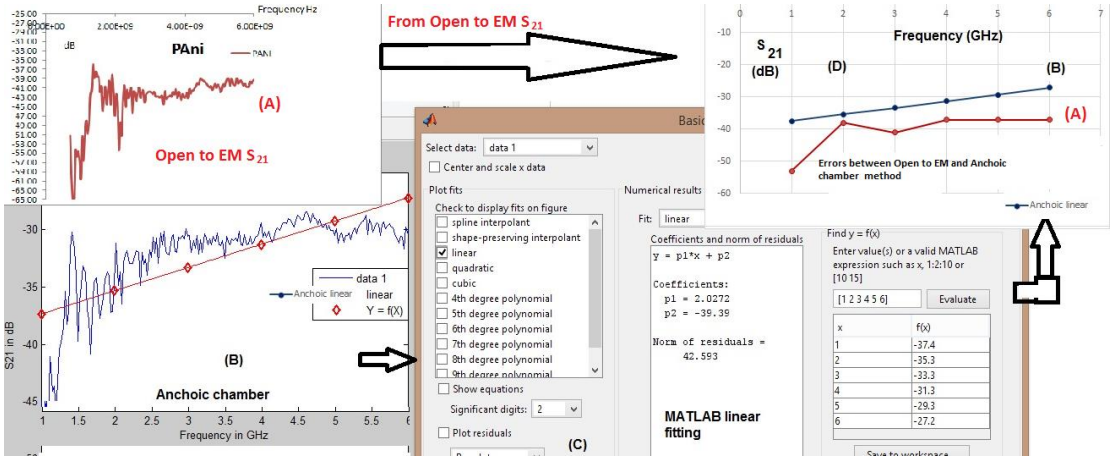

Figure 4-12 A summary of the verification pross

Manual Calibration of EC5071C VNA is important in reducing errors, the two VNA used different calibration methods. The EC5071C requires short, open and matched calibration, while the Rohde-Schwarz ZVL in the anechoic chamber method used an automated calibration method. However this shouldn't give any errors if calibration procedure is followed for EC5071C. The calibration process is described in details in the process is described in the manufacturer website link http://cp.literature.agilent.com/litweb/pdf/5989-5478EN.pdf .

Conclusion

In light of the literature reviewed in Chapter 2 and the methodology discussed in Chapter 3, this chapter outlined the results of narrowband and wideband experiments undertaken to address the research questions stated in Chapter 1. The OEMI experiment that is used in chapter 4 is justified by the acceptable error that is produced using a simple linear fit that relates the data values at three important frequencies.

The next chapter outlines the results of the simulations undertaken to address the research questions stated in Chapter 1.

Chapter 5. Modelling

Introduction

In the light of the literature reviewed in Chapter 2 and the methodology discussed in Chapter 3, this chapter outlines the results of the simulations undertaken to address the research questions stated in Chapter 1. It presents the results of:

- constructing COMSOL and HFSS simulation models to assess the transmission loss and generate the necessary data for comparing the modelling and experimental results,
- developing computational models of both the narrowband and wideband experiments to characterise the shielding devices and obtain the simulated transmission loss properties of each shielding device created to enable the ICPs to be compared with other materials used for EMI shielding, and
- comparing the computational shielding model results with the experimental results for both PPy and PAni.

Narrowband modelling

The narrowband modelling process was used to model shielding devices that protect systems from the interference that normally arises from deliberate transmissions such as radio and TV stations, pager transmitters, mobile phones, etc. and it is centred on the Wi-Fi frequency 2.45 GHz.

The following simulation results for transmittance loss S_{21} as function with narrowband frequency relate to the narrowband experiments in Chapter 4 with Wi-Fi transmitter and receiver of EM through Yagi-Uda antenna at operating frequency of 2.45 GHz. The 2D was the first step, in order to use the data that was acquired, with the second step is to visualise and then quantify through comparing the transmission loss of the ICPs shielding devices and try to correlate the visualisation the narrowband experiments. As the thickness was fixed and differ because of the scarcity of the ICPs materials and the variation of the materials state for two types shielding devices of liquid (coated on substrate) and felt materials. 2D simulation has many advantages in that it is easy and requires little computing time. COMSOL is the only commercial FEM that uses 2D.

The first simulation was done with a 2D square that measured the same as the aluminium screen 0.2m by 100 m compartments with no shielding device in the gap in the middle of aluminium screen as shown in Figure 5-1.

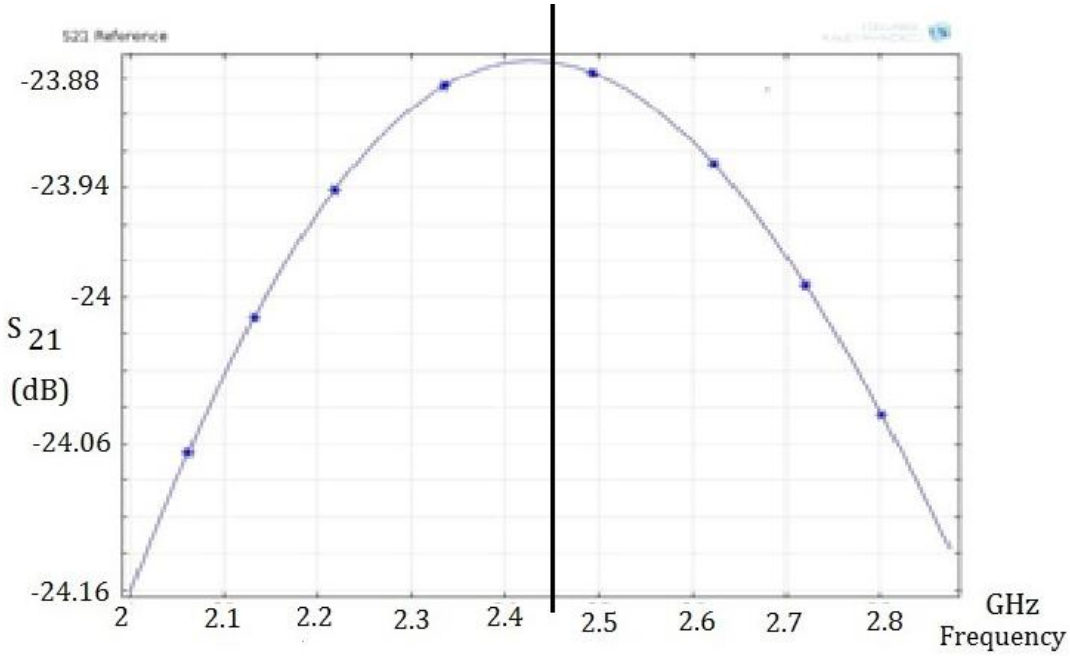

Figure 5-1. Reference with no shielding narrowband 2D model

Figure 5-2 shows the results of entering the relevant material parameters from the manufacturer's data sheet and simulating insertion of a PEDOT shielding device holder measuring 150mmX150mm.

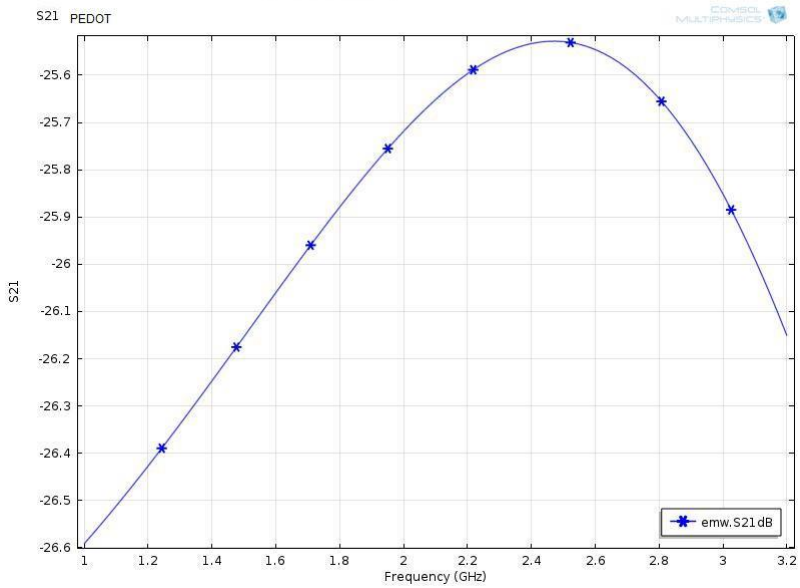

Figure 5-2. Narrowband 2D PEDOT model

Figure 5-3 shows the results of entering the relevant material parameters and simulating (insertion of a PPY shielding device in the shielding device holder).

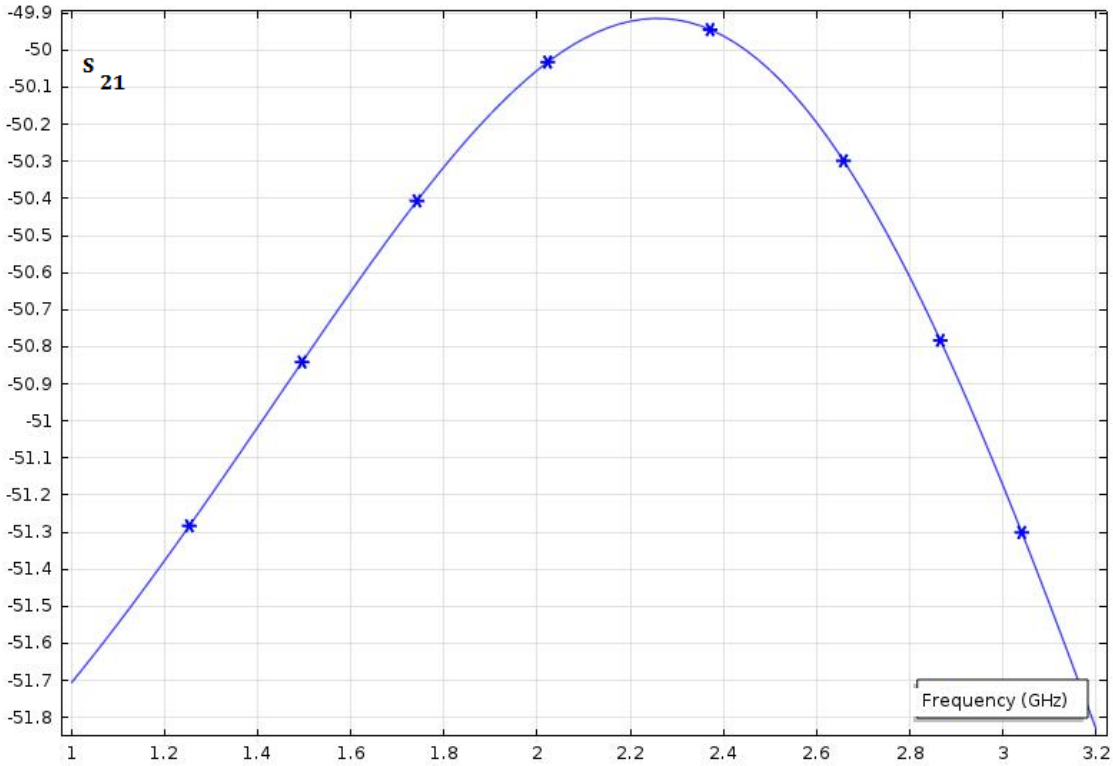

Figure 5-3. PPY narrowband 2D model

Figure 5-4 shows the result of entering the relevant material parameters and simulating the insertion of a PAni shielding device in the holder.

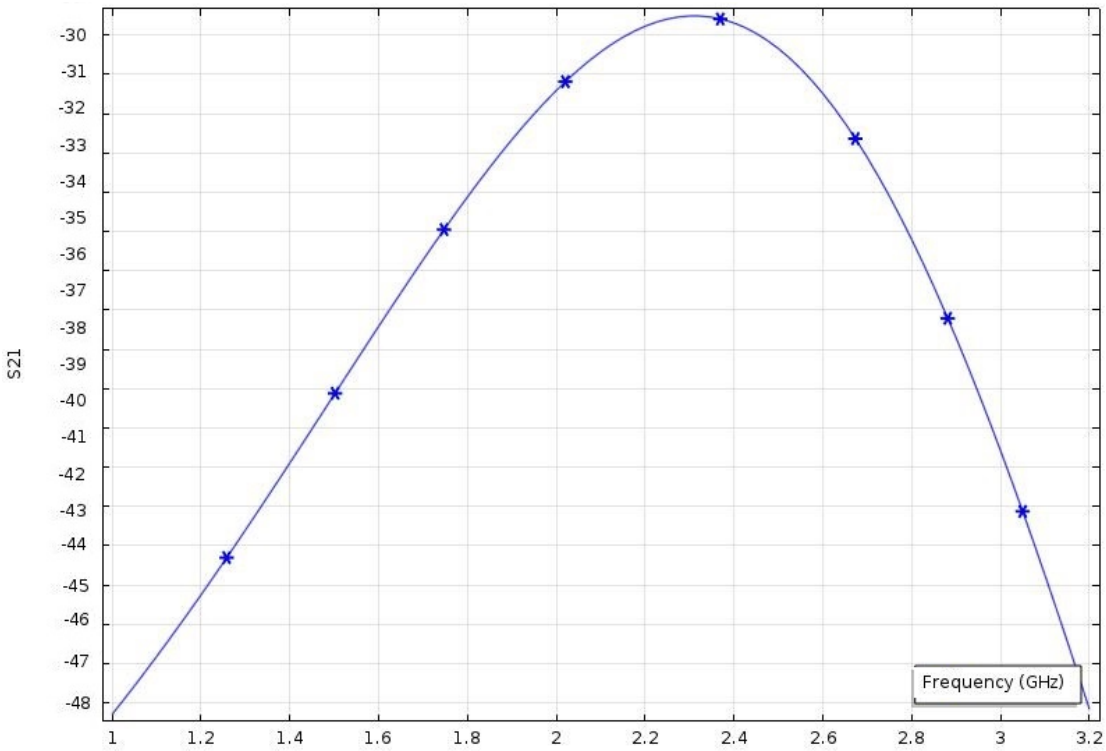

Figure 5-4. Narrowband 2D PAni S_{21} parameter

The figure below shows the S-parameters as a function of frequency of the Wi-Fi antenna of 2.45 GHZ.

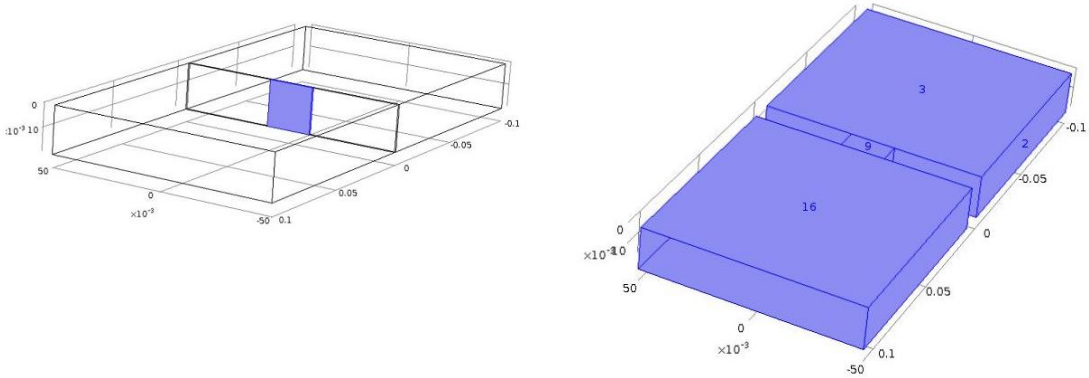

Figure 5-5. 3D wideband model

COMSOL 3D simulations

A 3D model was devised to add another dimension to the 2D model and better model the experimental results presented in Chapter 4. In this model, a 3D square aluminium box of size 0.1m is separated by a gap of 0.015m from another 3D aluminium box. The shielding device is inserted into the gap between the two metal

exterior boxes adjusted and scaled to simulate the 3D experimental results of Chapter 4.

The following simulation results for transmittance loss S_{21} as function with narrow band frequency 2.45 GHz that relates to the narrow band experiments in chapter 4 with Wi-Fi Yagi-Uda antenna with operating frequency of 2.45 GHz. Figure 5-10 shows the results of the first simulation done with a 3D square that measured the same as the aluminium screen 0.2m without any shielding device in the middle of aluminium screen.

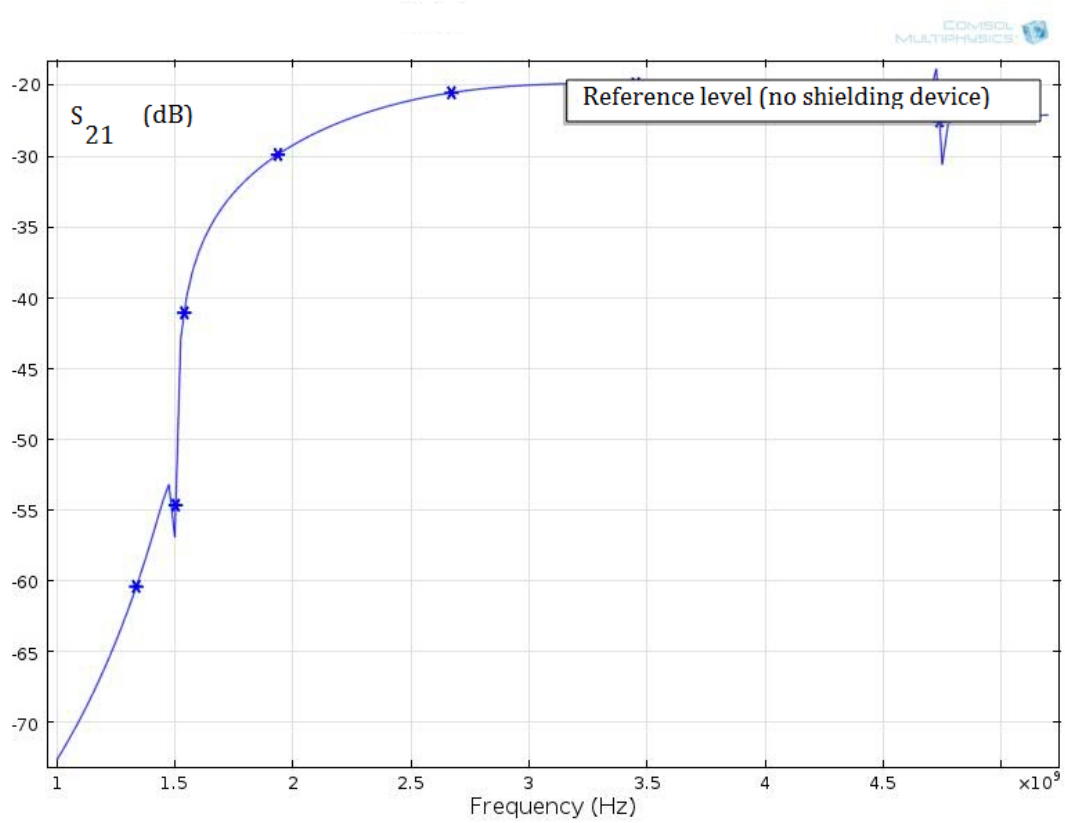

Figure 5-6. Reference 3D narrowband simulation (no shielding device)

Inserting a PPy shielding device between the transmitter and the receiver, the reduced the transmission losses S_{21} is shown in Figure 5-7.

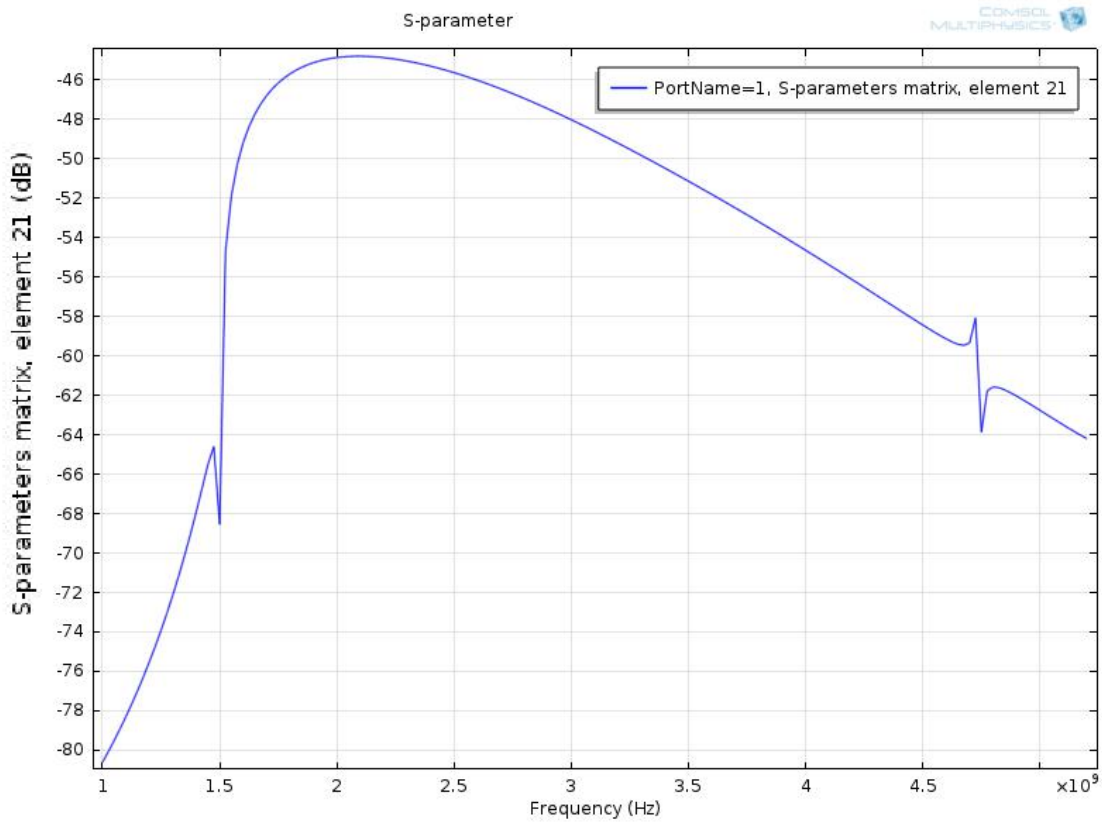

Figure 5-7. PPy S_{21} 2D shielding model

Figure 5-8 shows the results of a wideband 1-6 GHz simulation for a PPy 3D model with a PPy shielding device inserted between the transmitting horn antenna box and the receiving antenna box. The blue data points on the simulation plot are selected for comparison with the 3D experimental data at those frequencies.

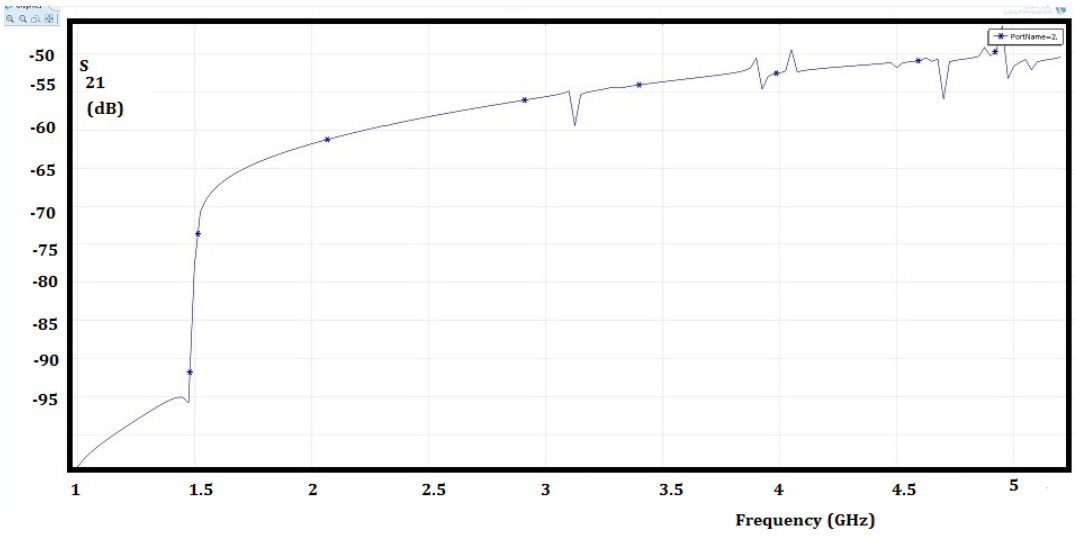

Figure 5-8. 3D wideband PPy shielding device simulation

The PPy shielding device was then replaced with the PAni shielding device.

HFSS 3D validation results

The first 3D simulation was attempted with current shielding device between the transmitter and the receiver and both the transmitter antenna and the receiving antenna encapsulated in a waveguide as shown in Figure 5-9 produced the results shown in Figure 5-10.

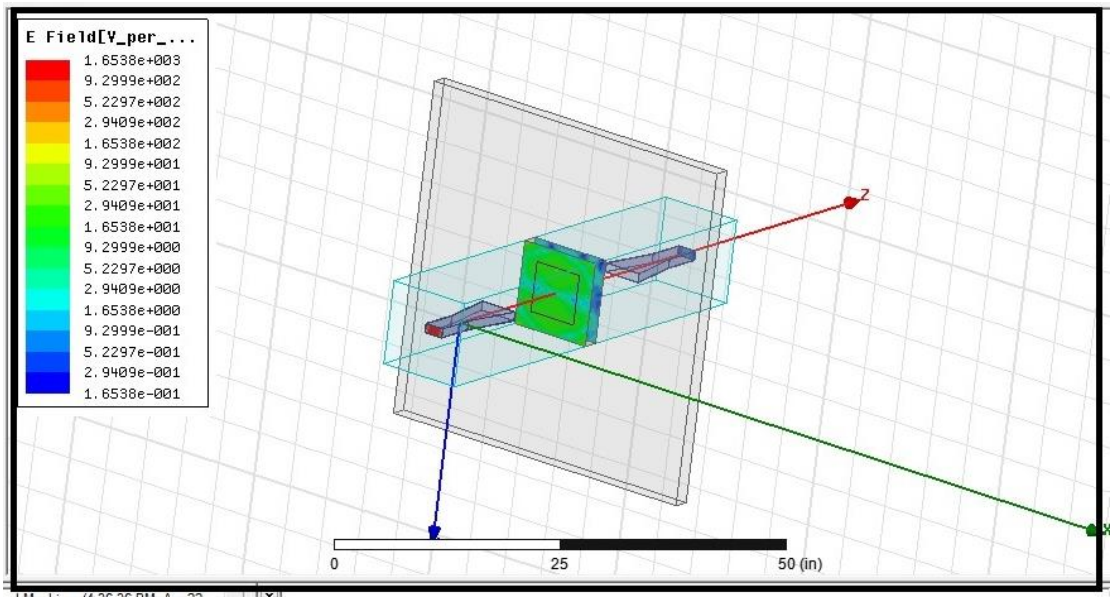

Figure 5-9: The first attempted HFSS 3D wideband model

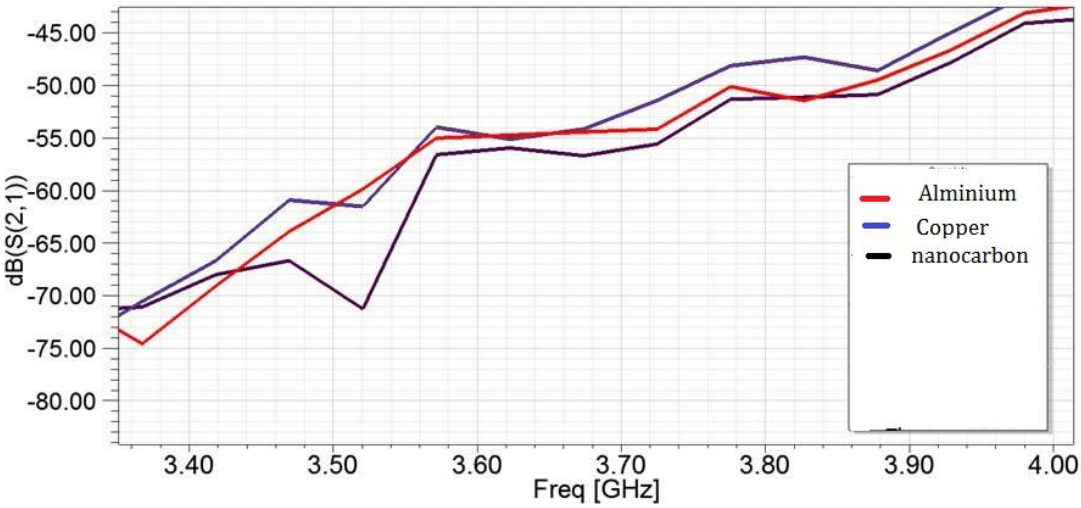

Figure 5-10. 3D-wideband S_{21} simulation with metal and carbon shielding devices

Running the HFSS simulation for material properties of current shielding device took a full day and for 1 GHz bandwidth, as it can be seen from the running time on figure 5-9. To reduce the running time, the model was simplified by removing the waveguide around the antennas as shown in Figure 5-11.

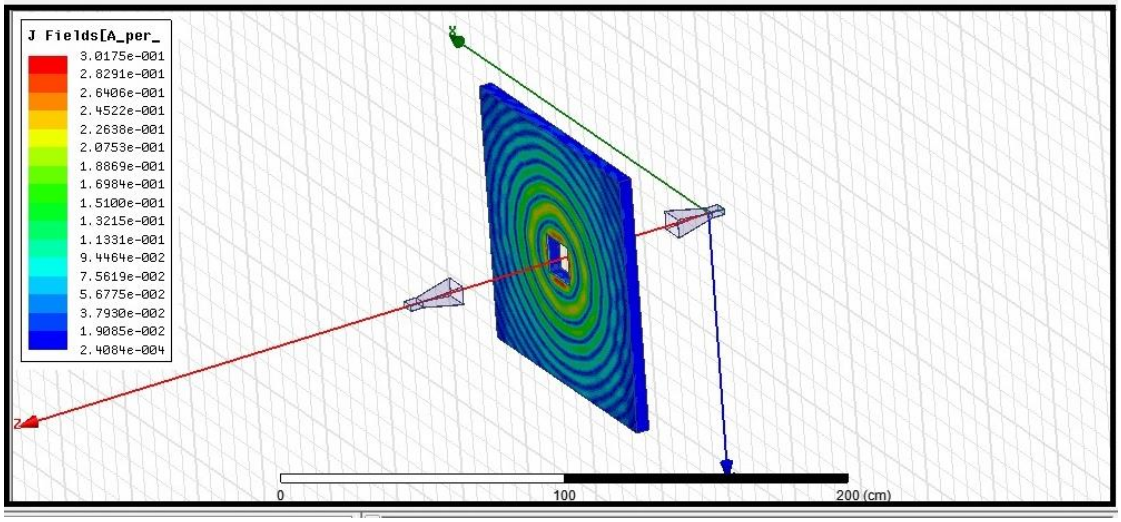

Figure 5-11: HFSS second validation model

This model was used to generate the transmittance loss S_{21} as a function with wideband frequency for 1-6 GHz that compares with the wideband COMSOL simulation results presented earlier in this chapter. Figure 5-12 shows the S_{21} versus the operating frequency for the HFSS simulation with PPy as a shielding device and Horn antennas operating in 1-6 GHz.

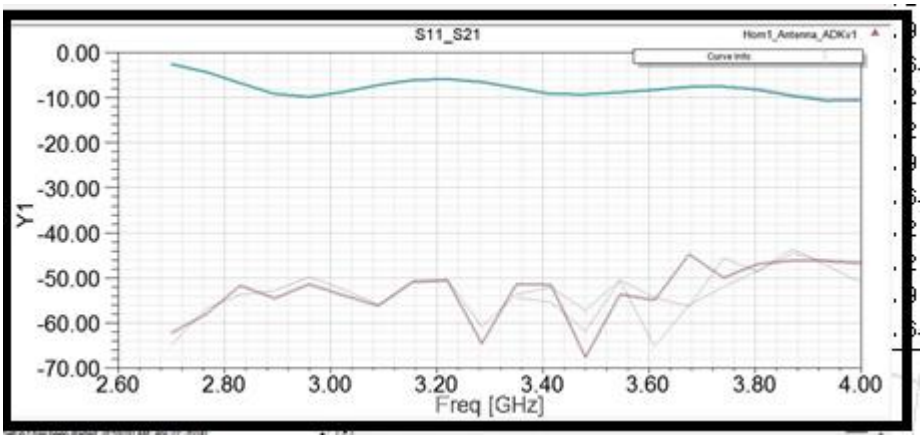

Figure 5-12. HFSS S_{11} and S_{21} simulation of PPy shielding device

The next step was to remove the shielding device in the simulation between the transmitting horn antenna and the receiving horn antenna. Figure 5-13 below shows

the 3D model results with no shielding device between the transmitting horn antenna box and the receiving antenna box.

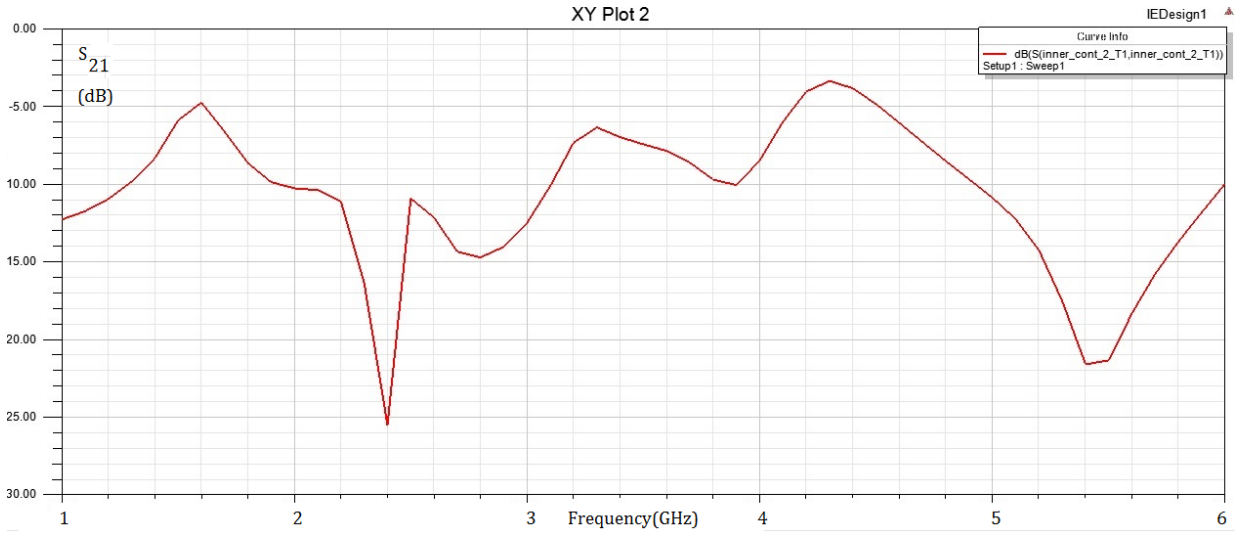

Figure 5-13. HFSS S_{21} simulation with no shielding device

The initial results were very limited in numbers compared to the results obtained with COMSOL software. These initial results showed the simple and easy-to-run COMSOL simulation closely approximated the more specialised HFSS simulation software.

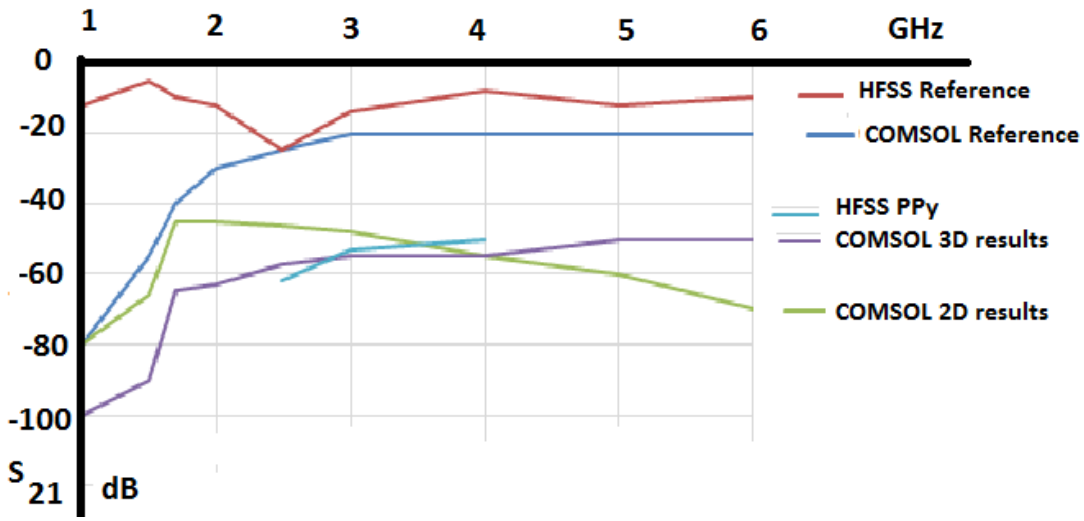

Figure 5-14 HFSS initial results compared to 2D and 3D COMSOL simulations

Although a very limited HFSS simulations that mainly concerned with PPy shielding devices that shown in figure 5-14. The simulation results of COMSOL 3D seems to follow closely the HFSS simulation while the COMSOL 2D simulation results diverge downwards.

Scope for further modelling research

Clearly, there is scope for further simulation work using methods other than Finite Elements Method (FEM) such as:

- Method of Moments (MoM) is used in ZELAD software, and is faster than other solvers that were used in this research.
- Finite Differences in the Time Domain (FDTD). Unlike other finite elements modelling methods. FDTD runs well with various arbitrary shapes also has a wide bandwidth and can be used in parallel computing.

Accuracy of the FEM results could be shown via the JCM suite software, which uses advanced mathematical methods and technologies from computer science to deliver exceptionally short computation times, compact data space requirements and highly robust software. JCM suite uses automatic Fourier decomposition to drastically cut the computation time while increasing accuracy.

Conclusion

This chapter outlined the results of the simulations undertaken to address the research questions stated in Chapter 1. The COMSOL modelling started with simple 2D narrowband around the Wi-Fi frequency 2.45 GHz before focusing on the 3D frequency band between 1 and 6 GHz.

Simulation of the S_{21} experimental results after the anechoic chamber verification and the experimental results proved to be 90% accurate based on straight line fit.

The 3D (HFSS) software was used to validate the COMSOL model results, but the completed HFSS model required both large amounts of memory and long processing time. The figure below shows the amount of time it took to draw the model, it took more than 24 hours to plot a more complicated model to the OEMI method.

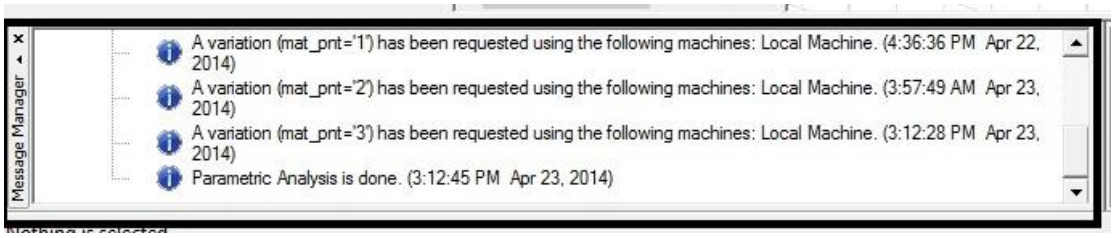

Verifying the COMSOL method through a very small number of HFSS simulation software runs showed that it had acceptable accuracy Use of general COM-SOL

software is therefore an appropriate method to solve Maxwell equations while usefully constraining both computation time and memory needs. However the interpretation of the data can be said that it is lacking substance and rigor because of the number of data points and also ignoring the antenna‘s parameters. In the present form, it is not possible to judge if the results are consistent or not but it is an initial step towards adapting the OEMI method for testing new types of ICPs shielding devices and comparing the transmission loss with other shielding devices. As a result of this modelling it would have been better to use the waveguide 3D model in COMSOL to represents a measurement in a rectangular waveguide. The next chapter compares the experimental results with the verified simulation results.

Chapter 6. Comparing experimental results and simulations

Introduction

This chapter compares the experimental results with the verified simulation results. It investigates whether the Electromagnetic Radiation (EMR) measurement simulated by COMSOL 4.3b provided valid results with the experimental data. This model has its advantages in EMC design with better cost effective design that include less Electromagnetic (EM) reflection, that can help improve the functionality of any device based on ICP materials.

A linear model was used to compare the modelling results and the experimental data. By comparison with other mathematical models (logarithmic, polynomials of different degrees, and moving average), the linear model is simple and shows the errors between the actual measurements and the simulation model.

PAni narrowband shielding device comparison

Figure 6-1 below shows the experimental data results in blue with the straight line approximation and the COMSOL simulation results for six selected frequencies between (2-2.7) GHz. As discussed in Chapter 5, this narrowband simulation positioned the PPy shielding device surrounded by two aluminium chambers in a mid-wall on which the s SDUT was placed. One chamber was attributed as the transmitter side and the other chamber is as a receiver chamber. The dimensions of the chamber were optimized for operating range of 2-3 GHz. Both the simulation and the experimental setups had a maximum dynamic range of approximately 60 dB over the entire frequency range and the various SDUT.

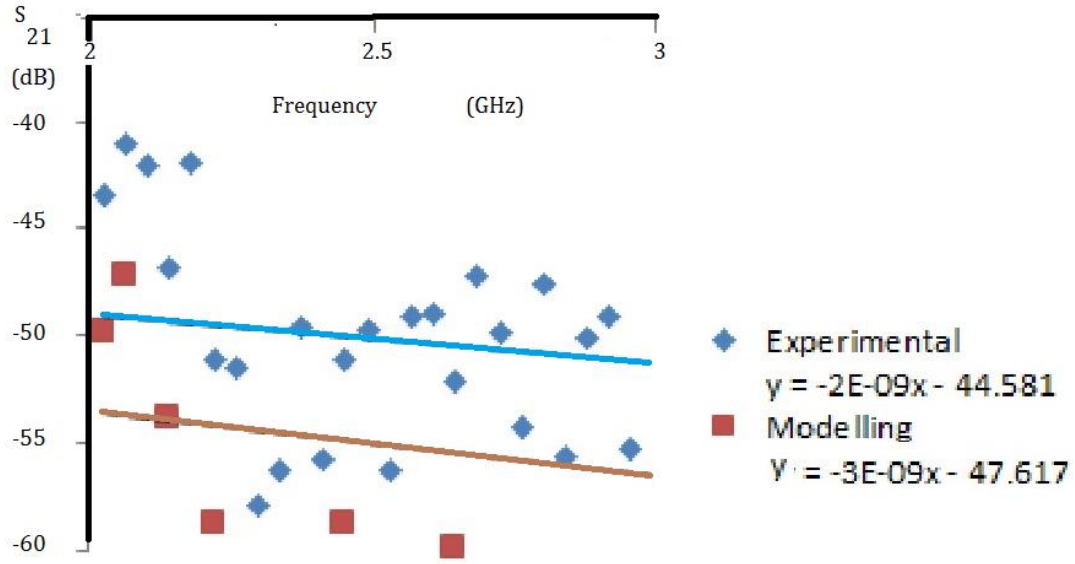

Figure 6-1. PPy narrowband shielding device simulation vs experimental results

COMSOL simulation results obtained from the 2D model were compared to the experimental results obtained for the narrowband of 2-3 GHz. These results were used to verify the electromagnetic transmission loss measurements that can be used in PAni shielding device applications such as radiated emissions & immunity, shielding characterization of connectors, antenna measurements, characterization of material properties, etc. The PAni experimental results presented in Figure 6-2 were obtained at room temperature for a square-shaped PAni-coated shielding device.

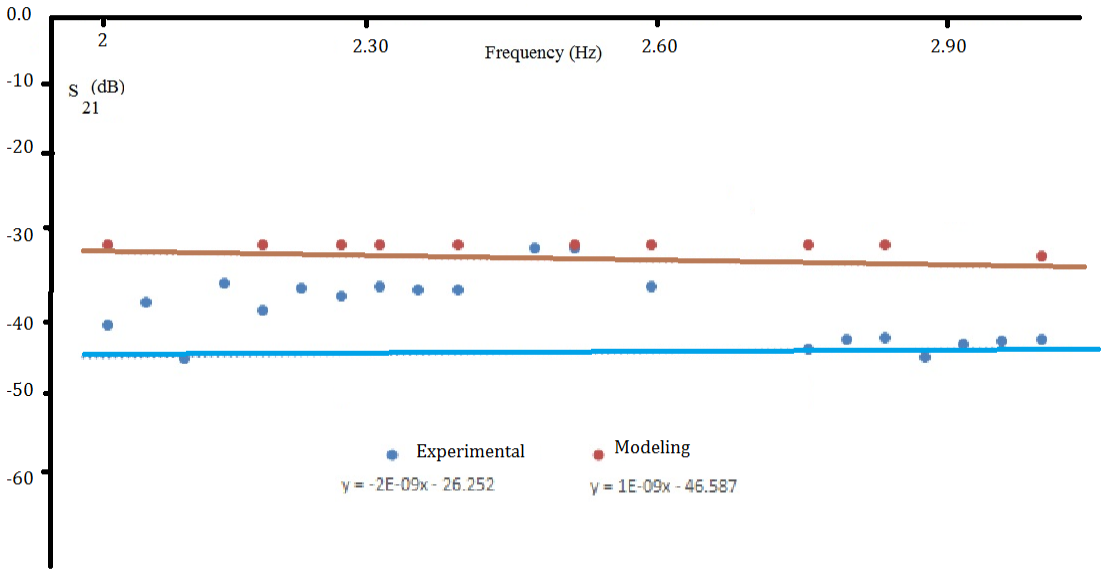

Figure 6-2: PAni narrowband shielding device experimental vs. modelling results

As the scatters in the data were imprecise, a straight line of best fit was generated via Excel using the method of least squares. The linear model for the modelling data is y = -2E-09x - 26.252, and the model for the experimental data is y = 1E-09x - 46.587. These results show a relationship between the experimental and simulation data points represented by two straight lines approximations with a constant error between the two straight lines. Error parameters could be added to correct the COMSOL model to take account of other experimental factors.

PAni wideband shielding device comparison

A new PPy shielding device was tested in Chapter 4 and then as discussed in Chapter 5, the simulation results of the wideband simulation data points were obtained with the PAni shielding device surrounded by two aluminium chambers in a mid-wall on which the SDUT was placed. One chamber was attributed as the transmitter and the other as a receiver. The dimensions of the chambers were optimised for operating range of 2-5 GHz. Both the simulation and the experimental setups had a maximum dynamic range of approximately 60 dB over the entire frequency range. The comparison of OEMI testing results with the COMSOL modelling results is shown in Figure 6-3 below.

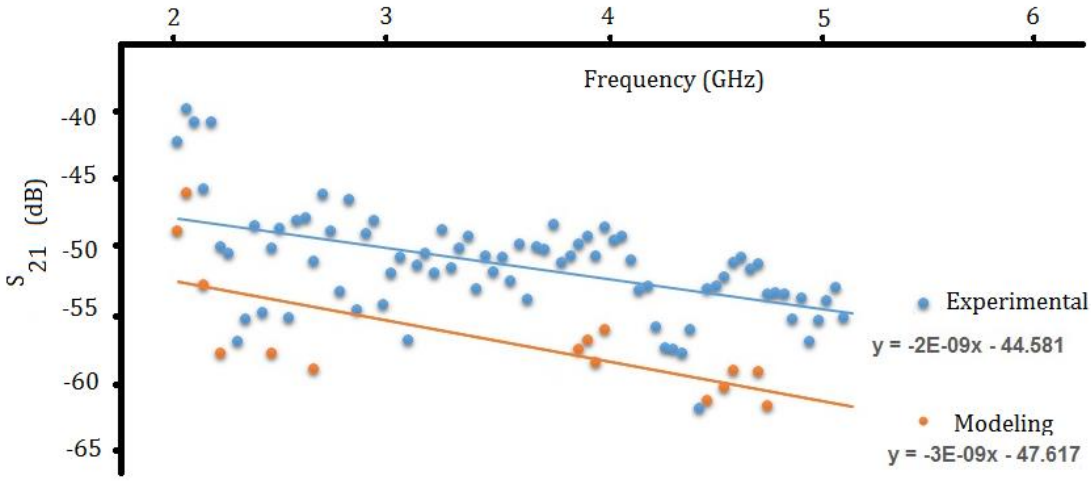

Figure 6-3: PPy wideband shielding device simulation vs experimental results

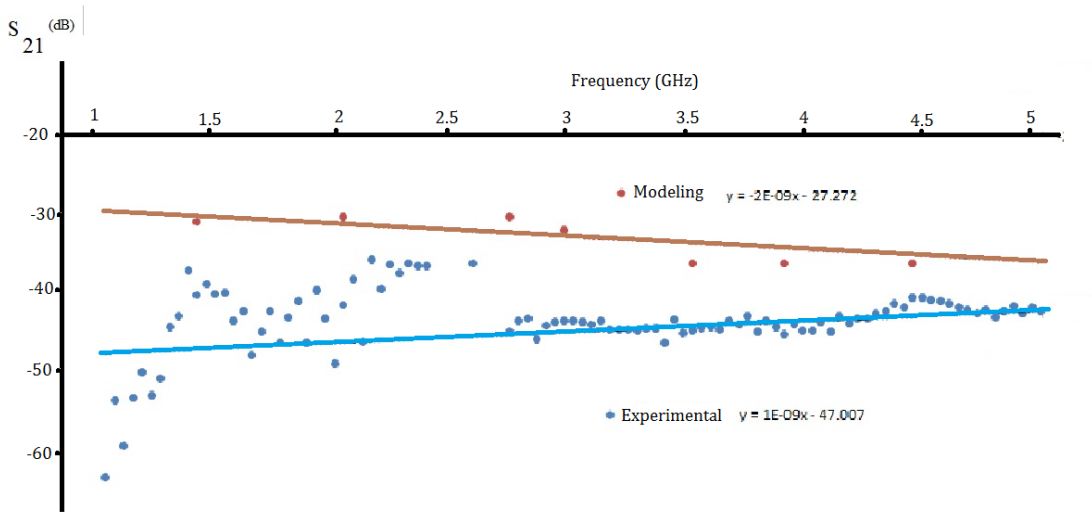

Figure 6.4: Modeling vs. Experimental PAni wideband shielding device

As the scatters in the data were imprecise, a straight line of best fit was generated via Excel using the method of least squares. In Figure 6-4, the experimental data results are shown in blue with the straight-line approximation of y = 1E-09x - 46.757. The more than 100 experimental data points were compared to the COMSOL simulation results for selected (7) COMSOL data points between 2-5 GHz that are shown in brown as a straight-line approximation of y = -2E-09x - 27.272.

These results show a relationship between the experimental and simulation data points represented by two straight lines approximations with a constant error between the two straight lines. Error parameters could be added to correct the COMSOL model to take account of other experimental factors.

Conclusion

This chapter compared the experimental results with the verified simulation results. The COMSOL simulation model approximated the experimental data points obtained from the OEMI experiments. These results show a relationship between the experimental and simulation data points represented by two straight lines approximations with a constant error between the two straight lines for both results of the PPy shielding devices. Error parameters could be added to correct the COMSOL model to take account of other experimental factors. One of those error sources is to select a method for measuring antenna far-field patterns, polarization,

input impedance, gain and directivity that those experiments in this chapter neglected if those experiments to develop further in the use in mobile communications and telecommunications shielding technologies.

Antennas experiments require sound theoretical background in antenna theory, radiation and state of art equipment capable of providing the necessary accuracy and purity of the measured data. Another error is the size of the aperture in the conductive plane is close to a free space wavelength. This causes major issues when the permittivity of the insert changes the effective size of the aperture.

Another source of error is the effect of cable radiation even though the cables are in relatively close proximity to each other. This elimination is done through the calibration process but the error source will affect the results.

The next chapter presents the results of laboratory experiments investigating the impact of EMI-shielding materials on the culturing of a much-studied species of bacteria.

Chapter 7. Can shielding materials influence bacterial growth?

Introduction

This chapter presents the results of laboratory experiments investigating the impact of the ICPs and other materials currently used in the mobile phone industry on the culturing of a common bacteria. It also highlights scope for further research on how greater use of ICPs could impact environmental and health matters.

Materials and Method

The main item is to grow the E.Coli in specially prepared Petra dishes. Blood agar with 5% blood is an excellent medium for growing E.Coli bacteria in nutrients and an environment that the E.Coli bacteria to grow, other materials like gloves and distilled water, . The samples of PPy ICP shielding devices compared to the most popular I Phone 3 as it is shown in Figure 7-1

Figure 7.1 Two samples of shielding devices (PPy and current IPhone 3)

The procedure of the experiment is explained briefly in chapter 3.

Results

The preliminary results summarised in Table 7-1 clearly show that the PPy shielding material inhibited bacterial growth to a greater extent than the material used in the iPhone 3 cover. These results indicate that ICP may offer significant advantages over conventional phone materials in terms of bacterial control.

Table 7-1: Number of coliform bacteria colonies present on agar plate

Shielding type	Trial 1	Trial 2	Trial 3
IPhone 3	1700	1800	1700
ICP (PPy)	700	700	500

This was an initial investigation into this aspect of mobile phone shielding devices, its results are indicative rather than definitive. This brief experiment did not aim to demonstrate a statistically significant difference in terms of a shielding material's ability to inhibit bacterial growth under controlled laboratory conditions. The marked difference in the results obtained for the two different types of shielding does, however, suggest scope for further research.

Scope for further research

There is clearly scope for further systematic tests of the PPy shielding device material and other ICP materials to verify the preliminary results presented in this chapter. Other investigations could also be conducted to see whether ICP shielding devices had any demonstrable short-term or long-term impact on sleep disturbances, heart palpitations, migraines and general health of people using mobile phones and Wi-Fi devices.

In term of health and environmental impacts, it is likewise worthwhile to contemplate what happens when these devices reach the end of their working lives. Mobile phones are currently discarded in large quantities each year as newer technologies emerge. The discarded mobile phones can have long-term damage on the environment. Work is needed to research the materials that can be recycled and ways to reduce toxic wastes at landfills. As ICP materials use no toxic materials, their

increasing use could protect the environment by reducing waste and encouraging recycling.

One of the key advantages of using ICP shielding devices is that they are made of 100% plastics and plastics are an area of significant manufacturer research. While having embedded metal parts makes some existing plastics difficult to reuse, eliminating metal parts facilitates recycling. Manufacturers are already exploring ways to improve ease of recycling and testing the suitability of compostable bio-plastics made from plant materials.

Conclusion

This chapter presented the results of laboratory experiments investigating the impact of the ICPs and other materials currently used in the mobile phone industry on the culturing of a much-studied common bacteria. It also discussed the scope for further research looking at the health and environmental impacts of incorporating ICPs into mobile phone and Wi-Fi devices.

The next chapter reviews the methods used to address the study's research questions and discusses findings obtained over the four years of the study, their significance and scope for further research.

Chapter 8. Conclusions and future work

Introduction

This chapter reviews the methods used to address the study's research questions and discusses findings obtained over the four years of the study, their significance and scope for further research.

Advantages and limitations of the methodology adopted

As noted in Chapter 3, this researcher encountered difficulties in getting ICPs materials for thickness measurements, payments, equipment, software license approvals, access to anechoic chambers, difficulties arranging the transfer of the test equipment to the anechoic chamber, delays in obtaining up-to-date computing facilities to run the selected simulation software. All of the factors constrained the methods adopted and the extent of experimentation and simulation. The methodology adopted was, however, able to adequately address all the research questions that were originally proposed at the start of the research.

The overarching research question

This thesis focused on the making, testing and modelling of ICP shielding devices for future use in mobile phones and Wi-Fi devices. My over-arching research question for this research study was whether ICPs tuneable (focused on the shielding device) to the frequency range between 1 - 6 GHz have potential to replace the current EMI shielding for mobile phones and Wi-Fi devices in OEMI environment. This study also explicitly addressed a number of subquestions (SRQs) relating to the ability of ICPs to shield and alter the transmission losses of the Electromagnetic Radiation (ER) at the main desired Wi-Fi microwave frequencies.

By successfully evaluating a selection of currently commercially available ICPs discussed in the recent literature (nature) in the Wi-Fi band between (1-6 GHz), I have shown that ICPs tunable (Focused on the shielding device) to the frequency range between 1 - 6 GHz do have potential to replace the current EMI shielding for mobile phones and Wi-Fi devices. Evidence that ICPs can enhance or replace the current shielding materials should promote the reduction or elimination of metals and carbon shielding materials in a new generation of

mobile phones and Wi-Fi devices. This use of ICPs could reduce the current environmental problems and health concerns.

The next few sections explicitly address each of the subquestions (SQs) within my overarching research question.

SQ1

This question asked 'Can simple experiments or simulations demonstrate whether ICPs can perform EMI shielding at least as well as the forms of shielding currently in use?"

I have shown that simple, inexpensive experiments and simulations do demonstrate that ICPs can perform EMI shielding at least as effectively as the forms of shielding currently in use. This thesis provided evidence obtained from experiments and simulations showing ICPs can provide effective EMI shielding for Wi-Fi devices and mobile phones.

This was achieved by:

- identifying the key ICPs to use in both the laboratory experiments and in simulations intended to realistically model the expected transmission loss (see Chapters 2 and 3),
- selecting the metals and microcarbon shielding devices to be compared with those ICPs through laboratory experiments (see Chapters 2 and 3),
- purchasing the required materials (see Chapter 3),
- designing and constructing the selected shielding devices to be used in the experiments and in simulation models to quantitatively assess each shielding device (see Chapter 3). This research used the new generation of VNA where calibration eliminated the many reflections and diffraction scenarios problems that had previously prevented use of an OEMI method,
- performing a series of narrowband experiments to assess transmission loss coefficients for each shielding device (see Chapter 4),
- performing a series of wideband experiments to assess transmission loss coefficients for each shielding device in anechoic chamber in order to verify the transmission loss shielding property of each by shielding device used in the OEMI method experiments,

- constructing COMSOL and HFSS simulation models to assess the transmission loss S_{21} and generate the necessary data for comparing the modelling results with a series of OEMI experiments,
- developing computational models of both the narrowband and wideband experiments to characterise the shielding devices and obtain the simulated transmission loss properties of each shielding device created to enable the ICPs to be compared with other materials used for EMI shielding, and
- comparing the computational shielding model results with the experimental results and produce a straight line fit for both PPy and PAni.

Comparison of the experimental modelling results showed the possibility of implementing the simulation model and applying it universally across all the shielding devices made from different IPC materials.

The accuracy of the modelling and the experimental data were analysed by a least squares straight-line approximation. The straight-line approximation was used because of the combination of different types of data that were taken under different conditions. Models fitted to the experimental data provide prediction rules for various ICP shielding devices in similar situations.

Future improvement on the modelling results is required to yield accurate material properties measurements. For this research, the relevant material properties were obtained from data sheets and the literature and no actual material measurements were undertaken to confirm the accuracy of those data. As the material properties affect the accuracy of the simulation, on-site measurements of the material properties of the shielding device might reduce the errors.

SQ2

This question asked ‘Which materials and forms (solids, liquids, gels) of ICPs are most effective as EMR shielding?’.

At present, the ICP materials investigated are expensive, difficult to manufacture and require ingredients not readily obtainable. Use of those materials in EMI shielding devices would, however, provide impetus for further development of ICP materials and enhancement of their technological performance.

Further research is still needed to address the process of improving the speed of producing high yield ICP materials with an accurate conductivity. The doping process should be classified according to the nature of the applications. The type of doping and the development of nanomaterials research produce better conductivity enable comparison of those nanomaterials with the current ICP materials.

All of the ICP shielding devices selected, constructed and tested by this researcher yielded results showing that these devices were similar or better than the current shielding materials. This research has shown that liquid and felt forms of ICPs can be effective as EMR shielding. The highest level of transmission loss S_{21} occurred when ICP device material was made of woven fabrics rather than a liquid PEDOT or PAni solution.

The narrowband experiments suggest the ICP transmission loss S_{21} could be improved by using a liquid rather than a woven PPy fabric, from solid to liquid and varying the frequency. The wideband experiments suggest liquid ICP shielding devices could be further improved by combining different doping chemicals with the PAni and the PEDOT and edge diffraction on the corners of the shielding device under test.

ICPs are already used in antistatic coating applications in electronics components. As an active component, ICP is used to make the windows and mirrors reflective when current is applied, poly(3,4-ethylenedioxythiophene)-poly(styrene sulfonate) (PEDOT-PSS). A product like Clevios P has been extensively used as an antistatic coating and commercialised by Bayer AG laboratory. The successful incorporation of new ICPs into the shielding devices would serve to introducing those materials into other fields such as industrial devices, agriculture, medical, car industry, aviation and military devices. Use of ICP materials should help to improving the 3D printing industry.

As a liquid conducting material, PAni is very effective for use in future printed circuit boards (PCB) with e-beam lithography. This process can make the PCB smaller, lighter and corrosion-resistant.

ICPs in the form of nonwoven fabrics clearly have many applications beyond their use in EMI shielding. There is potential to produce clothing items such as scarves, hats, socks, pajamas and anything else that can knitted from radiation-reducing fabric.

SQ3
This question asked “What other advantages might the ICPs confer?”

This thesis highlighted the potential benefits associated with the use of ICPs in EMI shielding in Chapter 1 and 2 as well as providing experimental evidence in Chapter 7 of the greater anti-bacterial properties of the ICPs compared with shielding materials used in an iPhone.

Scope for further research
This research suggests scope, and provides a firmer base for, more in-depth research regarding for future use of ICPs in shielding devices for mobile phones and Wi-Fi devices. The ICP shielding devices are also important in a new branch of military research called spectrum warfare and electronic warfare (EW) that are emerging in the top U.S. military priority.
The research was a pilot research in this field and further rsearch needs to observe the following points:

- Although all the shielding devices were tested in the same EM radiation environment but problems from cable radiation and cable coupling. Precautions regarding the feed cables and the radiation field distances.
- The balanced Yagi-uda antenna with integrated balun gave, high gain, good performance with large bandwidth to cover the shielding device at 2.45GHz frequency. In this research, the effects of antenna performance has not been

included and future research should include the antenna's description and parameters.

- Although aluminium tape was used to seal the edges which is a desirable to have good electrical contact across the aperture and acts as an enclosure comprises a lid and a box made of highly conductive material, preferably mild steel without adhesive. This practise improved the EMI of the device. In the future experiments there should be a pattern on the conductive tape that provide cancellation of the adjacent electric field lines. This practice will provide multiple point contact between the electric field lines on the tape that provides conductance and by earthing the experiment, the results can be improved.
- Thickness of the shielding devices was not considered and future research should look into how to include the thickness in the model, and also Frequency Selective Surface pattering if a method of accurate coating is successfully applied. The ICP's materials is great candidate for such application. In this thesis attempt to create FSS shielding was stopped when the spin coating was abended and replaced by dip coating method.
- The conductivity can be made to change by including ICPs materials in bulk materials pr conducting polymer, as seen in the changing of conductivity with 1dB and when the temperature was removed the conductivity returned back, a further experiments are needed to establish the rigger for this important application.
- The research is focused on "OEMI method" this method is used to compare rather than characterise the shielding device on the same EM condition without subjecting the device to absorbers or faraday cage. There was a suggestion by an expert in the field EM that "a parallel-plate arrangement of using two metallic plates (at distance of a few centimeters) and small quantity of absorber material (e.g. Eccosorb) to reduce echoes on side walls. This 2D equivalent of an anechoic chamber would allow also a direct comparison with 2D simulations, however this suggestion came at a very late stage of the research and this is was approved by the University for extra funding.

Other potential developments include electrostatic materials, conductive adhesives, printed circuited boards, artificial nerves, antistatic clothing, piezo ceramics, active electronics (diodes, transistors), aircraft structures, switches, molecular electronics, electric displays, chemical sensors, rechargeable batteries, drug release systems, optical computers, ion exchange membranes, electromechanical activators, and smart structures.

Use of PAni as a liquid conducting material has potential to make printed circuit boards (PCB) smaller, lighter and corrosion-resistant. Use of PAni to replace copper in telephone wires would confer similar advantage and enhance the reliability of telephone networks requiring both PCBs and copper wires.

Another potential research is the use of ICP's material in replacing the copper wires that are currently used for voice and data communications. The copper wires that currently are used is out of date and voice telecommunications. The following pictures shows the urgent need to start replacing them with ICP's wires.

Figure 8.1 The current state of the copper telecommunications underground wires and the various attempts to stop copper from rusting (curtesy of 3A Kathy Telecommunications Pty Ltd)

Figure 8.1 above shows the long term danger on the collapse of the data communication that banks, security alarms, and day to day broadband communications depends upon. The copper industry is out of date and the other alternative fibre optics is expensive to test, dangerous to handle and expensive to run. The time to start replacing millions of tons of copper wires with the future alternative had passed away and already the system is showing

signs of collapsing. The using a wired land line phone will reduce the effects of electromagnetic radiation and improve quality of life.

Conclusion

Using only simple experiments and simulation, this thesis has demonstrated the potential to make far greater use of ICPs in shielding devices for mobile phones and Wi-Fi devices. It has also highlighted the scope for use of ICPs in a wider range of applications and suggested directions for further research in solving the current problems in telecommunications and health issues in the transmitting of E-coli through mobile phones by introducing the ICPs materials to those applications. Further improvement of the modelling results is required to yield accurate material properties measurements.

References

1. M D'Amore and M Feliziani. Emp coupling to coaxial shielded cables. In Electromagnetic Compatibility, 1988. Symposium Record. IEEE 1988 International Symposium on, pages 3744. IEEE, 1988.
2. Zhuangjun Fan, Guohua Luo, Zengfu Zhang, Li Zhou, and Fei Wei. Electromagnetic and microwave absorbing properties of multi-walled carbon nanotubes/polymer composites. Materials Science and Engineering: B, 132(1):8589, 2006.
3. L Sandrolini, U Reggiani, and A Ogunsola. Modelling the electrical properties of concrete for shielding eectiveness prediction. Journal of Physics D: Applied Physics, 40(17):5366, 2007.
4. K Lakshmi, Honey John, KT Mathew, Rani Joseph, and KE George. Microwave absorption, reaction and emi shielding of pupani composite. Acta Materialia, 57(2):371375, 2009.
5. P Chandrasekhar and K Naishadham. Broadband microwave absorption and shielding properties of a poly (aniline). Synthetic metals, 105(2):115120, 1999.
6. Jiang, Daniel, and Luca Delgrossi. "IEEE 802.11 p: Towards an international standard for wireless access in vehicular environments." *Vehicular Technology Conference, 2008. VTC Spring 2008. IEEE*. IEEE, 2008.
7. Bo Han, Weijia Jia, and Lidong Lin. Performance evaluation of scheduling in ieee 802.16 based wireless mesh networks. Computer Communications, 30(4):782_792, 2007.
8. Wei Zhang, Abbas A Dehghani-Sanij, and Richard S Blackburn. Carbon based conductive polymer composites. Journal of materials science, 42(10):34083418, 2007. 118
9. Muhammad Faisal and Syed Khasim. Polyanilineantimony oxide composites for effective broadband emi shielding. Iranian Polymer Journal, 22(7):473480, 2013.
10. Jennifer M Pringle, Vanessa Armel, Maria Forsyth, and Douglas R MacFarlane. Pedot-coated counter electrodes for dye-sensitized solar cells. Australian journal of chemistry, 62(4):348_352, 2009.
11. Taosheng Wang, Guohua Chen, Cuiling Wu, and Dajun Wu. Study on the graphite nanosheets/resin shielding coatings. Progress in organic coatings, 59(2):101-105, 2007.
12. Köhler, Andreas R., et al. "Studying the potential release of carbon nanotubes throughout the application life cycle." *Journal of Cleaner Production* 16.8 (2008): 927-937.
13. PV Wright, B Chambers, A Barnes, K Lees, and A Despotakis. Progress in smart microwave materials and structures. Smart materials and structures, 9(3):273, 2000.

14. Christian Brosseau and Philippe Talbot. Instrumentation for microwave frequencydomain spectroscopy of lled polymers under uniaxial tension. Measurement Science and Technology, 16(9):1823, 2005.
15. Henry Greve, Christian Pochstein, Haile Takele, Vladimir Zaporojtchenko, FranzFaupel, Andreas Gerber, Michael Frommberger, and Eckhard Quandt. Nanostructured magnetic fenico/teon multilayers for high-frequency applications in the gigahertz range. Applied physics letters, 89(24):242501242501, 2006.
16. Irfan Ullah. Measuring and filtering microwave radiations using frequency selective surface through energy saving glass. 2012.
17. Mao-Sheng Cao, Wei-Li Song, Zhi-Ling Hou, Bo Wen, and Jie Yuan. The effects of temperature and frequency on the dielectric properties, electromagnetic interference 106 shielding and microwave-absorption of short carbon ber/silica composites. Carbon, 48(3):788796, 2010.
18. N. Li, Y. Huang, F. Du, X. He, X. Lin, H. Gao, Y. Ma, F. Li, Y. Chen, and P.C. Eklund. Electromagnetic interference (emi) shielding of single-walled carbon nanotube epoxy composites. Nano letters, 6(6):11411145, 2006.
19. Hao-Bin Zhang, Qing Yan, Wen-Ge Zheng, Zhixian He, and Zhong-Zhen Yu. Tough graphene- polymer microcellular foams for electromagnetic interference shielding. ACS applied materials & interfaces, 3(3):918924, 2011.
20. Abrikosov, Aleksej Alekseevič. Fundamentals of the Theory of Metals. Vol. 1. Amsterdam: North-Holland, 1988.
21. Deborah DL Chung. Applied materials science: applications of engineering materialsnin structural, electronics, thermal, and other industries. CRC Press, 2001
22. Wilson, Perry F., Mark T. Ma, and J. W. Adams. "Techniques for measuring the electromagnetic shielding effectiveness of materials. I. Far-field source simulation." *IEEE Transactions on Electromagnetic Compatibility* 30.3 (1988): 239-250.
23. Alan G MacDiarmid. Synthetic metals: a novel role for organic polymers. SyntheticMetals, 125(1):1122, 2001
24. Iain Thomas Learmonth. Pc card second generation shielding, April 11 2000. US Patent 6,049,468.
25. EMI Mesh. Emi shielding theory & gasket design guide.
26. Chun-Sheng Zhang, Qing-Qing Ni, Shao-Yun Fu, and Ken Kurashiki. Electromagnetic interference shielding effect of nanocomposites with carbon nanotube and shape memory polymer. Composites Science and Technology, 67(14):29732980, 2007.
27. Shang, S. M., and W. Zeng. "4-Conductive nanofibres and nanocoatings for smart textiles." *Multidisciplinary Know-How for Smart-Textiles Developers [Internet]. Woodhead Publishing* (2013): 92-128.

28. HT Feng, RF Zhuo, JT Chen, D. Yan, JJ Feng, HJ Li, S. Cheng, ZG Wu, J. Wang, and PX Yan. Synthesis, characterization, and microwave absorption property of the sno 2 nanowire/para-n composites. Nanoscale research letters, 4(12):14521457, 2009.
29. Wenrong Yang, Kyle R Ratinac, Simon P Ringer, Pall Thordarson, J Justin Gooding, and Filip Braet. Carbon nanomaterials in biosensors: should you use nanotubes or graphene? Angewandte Chemie International Edition, 49(12):2114 2138, 2010.
30. Chuizhou Meng, Changhong Liu, Luzhuo Chen, Chunhua Hu, and Shoushan Fan. Highly exible and all-solid-state paperlike polymer supercapacitors. Nano letters, 10(10):4025 4031, 2010.
31. Bibekananda Sundaray, V Subramanian, TS Natarajan, and K Krishnamurthy. Electrical conductivity of a single electrospun ber of poly (methyl methacrylate) and multiwalled carbon nanotube nanocomposite. Applied Physics Letters, 88(14):143114, 2006.
32. Gaozhi Xiao, Ye Tao, Jianping Lu, and Zhiyi Zhang. Highly conductive and transparent carbon nanotube composite thin lms deposited on polyethylene terephthalate solution dipping. Thin Solid Films, 518(10):28222824, 2010.
33. Zhong-Shuai Wu, Songfeng Pei, Wencai Ren, Daiming Tang, Libo Gao, Bilu Liu, Feng Li, Chang Liu, and Hui-Ming Cheng. Field emission of single-layer graphenemlms prepared by electrophoretic deposition. Advanced Materials, 21(17):17561760, 2009.
34. Alfredo M Morales and Charles M Lieber. A laser ablation method for the synthesis of crystalline semiconductor nanowires. Science, 279(5348):208211, 1998.
35. Dacheng Wei, Yunqi Liu, Yu Wang, Hongliang Zhang, Liping Huang, and Gui Yu. Synthesis of n-doped graphene by chemical vapor deposition and its electrical properties. Nano letters, 9(5):17521758, 2009.
36. Paola Ayala, R Arenal, M Rümmeli, Angel Rubio, and T Pichler. The doping of carbon nanotubes with nitrogen and their potential applications. Carbon, 48(3):575 586, 2010.
37. Yoshinori Ando, Xinluo Zhao, Toshiki Sugai, and Mukul Kumar. Growing carbon nanotubes. Materials today, 7(10):2229, 2004.
38. . David Robert King, Joseph C Rowan, Daniel D Johnson, and Bradley E Reis. Faraday cage, June 2 1998. US Patent 5,761,053.
39. Terje A Skotheim and John Reynolds. Handbook of Conducting Polymers, 2 Volume Set. CRC press, 2007
40. P Katta, M Alessandro, RD Ramsier, and GG Chase. Continuous electrospinning of aligned polymer nanobers onto a wire drum collector. Nano letters, 4(11):2215 2218, 2004.

41. Gordon G Wallace, Peter R Teasdale, Georey M Spinks, and Leon AP Kane- Maguire. Conductive electroactive polymers: intelligent polymer systems. CRC press, ISBN-13: 978-1420067095 Hardcover: {100-113) Publisher: CRC Press; 3 edition (October 22, 2008) ISBN-10: 1439828911 ISBN-13: 978-1420067095 ASIN: 1420067095 2008.
42. Yun-Hui Huang and John B Goodenough. High-rate lifepo4 lithium rechargeable battery promoted by electrochemically active polymers. Chemistry of Materials, 20(23):72377241, 2008.
43. Fengling Zhang, Mikael Johansson, Mats R Andersson, Jan C Hummelen, and Olle Inganäs. Polymer photovoltaic cells with conducting polymer anodes. Advanced Materials, 14(9):662665, 2002.
44. Alan J Heeger, Niyazi Serdar Sariciftci, and Ebinazar B Namdas. Semiconducting and metallic polymers. Oxford University Press, 2010.
45. M-A De Paoli, G Casalbore-Miceli, EM Girotto, and WA Gazotti. All polymeric solid state electrochromic devices. Electrochimica Acta, 44(18):29832991, 1999.
46. J. Simpson, S. Kirchmeyer, and K. Reuter. Advances and applications of inherently conductive polymer technologies based on poly (3, 4-ethylenedioxythiophene). In Proceedings of the 19th International Vacuum Web Coating Conference, Myrtle Beach, Dr. Jill Simpson*, Dr. Stephan Kirchmeyer§, Dr. Knud Reuter§ H.C. Starck, Inc., 45 Industrial Place, Newton, MA 02461 USA, Tel (617) 630-5878, fax (617) 559-3906, Email jill.simpson@hcstarck.com; § H.C. Starck, GmbH., C/o Bayer AG, Gebaude B 202, 51368 Leverkusen, Germany 2005.
47. E Falletta, C Della Pina, and M Rossi. Sustainable approaches for polyaniline and polypyrrole synthesis. Journal of Advanced Catalysis Science and Technology, 1:614, 2014.
48. Changling Li, Nicha Chartuprayoon, Wayne Bosze, Karen Low, Kyu Hwan Lee, Jin Nam, and Nosang V Myung. Electrospun polyaniline/poly (ethylene oxide) composite nanobers based gas sensor. Electroanalysis, 26(4):711722, 2014.
49. S. Kirchmeyer, A. Elschner, K. Reuter, W. Lovenich, and U. Merker. PEDOT as a Conductive Polymer: Principles and Applications. CRC Press, 2010.
50. JR Araujo, CB Adamo, MV Costa e Silva, and M-A Paoli. Antistatic-reinforced biocomposites of polyamide-6 and polyaniline-coated curau bers prepared on a pilot plant scale. Polymer Composites, 34(7):10811090, 2013
51. J. Huang. Syntheses and applications of conducting polymer polyaniline nanobers. Pure and applied chemistry, 78(1):1528, 2006.
52. Y. Niu. Preparation of polyaniline/polyacrylate composites and their application for electromagnetic interference shielding. Polymer composites, 27(6):627632, 2006.

53. HT Feng, RF Zhuo, JT Chen, D. Yan, JJ Feng, HJ Li, S. Cheng, ZG Wu, J. Wang, and PX Yan. Synthesis, characterization, and microwave absorption property of the sno_2 nanowire/para-n composites. Nanoscale research letters, 4(12):14521457, 2009.
54. Graeme A Snook, Pon Kao, and Adam S Best. Conducting-polymer-based supercapacitor devices and electrodes. Journal of Power Sources, 196(1):112, 2011.
55. David W Hatchett and Mira Josowicz. Composites of intrinsically conducting polymers as sensing nanomaterials. Chemical reviews, 108(2):746769, 2008. 109
56. Y. Wang and X. Jing. Intrinsically conducting polymers for electromagnetic interference shielding. Polymers for advanced technologies, 16(4):344351, 2005. 116
57. B. Belaabed, S. Lamouri, N. Naar, P. Bourson, and S.O.S. Hamady. Polyanilinedoped benzene sulfonic acid/epoxy resin composites: structural, morphological, thermal and dielectric behaviors. Polymer journal, Polymer Journal 42, 546–554; doi:10.1038/pj.2010.41; published online 2 June 2010.
58. Jaroslav Stejskal, Irina Sapurina, and Miroslava Trchová. Polyaniline nanostructures and the role of aniline oligomers in their formation. Progress in Polymer Science, 35(12):14201481, 2010
59. Mariana Ioniμ and Alina Prun . Polypyrrole/carbon nanotube composites: Molecular modeling and experimental investigation as anti-corrosive coating. Progress in Organic Coatings, 72(4):647652, 2011. 110
60. Kulesza, Pawel J., et al. "Network films composed of conducting polymer-linked and polyoxometalate-stabilized platinum nanoparticles." *Chemistry of materials* 16.21 (2004): 4128-4134.
61. Feng, Xiao-Miao, et al. "One-step electrochemical synthesis of graphene/polyaniline composite film and its applications." *Advanced Functional Materials* 21.15 (2011): 2989-2996.
62. D.C. Trivedi and S.K. Dhawan. Shielding of electromagnetic interference using polyaniline. Synthetic metals, 59(2):267272, 1993.
63. Drake, Neil. *Polymeric Materials for Electrostatic Applications: A Report from Rapra's Industry Analysis and Publishing Group*. iSmithers Rapra Publishing, 1996.
64. Yuan, Bingqing, et al. "Comparison of electromagnetic interference shielding properties between single-wall carbon nanotube and graphene sheet/polyaniline composites." *Journal of Physics D: Applied Physics* 45.23 (2012): 235108.
65. Sharma, Piyush Sindhu, et al. "Surface development of molecularly imprinted polymer films to enhance sensing signals." *TrAC Trends in Analytical Chemistry* 51 (2013): 146-157.

66. Wei, Li, Qi Chen, and Yingjun Gu. "Preparation and characterization of transparent PANI-SIO2 hybrid conducting films." *Polymer Engineering & Science* 50.5 (2010): 986-990.
67. L. Wei, Q. Chen, and Y. Gu. Eects of content of polyaniline doped with dodecylbenzene sulfonic acid on transparent pani-sio2 hybrid conducting lms. Synthetic Metals, 160(5-6):405408, 2010.
68. Yun-Hui Huang and John B Goodenough. High-rate lifepo4 lithium rechargeable battery promoted by electrochemically active polymers. Chemistry of Materials, 20(23):72377241, 2008.
69. J. Huang. Syntheses and applications of conducting polymer polyaniline nanobers. Pure and applied chemistry, 78(1):1528, 2006.
70. C.Y. Huang and C.C. Wu. The emi shielding effectiveness of pc/abs/nickel-coatedcarbon-bre composites. European polymer journal, 36(12):27292737, 2000.
71. J. Ouyang, C.W. Chu, F.C. Chen, Q. Xu, and Y. Yang. High-conductivity poly (3, 4-ethylenedioxythiophene): Poly (styrene sulfonate) lm and its application in polymer optoelectronic devices. Advanced Functional Materials, 15(2):203208, 2005.
72. H Gorter, MJJ Coenen, MWL Slaats, M Ren, W Lu, CJ Kuijpers, and WA Groen. Toward inkjet printing of small molecule organic light emitting diodes. Thin Solid Films, 532:11 15, 2013.
73. Frederik C Krebs, Thomas Tromholt, and Mikkel Jørgensen. Upscaling of polymer solar cell fabrication using full roll-to-roll processing. Nanoscale, 2(6):873886, 2010
74. Halit Arslan and Fatma Arslan. Preparation of a polypyrrole-polyvinylsulphonate composite _lm biosensor for determination of phenol based on entrapment of polyphenol oxidase. Arti_cial Cells, Blood Substitutes and Biotechnology, 39(5):341_345, 2011.
75. S Geetha, Chepuri RK Rao, M Vijayan, and DC Trivedi. Biosensing and drug delivery by polypyrrole. Analytica Chimica Acta, 568(1):119125, 2006.
76. Joseph Wang and Mustafa Musameh. Carbon-nanotubes doped polypyrrole glucose biosensor. Analytica Chimica Acta, 539(1):209_213, 2005.
77. Hua Bai and Gaoquan Shi. Gas sensors based on conducting polymers. Sensors, 7(3):267307, 2007
78. Mingming Sun, Shichao Zhang, Tao Jiang, Lan Zhang, and Jinhua Yu. Nano-wire networks of sulfurpolypyrrole composite cathode materials for rechargeable lithium batteries. Electrochemistry Communications, 10(12):18191822, 2008.
79. Babita Gaihre, Gursel Alici, Georey M Spinks, and Julie M Cairney. Synthesis and performance evaluation of thin lm ppy-pvdf multilayer electroactive polymer actuators. Sensors and Actuators A: Physical, 165(2):321328, 2011.

80. Fanhui Meng and Yi Ding. Sub-micrometer-thick all-solid-state supercapacitors with high power and energy densities. Advanced Materials, 23(35):40984102, 2011.
81. M Joshi and A Bhattacharyya. Nanotechnologya new route to high-performance functional textiles. Textile Progress, 43(3):155233, 2011.
82. M.A. Chougulea, S.G. Pawara, P.R. Godsea, R.N. Mulika, S. Senb, and V.B. Patila. Synthesis and characterization of polypyrrole (ppy) thin _lms. Soft Nanoscience Letters, 1, 2011.
83. Jian Wu, Dezhi Zhou, Chee O Too, and Gordon G Wallace. Conducting polymer coated lycra. Synthetic Metals, 155(3):698_701, 2005.
84. JH Ling. Polymers in electronics. Circuit World, 33(2), 2007.
85. Avloni, Jamshid, and Arthur Henn. "DEVELOPMENT OF NEW CONDUCTIVE AND MICROWAVE-LOSSY MATERIALS INVOLVING CONDUCTING POLYMER COATINGS."
86. Teodor Sandu, Andrei Sarbu, Floriana Constantin, Catalin Ilie Spataru, Raluca Augusta Gabor, Raluca Somoghi, and Horia Iovu. Characterization of functionalized polypyrrole. Rev. Roum. Chim, 57(3):177185, 2012.
87. Walter L Harmer, Leif Christensen, Gary J Drtina, and Harvey J Helmin. Abrasive article with conductive, doped, conjugated, polymer coat and method of making same, October 29 1991. US Patent 5,061,294.
88. Horacio Vasquez, Laura Espinoza, Karen Lozano, Heinrich Foltz, and Shuying Yang. Simple device for electromagnetic interference shielding eectiveness measurement. In Institute of Electrical and Electronics Engineers, http://www.emcs.org/acstrial/newsletters/winter09/pp2.pdf 2009.
89. Parveen Saini, Veena Choudhary, BP Singh, RB Mathur, and SK Dhawan. Polyanilinemwcnt nanocomposites for microwave absorption and emi shielding. Materials Chemistry and Physics, 113(2):919926, 2009.
90. Yonglai Yang, Mool C Gupta, Kenneth L Dudley, and Roland W Lawrence. Novel carbon nanotube-polystyrene foam composites for electromagnetic interference shielding. Nano letters, 5(11):21312134, 2005.
91. Akimasa Hirata, Ilkka Laakso, Takuya Oizumi, Ryuto Hanatani, Kwok Hung Chan, and Joe Wiart. The relationship between specic absorption rate and temperature elevation in anatomically based human body models for plane wave exposure from 30 mhz to 6 ghz. Physics in medicine and biology, 58(4):903, 2013.
92. Richard B Schulz, VC Plantz, and DR Brush. Shielding theory and practice. Electromagnetic Compatibility, IEEE Transactions on, 30(3):187201, 1988.
93. Christopher L Holloway, Ronald R Delyser, Robert F German, Paul Mckenna, and Motohisa Kanda. Comparison of electromagnetic absorber used in anechoic and semi-

anechoic chambers for emissions and immunity testing of digital devices. Electromagnetic Compatibility, IEEE Transactions on, 39(1):3347, 1997.

94. Habiba Hafdallah Ouslimani, Redha Abdeddaim, and Alain C Priou. Free-space electromagnetic characterization of materials for microwave and radar applications.PIERS Online, 1(2):128132, 2005.
95. Xingcun Colin Tong. Advanced materials and design for electromagnetic interference shielding. CRC Press, 2008.
96. Mohsen Jalali and Rolf Wuthrich. Improving electromagnetic shielding of composite structures with metallic nanoparticles synthesized by electrochemical discharges. In Electromagnetic Compatibility-EMC Europe, 2009 International Symposium on, pages 14. IEEE, 2009.
97. R Perumalraj, BS Dasaradan, R Anbarasu, P Arokiaraj, and S Leo Harish. Electromagnetic shielding eectiveness of copper core-woven fabrics. The Journal of The Textile Institute, 100(6):512524, 2009.
98. Juan C Carillo Jr and James S Carillo. Close-proximity radiation detection device for determining radiation shielding device eectiveness and a method therefor, December 10 2002. US Patent 6,492,957.
99. C Christopoulos. Electromagnetic compatibility. ii. Design principles. Power Engineering Journal, 6(5):239_247, 1992.
100. Inder J Bahl. Lumped elements for RF and microwave circuits. Artech house, 2003.
101. Wolfgang JR Hoefer. The transmission-line matrix method-theory and applications. Microwave Theory and Techniques, IEEE Transactions on, 33(10):882_893, 1985.
102. David M Pozar. Microwave engineering. John Wiley & Sons, 2009. 113
103. Christophe Caloz and Tatsuo Itoh. Electromagnetic metamaterials: transmission line theory and microwave applications. John Wiley Sons, 2005.
104. Leszek Demkowicz and L Vardapetyan. Modeling of electromagnetic absorption scattering problems using hp-adaptive nite elements. Computer Methods in Applied Mechanics and Engineering, 152(1):103124, 1998.
105. Lennart Hardell and Cindy Sage. Biological eects from electromagnetic eld exposureand public exposure standards. Biomedicine & Pharmacotherapy, 62(2):104109, 2008.
106. Tatia MC Lee, Sam MY Ho, Lucia YH Tsang, Serena YC Yang, Leonard SW Li, and Chetwyn CH Chan. Eect on human attention of exposure to the electromagnetic eld emitted by mobile phones. Neuroreport, 12(4):729731, 2001.

107. Stefan Schwarzer, Andréa De Bono, Gregory Giuliani, Stéphane Kluser, and Pascal Peduzzi. E-waste, the hidden side of it equipment's manufacturing and use. 2005, 114

108. Santosh Kumar, Wendy J Nilsen, Amy Abernethy, Audie Atienza, Kevin Patrick, Misha Pavel, William T Riley, Albert Shar, Bonnie Spring, Donna Spruijt-Metz, et al. 111

109. Ladou, Joseph, and Sandra Lovegrove. "Export of electronics equipment waste." *International journal of occupational and environmental health* (2013).

110. Chang, Jin-Hong. "Anti-electromagnetic interference material arrangement." U.S. Patent Application No. 12/207,107.

111. Neal Leavitt. Mobile phones: the next frontier for hackers? Computer, 38(4):2023, 2005.

112. Xiaofei Wang, Athanasios V Vasilakos, Min Chen, Yunhao Liu, and Ted Taekyoung Kwon. A survey of green mobile networks: Opportunities and challenges. Mobile Networks and Applications, 17(1):420, 2012.

113. Nicola Edelstyn and Anna Oldershaw. The acute eects of exposure to the electromagnetic eld emitted by mobile phones on human attention. Neuroreport, 13(1):119 121, 2002.

114. Ashok Agarwal, Nisarg R Desai, Kartikeya Makker, Alex Varghese, Rand Mouradi, Edmund Sabanegh, and Rakesh Sharma. Effects of radiofrequency electromagnetic waves (rf-emw) from cellular phones on human ejaculated semen: an in vitro pilot study. Fertility and sterility, 92(4):13181325, 2009.

115. Sabine Heinrich, Silke Thomas, Christian Heumann, diger von Kries, and Katja Radon. The impact of exposure to radio frequency electromagnetic elds on chronic well-being in young people a cross sectional study based on personal dosimetry. Environment international, 37(1):2630, 2011.

116. Maria Feychting. Mobile phones, radiofrequency fields, and health effects in children epidemiological studies. Progress in biophysics and molecular biology, 107(3):343348, 2011.

117. Sumana Bhattacharjee. Protective measures to minimize the electromagnetic radiation. Advance in Electronic and Electric Engineering, 4(4):375380, 2010.

118. Srikanth, Padma, et al. "Mobile phones: emerging threat for infection control." *Journal of infection prevention* 11.3 (2010): 87-90.

119. Karch, Helge, et al. "The enemy within us: lessons from the 2011 European Escherichia coli O104: H4 outbreak." *EMBO molecular medicine* 4.9 (2012): 841-848.

120. http://www.lshtm.ac.uk/newsevents/news/2011/mobilephones.html

121. Ramesh, AO Carter, MH Campbell, N Gibbons, C Powlett, H Moseley Sr, D Lewis, and T Carter. Use of mobile phones by medical staat queen elizabeth hospital, barbados: evidence for both benet and harm. Journal of Hospital Infection, 70(2):160165, 2008.

122. RRW Brady, A Wasson, I Stirling, C McAllister, and NN Damani. Is your phone bugged? the incidence of bacteria known to cause nosocomial infection on healthcare workers' mobile phones. Journal of Hospital Infection, 62(1):123125, 2006.

123. Supri A Ghani and Heah Chong Young. Conductive polymer based on polyanilineeggshell powder (pani-esp) composites. Journal of Physical Science, 21(2):81_97, 2010.

124. Ben Zhong Tang, Yanhou Geng, Jacky Wing Yip Lam, Bensheng Li, Xiabin Jing, Xianhong Wang, Fosong Wang, AB Pakhomov, and XX Zhang. Processible nanostructured materials with electrical conductivity and magnetic susceptibility: preparation and properties of maghemite/polyaniline nanocomposite _lms. Chemistry of materials, 11(6):1581_1589, 1999.

125. Naji Al-Dahoudi. Wet chemical deposition of transparent conducting coatings made of redispersable crystalline ITO nanoparticles on glass and polymeric substrates. Journal of sol-gel science and technology 27 (1), 81-89 2007

126. R Patil, E Matveeva, and V Parkhutik. Simple chemical polymerization method for deposition of conducting polyaniline on surface of acrylonitrile butadiene styrene. Journal of Applied Polymer Science, 85(9):1904_1910, 2002.

127. Vandana Singh, Swati Mohan, G Singh, PC Pandey, and Rajiv Prakash. Synthesis and characterization of polyaniline_carboxylated pvc composites: application in development of ammonia sensor. Sensors and Actuators B: Chemical, 132(1):99_106, 2008.

128. M Vukadinovic, B Malic, Marija Kosec, and D Krizaj. Modelling and characterization of thin lm planar capacitors: inherent errors and limits of applicability of partial capacitance methods. Measurement Science and Technology, 20(11):115106, 2009.

129. COMSOL Multiphysics. Comsol multiphysics user guide (version 4.3 a). COMSOL, AB,https://cdn.comsol.com/documentation/5.2.1.229/IntroductionToCOMSOLMultiphysics.pdf. 2012.

130. Roger W Pryor. Multiphysics Modeling Using COMSOL?: A First Principles Approach. Jones & Bartlett Learning, https://www.amazon.com/Engineering-Physics-Rajesh-Kumar/dp/9380298609/ref=mt_paperback?_encoding=UTF8&me= 2011.

131. Claes Johnson. Numerical solution of partial dierential equations by the nite element method. Courier Corporation, 2012.

132. John Rodgers and Edo Waks. Protection of electronic systems from the effects of high-power microwave (hpm) and ultra-wideband (uwb) sources. Technical report, DTIC Document, 2012.

133. D Gaston, G Hansen, S Kadioglu, DA Knoll, C Newman, H Park, C Permann, and W Taitano. Parallel multiphysics algorithms and software for computational nuclear engineering. In Journal of Physics: Conference Series, volume 180, page 012012. IOP Publishing, 2009.

134. Michael R Tonks, Derek Gaston, Paul C Millett, David Andrs, and Paul Talbot. An object-oriented nite element framework for Multiphysics phase field simulations. Computational Materials Science, 51(1):2029, 2012.

135. AS Al-Shibib, KM Khammas, and R Taher. Pyocyanin preparation frompseudomonas aeruginosa isolated from heterogeneous clinical materials. Folia micro- biological, 31(3):215219, 1986.

136. SA Kandela, AS Al-Shibib, and BH Al-Khayat. A study of puried pyorubrin produced by local pseudomonas aeruginosa. Acta microbiologica Polonica, 46(1):3743, 1996.

137. Asfar Al-Shibib. Medical biology and antibiotics science. neelwafurat, 1997.

138. Al-Khalil Suleiman Al-Shibib, Asfar, Ahmad Alkofahi, and Dawud El-Eisawi. Transitorine, a new quinoline alkaloid from ephedra transitoria. Journal of natural products, 62(8):12141214, 1999.

139. AS Al-Shibib, FK Hassan, FY Al-Ani, and SM Mudaar. Pyocin typing of pseudomonas aeruginosa isolated from hospital of iraq. Indian Journal of Comparative Microbiology, Immunology and Infectious Diseases, 4:l9697, 1983.

140. Mahiar Hamedi, Anders Elfwing, Roger Gabrielsson, and Olle Inganäs. Electronic polymers and dna self-assembled in nanowire transistors. Small, 9(3):363_368, 2013.

141. B Zhang, J Sun, HE Katz, F Fang, and RL Opila. Promising thermoelectric properties of commercial pedot: Pss materials and their bi2te3 powder composites. ACS applied materials & interfaces, 2(11):3170-3178, 2010.

142. Ali Hellany, Mahmood H Nagrial, and Jamal Rizk. Emc compliance with reference to Australia. In High-Capacity Optical Networks and Enabling Technologies (HONET), 2010, pages 232236. IEEE, 2010**.**

143. Parveen Saini and Manju Arora. Microwave absorption and emi shielding behavior of nanocomposites based on 2 intrinsically conducting polymers, 3 graphene

and carbon nanotubes 4. book edited by Ailton De Souza Gomes, ISBN 978-953-51-0744-6, Published: September 12, 2012.

144. Tatia MC Lee, Sam MY Ho, Lucia YH Tsang, Serena YC Yang, Leonard SW Li, and Chetwyn CH Chan. Eect on human attention of exposure to the electromagnetic eld emitted by mobile phones. Neuroreport, 12(4):729731, 2001.

145. Chung, D. D. L. "Review Electromagnetic interference shielding effectiveness of carbon materials." *carbon* 39.2 (2001): 279-285.

146. W Al-Shabib, "Identifying smart conducting materials for Wi-Fi electromagnetic interference shielding" http://ro.ecu.edu.au/cgi/viewcontent.cgi?article=1192&context=ecuworks2012

147. Ding-Xiang Yan, Peng-Gang Ren, Huan Pang, Qiang Fu, Ming-Bo Yang, and Zhong-Ming Li. E-cient electromagnetic interference shielding of lightweight graphene/polystyrene composite. J. Mater. Chem., 22(36):18772-18774, 2012

148. C.D. Liu and K.H. Hsieh. Synthesis and characterisation of conducting pedot/watersoluble polymer.

149. Hammo, Shamil M. (2012). "Effect of Acidic Dopants properties on the Electrical Conductivity of Poly aniline". Tikrit Journal of Pure Science. (17) 2-14

150. W.Al-shabib, “The characterization of Polar-Loop transmitters in co-sited operation” May 1981

151. Sook Wai Phang, Masato Tadokoro, Jiro Watanabe, and Noriyuki Kuramoto. Synthesis, characterization and microwave absorption property of doped polyaniline nanocomposites containing tio 2 nanoparticles and carbon nanotubes. Synthetic Metals, 158(6):251 258, 2008

152. L. Wei, Q. Chen, and Y. Gu. Effects of content of polyaniline doped with dodecylbenzene sulfonic acid on transparent pani-sio2 hybrid conducting lms. Synthetic Metals, 160(5-6):405408, 2010.

153. L Groenendaal, Friedrich Jonas, Dieter Freitag, Harald Pielartzik, and John Reynolds. Poly (3, 4 ethylenedioxythiophene) and its derivatives: past, present,and future. Advanced Materials, (12):481494, 2000.

154. John Thompson, Xiaohu Ge, Hsiao-Chun Wu, Ralf Irmer, Hong Jiang, Gerhard Fettweis, and Siavash Alamouti. 5g wireless communication systems: Prospects and Challenges, 2014.

155. Min Li, Joe Nuebel, James L Drewniak, Richard E DuBro, Todd H Hubing, and Thomas P Van Doren. Emi from cavity modes of shielding enclosures-fdtd modeling and measurements. Electromagnetic Compatibility, IEEE Transactions on, 42(1):29 38, 2000.

156. Brian C Warren, Mohamed H Awida, and Aly E Fathy. Nonlinear multi-physics model for casting metal in an industrial microwave furnace. In Microwave Symposium Digest (MTT), 2011 IEEE MTT-S International, pages 1-4. IEEE, 2011.

157. BR Kim, HK Lee, SH Park, and HK Kim. Electromagnetic interference shielding characteristics and shielding effectiveness of polyaniline-coated lms. Thin Solid Films, 519(11):34923496, 2011**.** 92

158. S Hamilton, MJ Hepher, and J Sommerville. Polypyrrole materials for detection and discrimination of volatile organic compounds. Sensors and Actuators B: Chemical, 107(1):424_432, 2005.

159. Jung-Sim Roh, Yong-Seung Chi, Tae Jin Kang, and Sang-wook Nam. Electromagnetic shielding effectiveness of multifunctional metal composite fabrics. Textile Research Journal, 78(9):825835, 2008.

160. H. Ott, Electromagnetic Compatibility Engineering, John Wiley & Sons, New York, 2009.